DEPARTMENT OF BIOLOGY, UNIVERSITY OF CRETE

INSTITUTE OF MOLECULAR BIOLOGY AND BIOTECHNOLOGY, FOUNDATION FOR RECEARCH AND TECHNOLOGY

PhD THESIS

Molecular analysis of protein secretion through Type III secretion system from Enteropathogenic E. coli

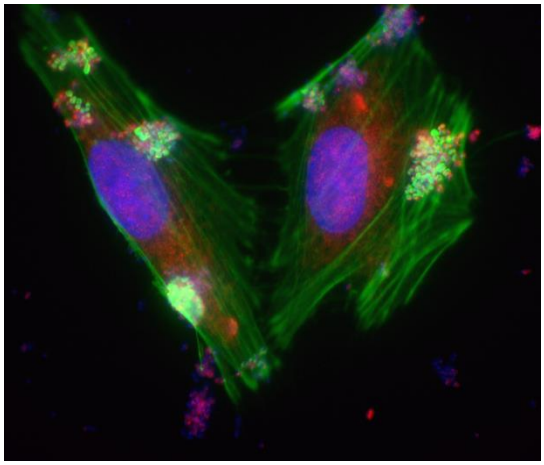

Portaliou Athina

Supervisor: Prof. Anastasios Esonomou

Iraklion, 2015

....To God who instead of strength, gave me courage

and to my supportive family....

Contents

Content of figures and tables

Acknowledgments

In order to fulfill the requirements needed so to be able to finish your PhD thesis, the help and support from other people is essential. In a daily basis, one needs to be surrounded from people that will care about him/ her. Otherwise, is not possible to survive this procedure….

During this PhD thesis, many people were there for me, to help me and support me, in their own special way. For this reason, I would like to devote a few lines in here to thank them.

At this point, I would like to say a great thanks to Prof. Anastassios Economou firstly because he accepted me to be a member of his lab team; but more importantly because all these years, every single day, he was there for me, tolerating my insecurity and advising me, so to become the person-scientist I am today. Secondly, I would like to thank Dr. Spyridoula Karamanou for her constant scientific and general support to my every-day-experimental problems where she always had something to suggest.

Afterwards, I would like to thank Dr. Vassileia Balabanidou, because not only she recruited me to the fascinating world of T3SS, but also she bequeathed me with almost all the tools to do so.

Furthermore, I would like to thank all the members of the lab, past and new, that helped to maintain a nice environment there, support each other when need arised, resulting in a perfect place to spent your daily life. Specifically, a great thanks to: Giorgia Orfanoudaki, Giorgos Gouridis, Michalis Aivaliotis, Nikos Kountourakis, Kostas Tsolis, Alexandra Tsirigotaki, Nikos Famelis, Marina Koukaki, Katerina Chatzi and Marios Sardis.

A great thank also to my family, for all these years of the embracement and the support to everything I do.

Last, but no least, I would like to give special thanks to my partner in life, Konstantinos Giakoumakis, because he stood by me for all these years now, and still does…..

Summary

Type III secretion system (T3SS) is a widespread virulence system, in Gram negative bacteria, used to transport effector proteins directly into the eukaryotic host cell by spanning three membranes, two bacterial and one eukaryotic. The T3SS is a unique nanomachine that resembles a needle and can be divided in three basic compartments. First, the basal body, which forms a ring-like structure, is used to bridge the inner with the outer membrane of the bacterium. From the basal body a needle-filament construction is generated that will be attached to the host cell. In the cytosolic domain of the inner membrane the cytosolic ring and the ATPase complex is assembled in order to regulate and coordinate the secretion process. In order the system to become functional and active more than 50 proteins need to be synchronized so the assembly of the system and the protein secretion through it undergo sophisticated regulation. Although recent structural and biochemical studies provide information about the assembly of the system, the understanding of the molecular mechanism behind the translocation process remains elusive.

The main goal of this thesis was to shed more light to the molecular mechanism that proteins follow so to be secreted from T3SS. The aim was to investigate and map the pathway proteins follow from the bacterial cytosol towards the membrane at the base of the translocation pore. Determination of the protein-protein interactions that occur and elucidation of the mechanism that lies behind the membrane targeting of the secretory protein- chaperone complexes was our ultimate target.

Using Enteropathogenic *E. coli* as a model organism we combined structural, biochemical and biophysical approaches to achieve our goal.

Towards this end, first we performed a comprehensive analysis of the protein complexes formed in the bacterial cytosol during protein secretion through T3SS. For this analysis we combined Native Polyacrylamide gel electrophoresis and/or Size exclusion chromatography for protein separation in line with high resolution Mass spectrometry analysis. From this analysis, we identified many protein complexes related with T3SS. Moreover, we ended up with important information regarding protein complex formation in the cytosol as a function of time, hierarchy that is followed and regulation of the procedure, which were also correlated with real-time secretion analysis from the system. We established a general pipeline that could be

followed for the protein identification and determination of protein complexes formed in different biological states.

Additionally, in a more targeted approach to map the interactions between the specialized chaperones of the system with the secretory proteins, and how these interactions are regulated, we used biochemical and biophysical methods in concert with *in vivo* experiments. As a model for secretory protein-chaperone complex, the CesAB chaperone in complex with its cognate substrate EspA was used.

First, we determined the mechanism that is followed in order for the chaperone to avoid aggregation and unspecific interactions in the cytoplasm. According to this model, the chaperone forms a homo-dimer when is on its own in solution that mimics the structure that it would occur if the secretory protein was bound. The main difference between these two similar overall structures, the homo- and hetero-dimers is that the homodimer retains a partially loose and unfolded structure, due to unfavored interactions between the two CesAB protomers.

Once the secretory protein EspA is added in solution, the homodimer of the chaperone dissociates and a stable heterodimer is generated with the chaperone CesAB and the secretory protein EspA. The formation of the 1:1 protein complex is essential so to keep the secretory protein in an unfolded and translocation-competent state. Conformational changes that occur on CesAB main body, upon EspA-binding, lead to a transition disorder-to-order state. These structural changes are important for the exposure of a targeting signal on the chaperone's surface, which enables the interaction of the protein complex with the ATPase of the system.

Overall the results obtained, revealed, on one hand, a self-regulation mechanism that the chaperones follow so to prevent unspecific protein interactions. On the other hand, we established a substrate –activated conformational switch on the chaperone which encodes a targeting signal that could be the mechanism for protein targeting to the ATPase of the system.

Finally, in order to fulfill our goal for elucidating the membrane targeting procedure, we reconstituted the process *in vitro*. We established an *in vitro* assay where the binding of the cytoplasmic complexes at the T3SS can be monitored and quantified.

From the data derived from the *in vitro* analysis of the targeting process, we have clearly demonstrated that the carboxyl-terminal tail (hereafter C-tail) of the chaperone

CesAB is essential for the targeting of the secretory protein-chaperone complex at the T3SS export apparatus. We have signified that when CesAB is bound on the secretory protein EspA, the protein complex can interact with the membrane, via the C-tail. This targeting process is independent of the existence of the ATPase, and other proteins that are located at the export apparatus of the system, like SepL, EscV and EscU are essential for the binding event to occur.

Collectively, a two-step targeting hypothesis is proposed. During the first step, once the chaperone-secretory complex has been formed it is targeted to the membrane of the T3SS, via the C-tail of the chaperone. Afterwards, the ATPase can bind to the main body of the CesAB, as a second docking event.

Περίληψη

Το σύστημα έκκρισης τύπου ΙΙΙ (T3SS) είναι ένα ευρέως διαδεδομένο σύστημα που χρησιμοποιείται από πολλά παθογόνα, κατά Gram αρνητικά βακτήρια. Το σύστημα τύπου ΙΙΙ, είναι μια εξειδικευμένη μικρο-μηχανή που χρησιμοποιείται για τη μεταφορά των μολυσματικών παραγόντων του βακτηρίου από το κυτταρόπλασμά του κατευθείαν μέσα στο κύτταρο ξενιστή, διαπερνώντας τρεις μεμβρανικές δομές, δύο βακτηριακές και μία ευκαρυωτική. Το σύστημα έκκρισης τύπου ΙΙΙ σχηματίζει μια δομή στο χώρο που μπορεί να παρομοιαστεί με βελόνα (injectisome). Η βελονοειδής αυτή κατασκευή, διαχωρίζεται σε τρία δομικά στοιχεία: το βασικό σωμάτιο, που απαρτίζεται από κυλινδρικές κατασκευές και ενώνει την εξωτερική με την εσωτερική μεμβράνη του βακτηρίου ˙ το ινίδιο το οποίο εξέρχεται από το βασικό σωμάτιο και προσκολλάται στη μεμβράνη του κυττάρου ξενιστή, ώστε να δημιουργηθεί ένας συνεχόμενος κενός δίαυλος από το βακτηριακό κυτταρόπλασμα στο ευκαρυωτικό. Τέλος, στη βάση του βασικού σωματίου από τη μεριά της εσωτερικής βακτηριακής μεμβράνης συναντάμε τον κυτταροπλασματικό δακτύλιο. Ο κυτταροπλασματικός δακτύλιος, απαρτίζεται από έναν πρωτεϊνικό δακτύλιο και το πρωτεϊνικό σύμπλοκο με την ΑΤΡαση του συστήματος, οι οποίοι είναι υπεύθυνοι για τη σωστή λειτουργία του συστήματος και την αποτελεσματική έκκριση των πρωτεϊνών από αυτό.

Για τη δημιουργία και ενεργοποίηση του συστήματος περίπου 50 πρωτεΐνες πρέπει να συντονιστούν ώστε το σύστημα να αποκτήσει τη σωστή διαμόρφωση στο χώρο και οι πρωτεΐνες που πρόκειται να εκκριθούν από αυτό να μεταφερθούν εκεί. Η όλη διαδικασία υπόκειται πολύπλοκο και σύνθετο έλεγχο από διάφορους παράγοντες σε διάφορα επίπεδα, κατά το μονοπάτι εξόδου των πρωτεϊνών από το κύτταρο. Παρόλο που πάρα πολλές δομικές και βιοχημικές μελέτες έχουν συμβάλει στην κατανόηση και δομική ανάλυση του συστήματος, ελάχιστες πληροφορίες σχετικά με το μονοπάτι που ακολουθούν οι πρωτεΐνες με στόχο την έξοδό τους από το κύτταρο και τη ρύθμιση αυτού είναι γνωστές.

Βασικός στόχος της παρούσας διδακτορικής διατριβής είναι η κατανόηση και αποσαφήνιση του μονοπατιού που ακολουθούν οι πρωτεΐνες οι οποίες πρόκειται να εκκριθούν, κατά τη μετατόπιση αυτών από το βακτηριακό κυτταρόπλασμα μέχρι τη μεμβράνη, στον πόρο εξόδου του συστήματος έκκρισης τύπου ΙΙΙ. Μέλημά μας ήταν ο εντοπισμός και χαρακτηρισμός των αλληλεπιδράσεων που συμβαίνουν ανάμεσα

στις πρωτεΐνες του συστήματος και η χαρτογράφηση αυτών με στόχο τη διασαφήνιση του μηχανισμού που ακολουθείται κατά τη στόχευση των πρωτεϊνών στη μεμβράνη.

Για την επίτευξη του παραπάνω στόχου χρησιμοποιήθηκε σαν οργανισμός-μοντέλο το Εντεροπαθογόνο *E. coli*, και συνδυάστηκαν διάφορες βιοχημικές, δομικές και βιοφυσικές μεθοδολογίες.

Αρχικά πραγματοποιήθηκε μια περιεκτική και ολοκληρωμένη ανάλυση των πρωτεϊνικών συμπλόκων που εντοπίζονται στο βακτηριακό κυτταρόπλασμα κατά τη διάρκεια της ανάπτυξης του βακτηρίου και την έκκριση των πρωτεϊνών από το σύστημα τύπου ΙΙΙ, συνδυάζοντας τεχνικές εγγενούς ηλεκτροφόρησης ή/ και χρωματογραφία μοριακής διήθησης, με υψηλής ευκρίνειας φασματομετρία μάζας.

Από την ανάλυση αυτή ταυτοποιήθηκαν πολλές πρωτεΐνες που σχετίζονται με το σύστημα έκκρισης τύπου ΙΙΙ. Επιπλέον, προέκυψαν σημαντικές πληροφορίες αναφορικά με τα πρωτεϊνικά σύμπλοκα που δημιουργούνται στο κυτταρόπλασμα και πως ο σχηματισμός αυτών συνδέεται με τη ρύθμιση και λειτουργία του συστήματος, καθώς και με την σειρά που ακολουθείται κατά την διαδικασία της έκκρισης των πρωτεϊνών από το βακτήριο. Επιπλέον, αναπτύξαμε μια πειραματική διαδικασία η οποία μπορεί να χρησιμοποιηθεί για την ανίχνευση, τον προσδιορισμό και τη σύγκριση πρωτεϊνικών συμπλόκων σε οποιοδήποτε κύτταρο, κατά τη διάρκεια διαφορετικών φάσεων της ανάπτυξη αυτού.

Στα πλαίσια μιας πιο στοχευόμενης προσέγγισης, για την αποσαφήνιση των αλληλεπιδράσεων δυο πρωτεϊνών, χρησιμοποιήθηκε η σαπερόνη CesAB σε σύμπλοκο με την εκκριτική πρωτεΐνη EspA, και συνδυάστηκαν τόσο βιοχημικά, και βιοφυσικά πειράματα όσο και πειράματα *in vivo*.

Αρχικά χαρακτηρίστηκε η δομή της σαπερόνης μόνη της ή σε σύνδεση με την πρωτεΐνη EspA. Από το χαρακτηρισμό αυτό προέκυψε ότι η σαπερόνη σε μια προσπάθεια να αποτρέψει τον εαυτό της από μη ειδικές πρωτεϊνικές αλληλεπιδράσεις, αλληλεπιδρά με τον εαυτό της, μιμούμενη τον τρόπο που θα αλληλεπιδρούσε με την πρωτεΐνη EspA. Αυτό έχει σαν αποτέλεσμα, να παίρνει μια δομή στο χώρο σχεδόν όμοια με αυτή που έχει όταν βρίσκεται σε σύνδεση με την εκκριτική πρωτεΐνη EspA. Η μεγάλη διαφορά των δυο αυτών δομών είναι ότι όταν η σαπερόνη βρίσκεται σε σύνδεση με τον εαυτό της, το ομοδιμερές που προκύπτει έχει μια πιο χαλαρή δέσμευση και είναι μερικώς αναδιπλωμένο. Αυτό οφείλεται σε μη ευνοϊκές αλληλεπιδράσεις μεταξύ των δυο μορίων της σαπερόνης. Αποτέλεσμα αυτής της

χαλαρής σύνδεσης είναι το γεγονός ότι αμέσως μετά την εισαγωγή της πρωτεΐνης EspA στο διάλυμα, το ομο-διμερές της σαπερόνης να διασπάται και ένα σταθερό και καλά αναδιπλωμένο ετερο-διμερές δημιουργείται μεταξύ της σαπερόνης CesAB και της εκκρινόμενης πρωτεΐνης EspA, με μοριακή αναλογία 1:1.

Επιπλέον, δείχθηκε ότι συγκεκριμένες αλλαγές στη στερεο-διαμόρφωση της σαπερόνης CesAB που προκύπτουν μετά από την πρόσδεση της πρωτεΐνης EspA, οδηγούν στη δημιουργία και έκθεση ενός σήματος στόχευσης στην ATPαση του συστήματος, την πρωτεΐνη EscN.

Συμπερασματικά, από τις δυο αυτές μελέτες προκύπτει ένας μηχανισμός κατά τον οποίο αρχικά η σαπερόνη «αυτορυθμίζεται» ώστε να αποτρέπει μη ειδικές αλληλεπιδράσεις στο κυτταρόπλασμα. Στη συνέχεια, αφού αλληλεπιδράσει με το σωστό πρωτεϊνικό μόριο, την εκκρινόμενη πρωτεΐνη EspA, εκθέτει ένα σήμα στόχευσης ώστε να μπορέσει να αναγνωριστεί και να προσδεθεί το σύμπλοκο στην ATPαση του συστήματος. Η αλληλεπίδραση αυτή ρυθμίζεται με ένα μηχανισμό μετάβασης από μια μη αναδιπλωμένη κατάσταση με μια καλά αναδιπλωμένη κατάσταση (disorder-to-order state), και εξαρτάται αποκλειστικά από την πρωτεΐνη EspA.

Τέλος, για τη διαλεύκανση του μηχανισμού στόχευσης των πρωτεϊνών στον πόρο μετατόπισης του συστήματος, απομονώθηκε το σύστημα και δημιουργήθηκε μια πειραματική διαδικασία κατά την οποία μπορούσαμε να μελετήσουμε την αλληλεπίδραση ή μη πρωτεϊνικών μορίων με τη μεμβράνη του βακτηρίου, *in vitro*.

Κατά τη διαδικασία αυτή, μελετήσαμε διαφορετικά πρωτεϊνικά μόρια της σαπερόνης CesAB, αγρίου τύπου ή μεταλλάγματα αυτής, ως προς την ικανότητά τους να προσδένονται στη μεμβράνη παρουσία ή απουσία της πρωτεΐνης EspA. Από την ανάλυση αυτή, προέκυψε ότι για την πρόσδεση του πρωτεϊνικού συμπλόκου στην μεμβράνη, απαραίτητο είναι το καρβοξυτελικό τμήμα της σαπερόνης CesAB. Επιπλέον, η πρόσδεση αυτή γίνεται μόνο παρουσία της εκκρινόμενης πρωτεΐνης EspA, αλλά όχι στην ATPαση του συστήματος, EscN. Η αλληλεπίδραση συμβαίνει με κάποιον άλλο πρωτεϊνικό υποδοχέα του συστήματος στον πόρο εξόδου, ενδεχομένως στην πρωτεΐνη EscU ή/ και στην EscV.

Συμπερασματικά, αναφορικά με τη διαδικασία στόχευσης των πρωτεϊνών στη μεμβράνη του βακτηρίου, με στόχο την έξοδο από αυτό, προτείνουμε το μοντέλο δυο φάσεων (two-step model). Κατά την πρώτη φάση, το πρωτεϊνικό σύμπλοκο, CesAB-

EspA μεταφέρεται στη μεμβράνη του βακτηρίου και αλληλεπιδρά με τον πρωτεϊνικό υποδοχέα στην κυτταροπλασματική πλευρά της εσωτερικής μεμβράνης, στον πόρο μετατόπισης του συστήματος. Για την αλληλεπίδραση αυτή χρησιμοποιείται το σήμα στόχευσης στο καρβοξυτελικό άκρο της σαπερόνης CesAB. Η πρόσδεση αυτή του συμπλόκου στον πόρο μετατόπισης, έχει σαν αποτέλεσμα να έρχεται σε κοντινή απόσταση η ΑΤΡαση του συστήματος, η πρωτεΐνη EscN και να αλληλεπιδρά με το κεντρικό σώμα της σαπερόνης, στο οποίο βρίσκεται το δεύτερο σήμα στόχευσης (δεύτερη φάση).

Publications derived from this thesis

- "*Structural instability tuning as a regulatory mechanism in protein-protein interactions*."
  Chen, L., Balabanidou, V., Remeta, D.P. Minetti, C., Portaliou, A.G**.,** Economou, A. and Kalodimos, C.G. Molecular Cell 44, 734-744
  (Thesis' Chapter 3)
- «*Substrate-induced structural transition on chaperones encodes targeting signal in type III secretion*» ,
  Chen, L., Ai, X., Portaliou, A G., Economou, A., and Kalodimos, C.G. Cell Rep. 2013 May 30;3(5):1754.
  (Thesis' Chapter 4)
- «*Chaperone-mediated membrane targeting during Type III protein secretion*"
  A.G. Portaliou, V. Balabanidou, K. Tsolis, M. Aivaliotis, M. Loos, S. Karamanou, C. Kalodimos and A. Economou (in preparation)
  (Thesis' Chapter 5)
- "*Dissecting Type III Protein Secretion Mechanism in Enteropathogenic E. coli by Dynamic Complexome and Secretome Analysis*."
  M. Aivaliotis, A.G. Portaliou, V. Balabanidou, N. Kountourakis, G. Orfanoudaki, S. Karamanou, A. Enonomou (in preparation)
  (Thesis' Chapter 2)

- *"Type III Secretion System: building and operating a remarkable nanomachine"*

  A.G. Portaliou, A. Economou, Review Article (submitted**)**

1. Chapter: Introduction

In the bacterial cytosol more than 4,500 proteins are being synthesized in the ribosome, from which about 500 of them or more need to be embedded at the membrane, secreted to the periplasm, or to the external milieu [1]. Protein transportation into or through the two lipid bilayers is a challenging procedure. Taking under consideration that the plethora of proteins are huge macromolecules, mainly hydrophobic, their translocation through the solid hydrophilic environment of the membranes, that was evolved to keep cells intact and impermeable, sounds quite impossible. Having in mind that a typical bacterium lives for about 30-45 minutes it is of high importance to evolve ways to mediate protein translocation and secretion fast and efficient. On the other hand, due to the fact that protein secretion is an energy-consuming process the regulation and the proper function of it are important. For these reasons, only in bacteria, natural selection has given rise to 16 different protein export apparatuses indicating how important protein secretion is (Figure 1-1) [2]. Although, only one protein translocation system is essential to all facets of life, the Sec system [3], all the secretion systems have been evolved to serve specific processes when it is necessary, during bacterial growth. In many different cellular pathways, such as membrane biogenesis, cell motility and pathogenesis, protein translocation and secretion play a crucial role or it is even essential for them to occur [2]. Due to the high necessity of protein secretion for the mediation of many cellular processes, the understanding of the molecular basis of this procedure is of high importance, in order to elucidate main cellular pathways.

A protein secretion system that is very common in Gram negative bacterial pathogens and is essential for their pathogenicity is the Type III secretion System (T3SS, hereafter) [4]. Determination of how the system functions and is regulated, is essential so to elucidate the molecular basis of pathogenesis from these bacteria.

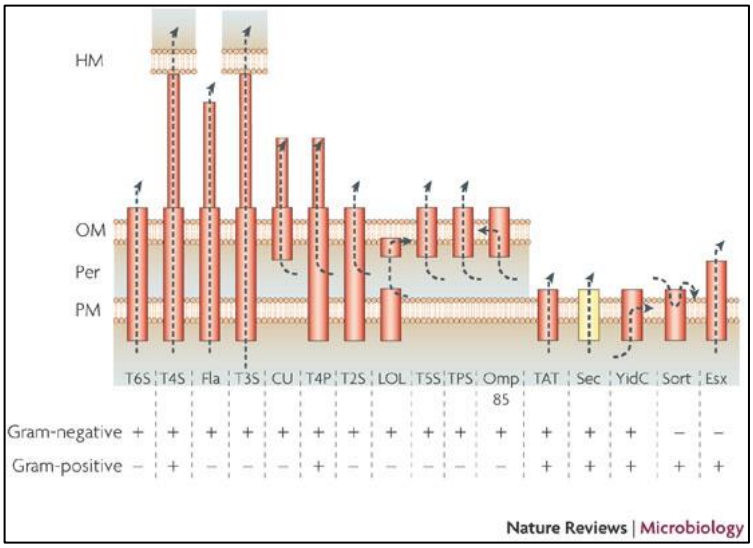

Figure 1-1: Simplified schematic representation of the protein export apparatuses found in bacteria. Translocation systems in bacteria are used for protein export, protein secretion and protein localization at the membrane.

Enteropathogenic *Escherichia coli* (EPEC)

EPEC and pathogenesis

T3SS is a widespread secretion system found in bacterial pathogens like *Yersinia, Salmonella,* Enteropathogenic *E.coli* (EPEC) and is responsible for secreting proteins into the host cell, causing bacterial diarrhea, which sometimes is lethal for the infected organism [4].

EPEC is a Gram negative bacterium that infects human intestinal epithelium causing diarrheal disease, first discovered in early 40's [5] . Since then, infections caused by EPEC, are very common in infants, under the age of two years. It is responsible for many diarrhea incidents in schools and hospitals. Although EPEC infections are generally treatable with antibiotics, in some cases the symptoms are very heavy and can last for a long period of time, or they are so severe that can be lethal. Especially in the developing world, EPEC infections are a daily phenomenon that leads children to death, ranking the EPEC infection as the fifth death-cause worldwide [6].

During infection from EPEC, bacteria are attached to the host cell at the plasma membrane and secrete the effector proteins directly from the bacterial cytoplasm into the host cell. Proteins that are secreted from EPEC interfere in various essential for viability cellular processes resulting cell death. The significant feature of EPEC infection is the Attaching and Effacing lesions (A/E lesions) detected in the destroyed tissues after biopsies of the small intestine from infected patients (Figure 1-2). Infection from EPEC is followed by severe diarrhea, high fever and vomiting which can be treated with antibiotics [7]–[9].

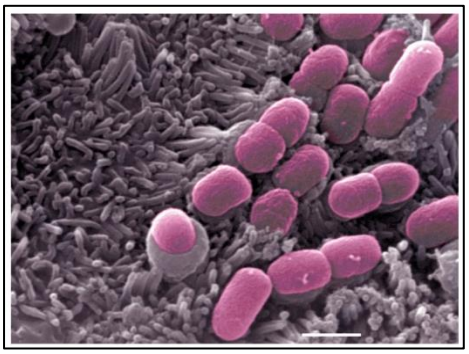

Figure 1-2: **Small intestine infected from EPEC**. After biopsy of the destroyed tissue A/E lesions that have been formed can be detected and are distinct characteristic for EPEC infection. Image was taken from Dr. St. Schuller, University of East Anglia (UEA)

Attaching and Effacing Infection

Locus of Enterocyte Effacement, LEE locus

In contrast with the common *E. coli* strains that exist naturally at the human intestine, EPEC pathogens contain at their genome specific genes that encode the proteins related to the pathogenesis of the bacteria. All the genes that are responsible for the formation of A/E lesions are located in a special genetic locus on the bacterial chromosome. This locus is called Locus of Enterocyte Effacement (LEE) and it has been identified, characterized and completely sequenced from the human EPEC strain E2348/69. All the different EPEC pathogens from dogs to humans share the same LEE locus as recently revealed from comparative genomic analysis [10]. The LEE locus is 35,5 Kbp long and all the genes are clustered into 5 operons. These operons consist of genes coding for: a type III secretion system (genes esc and sep), the translocated intimin receptor (gene tir), the outer membrane protein intimin (gene eae) and the *E. coli* secreted proteins EspA, EspB, and EspD (genes esp) [11]. Apart from the LEE genes, there are some more genes that encode proteins that are being secreted

through T3SS, and are related to the infection procedure, these proteins are called Non-LEE effectors [12], [13].

EPEC localized adherence on the host cell

EPEC infection is a very complicated procedure and undergoes sophisticated regulation. Although, in general this procedure can be discriminated in three phases, these steps are not very distinct in real life.

During the first step, bacteria cluster around the host cell forming micro-colonies. This micro-colony formation follows a specific pattern and is essential for the pathogenicity of the bacteria. Bacteria that fail to form micro-colonies on the host cell, fail to form functional T3SS resulting no infection. After observation of infected cells or tissues it has been determined that around 35 bacteria are clustered per colony, and 5-6 colonies are detected per host cell. The localized adherence from EPEC depends on different environmental parameters, like CO_2 concentration, temperature, and glucose concentration [14], [15].

The Bundle forming pilus (BFP pilus) is an adhesin associated with the initial stages of adherence of EPEC to epithelial cells. BFP is encoded by the *bfp* operon located in plasmid EAF, present only in typical EPEC isolates. However, strains that lack pilus formation can still be found attached on the host cells, although the colonies formed are smaller and the A/E lesions fewer [16], [17].

EPEC Secreted proteins (Esps)

During the second phase of EPEC infection, the EPEC secreted proteins (Esps, or translocators) are being secreted. Esp proteins are proteins that are being expressed from the 4^{th} LEE operon and are the first proteins secreted at the external milieu in order to form the outer structure of the T3SS. Specifically, EspA protein due to self-oligomerization forms an external filamentous tube, up to 25nm long [18], [19]. On top of the EspA filament, translocator proteins EspB and EspD are attached. The formation of this filament structure connects the bacterial membrane with the host plasma membrane, where the translocator protein EspB and EspD are inserted into the plasma membrane so to form a pore-like structure and it will connect the bacterial cytoplasm with the eukaryotic one (Figure 1-3) [20]. This needle-like structure enables the bacteria to secrete the effector proteins directly to the host cell cytoplasm in one step, which makes these proteins essential for EPEC pathogenesis [21], [22].

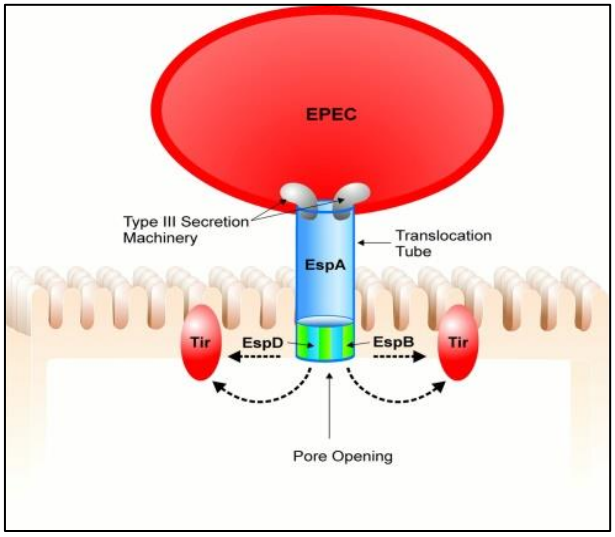

Figure 1-3: **Translocation of EPEC secreted proteins.** They are secreted through T3SS and once tranclocated outside of the bacteria, EspA forms a filamentous tube, while EspB and EspD are inserted into the plasma membrane to form a pore like structure. This structure will enable the bacteria to secrete the effectors directly in the host cell cytoplasm. Picture from Vallance B.A and Finlay, "*Exploitation of host cells by Enteropathogenic E. coli*", PNAs, 97(16):8799-806 (2000)

Close adherence and pedestal formation of A/E lesions

The third and last phase of the A/E lesions is characterized from close adherence of the bacteria on the host cell and the formation of the actin pedestals. The third step is signaled by the secretion of Tir protein (translocator intimin receptor) through T3SS [15]. Protein Tir is being translocated through the T3SS needle and is embedded to the eukaryotic membrane. Upon phosphorylation from Kinase A, Tir forms dimers at the membrane where it can interact with the intimin protein on the bacterial surface [23]. The association between the intimin and its receptor leads to the anchoring of the bacteria to the host cell, leaving a distance in between them approximately 10nm[24] .

Once the Tir-intimin protein complex is formed, a series of cytoskeleton re-arrangements take place into the host cytoplasm in order to form the typical actin pedestals beneath the bound bacteria. The formation of the actin pedestals is a Tir-mediated procedure, where upon Tir secretion and binding to intimin, actin polymerization process is being transferred to the membrane of the host [15], [24]. At that point, Tir protein binds Nck adaptor proteins, which in turn recruit and activate N-WASP, a member of the Wiskott-Aldrich syndrome protein-family. N-WASP afterwards, activates the Arp2/3 complex so to promote actin polymerization, at the membrane where EPEC have been attached (Figure 1-4) [25].

The formation of actin pedestals, upon EPEC infection, is so typical, that is used as an *in vitro* assay to characterize bacterial strains as far as function of T3SS is

concerned, by observing the formation or not of the actin pedestals using fluorescence microscopy [26].

Once the pedestals are formed, the effector proteins (LEE- or NON LEE) are being secreted through the T3SS. Effectors from EPEC are characterized by multifunctional nature and their ability to participate in redundant, synergistic or antagonistic relationships, acting in a co-ordinated spatial and temporal manner on different host organelles and cellular pathways during infection, resulting in cell lysis. Many of these proteins have been characterized and it is known that interfere in a plethora of essential cellular pathways, like with the inflammatory signaling pathways, the phagocytosis pathway, and Golgi, ER and mitochondria function is also inhibited (Figure 1-5) [13], [27], [28].

Figure 1-5 EPEC attached to the host cell membrane. The typical actin pedestals have been formed underneath the bacteria. Picture was taken from Finlay lab, Michael Smith laboratories

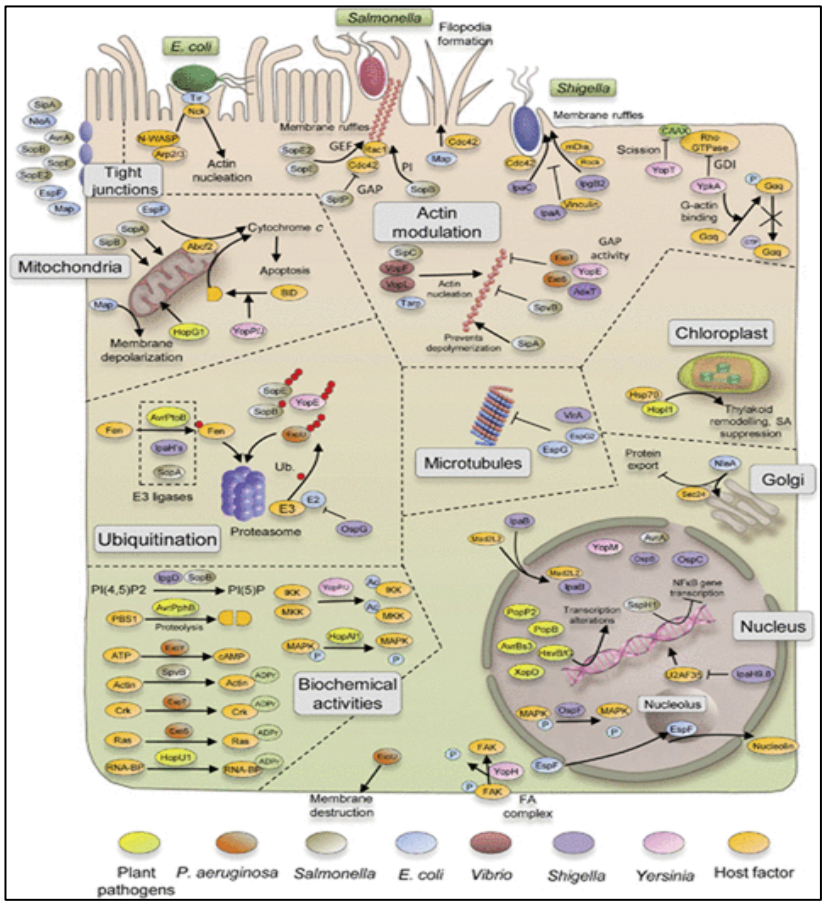

Figure 1-4 : The complexity of effector's function. The multifunctional and overlapping properties of the T3SS effectors are depicted here by grouping effector functions together. Picture was taken from Paul Dean, *"Functional domains and motifs of bacterial Type III effector proteins and their in infection"*, Review article, FEMS Microbiol Rev 35 (2011) 1100–1125

Type III secretion system in EPEC

General structural characteristics

The Type III secretion system (T3SS) forms a macromolecular syringe –like structure nanomachine, used by Gram negative bacteria to transfer or to "inject" proteins into the host cell, spanning 3 membranes, two bacterial and one eukaryotic. Due to the fact that more than hundred copies of up to twenty different proteins need to be co-ordinated in order to be assembled into a multi-MDa transmembrane complex, the T3SS is one of the most complex known bacterial systems [29].

Overall the structure of the system can be divided in three distinct parts, the needle and the filament or the tip complex, the basal body and the Cytosolic ring. The needle with the basal body and the cytoplasmic ring is often termed as the injectisome (Figure 1-6). The formation of such machinery is a complicated procedure and depends on precise orchestration [30].

The T3SS injectisome- Basal body composition

The availability of high-resolution structures of several domains of T3SS components [31]–[34], in combination with electron density maps obtained from cryo-EM analysis, has given the opportunity to gain some structural insight of the T3SS assembly [35]–[37]. The basal body consists of two membrane ring-like structures. The outer membrane (OM) ring extends into the periplasm and is made of 12–15 copies of a protein from the secretin family (EscC) [38]. The IM ring, also called MS ring (membrane and supramembrane) spans the IM of the bacterium and consists of a lipoprotein that constitutes the inner side of the ring (EscJ) [30], [31], and a transmembrane protein composing the outside (EscD). EscD also connects the two membrane rings through its periplasmic domain. The MS ring has been proposed to have a 12- or 24-fold symmetry [37], [39], [40].

Five highly conserved IM proteins EscR, EscS, EscT, EscU and EscV form what is called the export apparatus. These proteins span the IM with up to eight transmembrane domains and are essential for secretion [29], [32]. They are proposed to be located within the membrane patch surrounded by the MS ring machinery.

While the three components of the apparatus EscRTS consist mainly of transmembrane or periplasmic domains, each of the two major proteins EscU and EscV contain a large cytosolic C-terminal domain [41]. EscU is being auto-cleaved and somehow regulates protein secretion [32], [42], and EscV forms a cirlular nonamer [33], [43]. Due to these results they are thought to be either the targeting platform for secretory proteins or play a critical role at the secretion switch process [36], [44], [45].

The T3SS injectisome- Needle-filament composition

The extracellular needle is generated by helical polymerization of a small hairpin protein (EscF) and is possibly anchored to the base by the alpha-helical inner rod protein EscI [46], [47]. In attaching and effacing animal pathogens such as EPEC and EHEC, the needle is surrounded from a hydrophobic protein forming a pilus or filament, EspA [48], [49]. EspA after self-polymerization forms the filament which is extended above the needle and its length is regulated by a molecular ruler protein, EscP [18], [50], [51]. Finally, two hydrophilic translocator proteins, EspB and EspD are anchored on top of the EspA-filament and are inserted to the membrane of the host, where upon oligomerization they form the pore, through which effector proteins will be inserted to the host cytoplasm.

The T3SS injectisome- cytoplasmic ring (C-ring)

The C-ring consists of five essential for the secretion through T3SS cytosolic proteins, which are peripherally associated with the basal body of the system at the inner membrane. Protein SepQ or EscQ, forms again a ring-like structure that is anchored to the EscD protein [44], [52]. SepQ protein, in complex with the gatekeeper protein, SepL, has been considered to serve as the sorting platform that regulates the hierarchy of protein secretion [53], [54].

The ATPase of the system, protein EscN, is also essential for protein secretion and is thought to be the energy producer so that the secretory proteins will be released from their chaperones and become unfolded so to be tranclocated through the channel [55], [56]. In order for EscN, the ATPase to be localized and stabilized at the membrane two proteins are needed. First, the stator protein EscL that is thought to act

as a chaperone of the ATPase in the cytoplasm and escorts it to the membrane. Once the complex is at the membrane, it is attached to the C-ring, by interactions occur between EscL and SepQ [36], [57]. The second protein is the stalk protein EscO, which interacts with the ATPase and connects the ATPase complex to the major export apparatus protein (EscV). Furthermore, EscO promotes the oligomerization of the ATPase and stimulates its enzymatic activity [36], [58], [59]. For the EscN ATPase, the localization at the membrane and the regulation mechanism of its activity, more details can be found in the sub-chapter "Energy requirements for protein secretion".

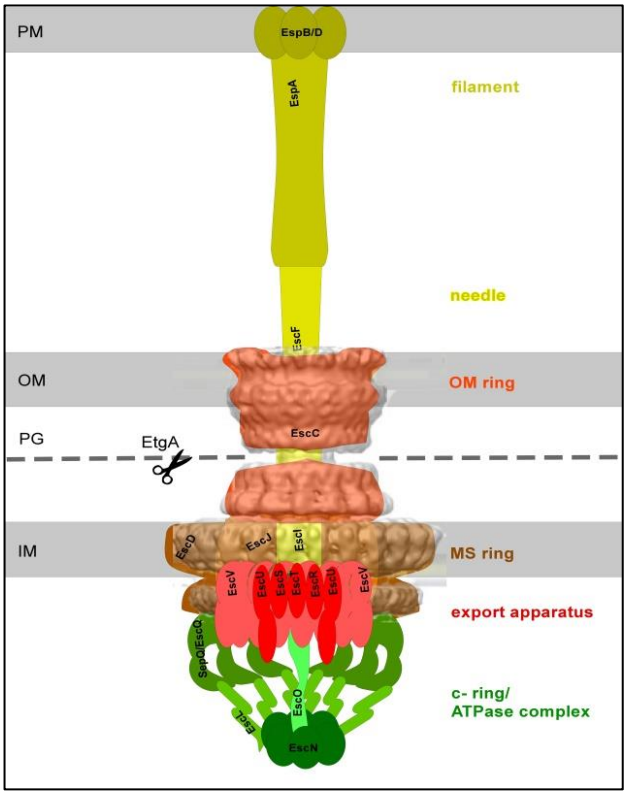

Figure 1-6 : Schematic representation of T3SS injectisome from EPEC. Protein components of needle/ filament, basal body and C-ring are shown. PM=plasma membrane of host cell,, OM= outer membrane, PG=peptidoglycan layer, IM= inner membrane of the bacterium

Similarities between T3SS and flagellum

Since middle 90's, it has been demonstrated from genetic studies and high resolution EM that the T3SS injectisome shares similar overall structure with the flagellum [35], [60], [61]. The flagellum is an organelle used for motility and consists of the basal body, the hook and the filament. It is also used to secrete proteins from the bacterial cytoplasm to the external milieu, mostly filament or hook components

though [30]. Due to the high structural similarity and same genetic origin, it is very common to refer to flagellum and T3SS as two highly homologous families: the flagellar T3SS which drives cell motility, and the non-flagellar T3SS that injects effector proteins into eukaryotic host cells. In this thesis, however, the term T3SS refers to the pathogenic system.

Electron microscopy studies, verified the comparative sequence analysis that have revealed high homology between the basic structural components of the flagellum and the T3SS. Both systems consist of ring-like structures at the OM and IM that enclose an export apparatus. The proteins that form the OM rings share similar structure and symmetry. However, in the flagellum there are no secretins, thus a lipoprotein forms a ring that is connected to the peptidoglycan ring. These two rings (L and P) serve for the rotation of the hook. In both cases the export apparatus is almost identical and the proteins that it is consisted of share high homology among species. Due to this reason, it is assumed that in both cases the export apparatus share the same function as far as targeting and secretion regulation is concerned. Moreover, the IM ring is connected in both cases with the cytoplasmic ring, which is also where a homologous ATPase in complex with its partners is anchored [30], [35], [62].

Moreover, although the needle protein from the T3SS share almost no sequence similarity with the respective one in flagellum, the needle-like structure, which is termed hook in the flagellum, shares the same helical structure and follows the same assembly process in both cases [47], [63].

Additionally, the filament protein EspA has a similar overall helical structure and composes a tube-like machinery with an inside diameter around 2.5 nm, like the flagellum filament protein, FliC. However, the length and external diameter of these two filaments are different, which could be due to different in overall protein size (EspA is 192 residues while FliC is 494) [64], [65]. Regarding the localization of the ATPase complex and the regulation mechanism of the ATPase activity, more details can be found in the sub-chapter 1.8, Energy requirements for protein secretion.

Collectively, although the structures and symmetries of some components of the T3SS have diversified to match requirements of different species, recent genetic, molecular and structural studies demonstrate that these systems are built by arranging homologous protein assemblies (Figure 1-7), and share same regulation strategies [62], [66], [67]. For these reasons, it is very common in the field that new

experimental findings related to structure or function of the flagellum to be used also for the T3SS and vice versa.

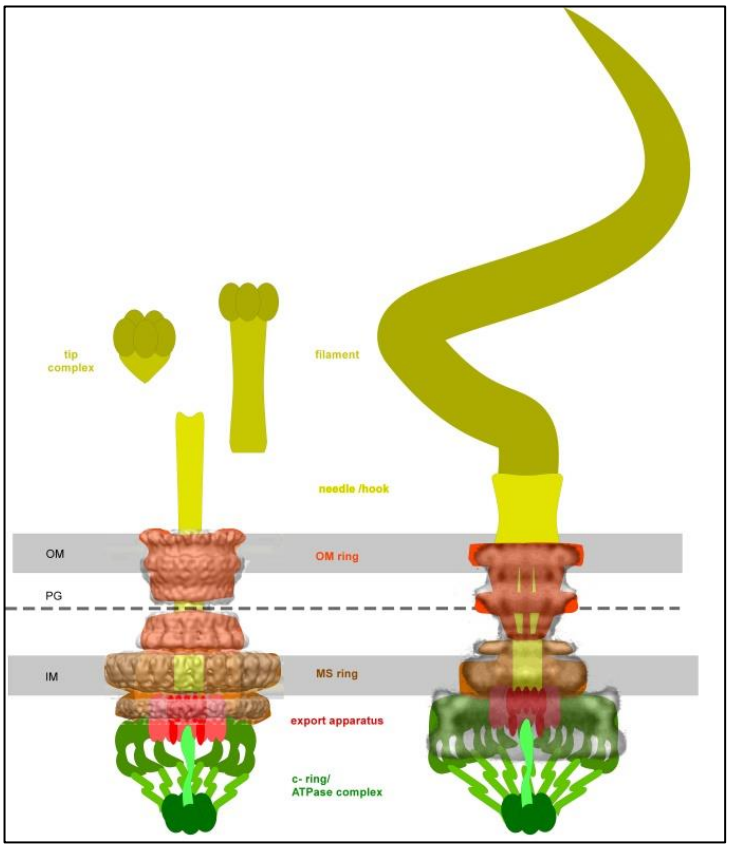

Figure 1-7 : Schematic representation of the structures of T3SS (left) and flagella (right). On the background of each cartoon cryo-EM sub-tomograms for each one are being presented. Common colors indicate common elements of common or similar proteins/structures.

Biogenesis of the T3SS basal body

The transmebrane proteins that form the basal body structure of the injectisome are localized to the inner membrane or translocated to the peripasm through the Sec system, once their genes are expressed. It has been demonstrated in various bacteria with protein-protein interactions studies, that in order to form a stable structure and the two rings to be connected (OM and MS) all three base components, EscJ, EscC, EscD are required [68]. However there is a controversy in the field regarding the order of ring-like structure formation. On one hand, it is believed that the injectisome assembly is initiated at the IM, like in flagellum, and afterwards, the MS ring will be attached to the secretin ring in the OM [29], [69]. On the other hand, the outside-in assembly has been demonstrated. According to it, the assembly starts from the stable

secretin ring in the OM and progressively via the outer membrane the inner MS ring components YscD and YscJ are being attached [39]. In both cases the formation of the secretin ring assembles efficiently in the absence of the MS ring components and vice versa.

As the secretin ring bridges the largest part of the periplasm, an outside-in assembly order would accomplish the necessary penetration of the peptidoglycan layer in the first assembly step, which could facilitate the attachment of subsequent components [40],[52].

The export apparatus, which is formed from proteins EscR, EscT, EscS, EscU and EscV, is localized at the inner membrane and is surrounded by the MS rings proteins EscJ and EscD [70], [71]. Combination of complex purification and EM analysis in *Salmonella* sp. and *Yersinia* sp. have demonstrated that the export apparatus components can form a complex on their own and moreover, this complex can be divided in two sub-complexes. One sub-complex of the minor export apparatus proteins EscR,S,T,U and one formed after oligomerization of protein EscV [39], [70]. It has been demonstrated though that in order for the major export component to be localized at the membrane (protein EscV) the minor export apparatus needs to be there, independent from the existence of the IM rings [33]. These results demonstrate that the assembly of the export apparatus *per se* is independent from the formation of the OM and IM rings, indicating that the outside-in assembly mechanism cannot be the only case. It is more possible that two different assembly pathways are followed for the formation of the basal body and the export apparatus and afterwards they are attached possibly by electrostatic interactions that bridge them together [29], [67].

As far as the cytoplasmic ring is concerned, data have indicated that it can assemble independent of the existence of the export apparatus, but the IM ring is important. It has been demonstrated that protein SepQ/EscQ interacts with the IM ring component, EscD upon phosphorylation, and this is how it is stabilized at the cytoplasmic domain of the inner membrane [52]. However, the c-ring has never been visualized, due to the fact that is easily lost during purification techniques. Thus, this also implies that it is not needed for the assembly of the basal body apparatus.

The ATPase complex is also being lost during purification, however after *in vivo* analysis it has been shown to interact with the C-ring and stabilized to it by interactions between the C-ring and the stalk protein EscL [33], [36], [39]. Overall,

the cytosolic components (C-ring and ATPase complex) can assemble independently, and are possible dock in a downstream event during injectisome formation. For this docking step, the IM ring is important and not the export apparatus (Figure 1-8).

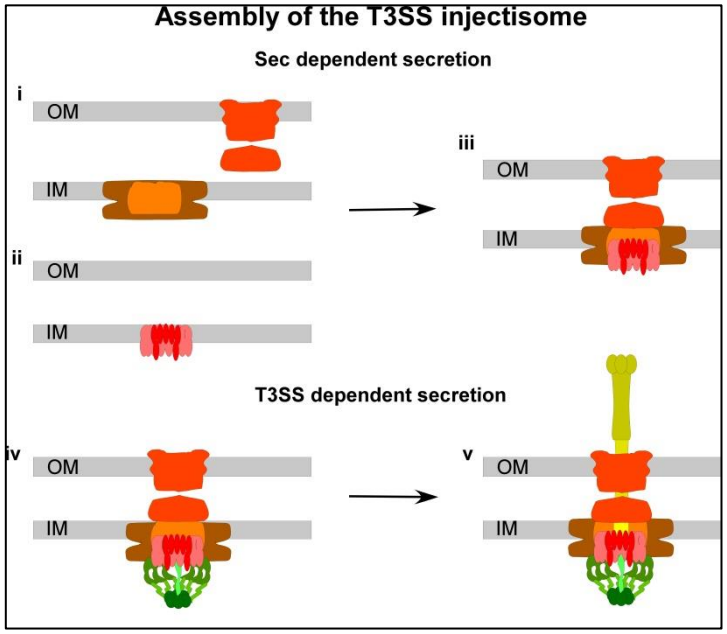

Figure 1-8: **Bipolar model of injectisomme assembly.** The IM and OM rings are formed and bridged together. Independently, the export apparatus is formed. Once the basal body of the injectisome is attached, the C-ring and ATPase complex are associated, probably by interacting with the IM ring.

Assembly and Regulation of the T3SS needle and filament

It is known for a long time that overall transcription levels of the T3SS genes are compromised; expression of the T3SS genes is up-regulated from environmental conditions, such as pH, temperature and contact to the host cell. Nevertheless, all system components are likely to be present at the same time, and the assembly order will largely depend on affinities and kinetics of protein–protein interactions [72]. As a result, the system needs to undergo sophisticated regulation, so to prevent unspecific protein secretion and to maintain the hierarchy of the process according to which the needle and filament proteins are secreted first; afterwards the translocators and finally the effector proteins are being secreted. The proteins forming the export apparatus at the IM and components of the C-ring and the ATPase complex are thought to be responsible for substrate targeting, unfolding and finally export. However, these proteins are easily lost during the classical purification of the machinery used for electron microscopic studies [33], [37], [70]. Moreover, *in vivo* analysis, co-purification experiments and protein-protein interaction studies could be misleading,

regarding the mechanism followed for secretion regulation, membrane targeting and protein export through the apparatus of the secretory proteins. As a result, although the central role in substrate export has been attributed to these proteins, very little is known about their interactions and how they function within the injectisome.

A well-studied protein from the export apparatus that has been attributed the role of secretion switch protein is EscU. EscU protein shares high sequence and structural homology among different bacteria. EscU possess four transmembrane helices and a long cytoplasmic domain that undergoes auto-cleavage and is suggested to be the mechanism used from the system to switch from tranclocator to effector protein secretion. This cleavage has been proposed to generate conformational changes to the export apparatus and modifications to the local electrostatic surface, preventing or advocating T3SS-related components to bind [32], [34], [42]. However, the molecular mechanism of this switch is not clear yet.

It has been demonstrated that the inner-rod protein, EscI interacts with the inner-membrane protein EscU, regardless of the EscU cleavage state. This allows secretion of EscI together with the needle protein EscF. It has been proposed that as secretion of the early substrates proceeds, the inner rod and the needle structure are assembled allowing EscI to interact with EscC at the outer membrane ring. This interaction, in combination to reduced levels of needle protein accumulated at the export apparatus, led to EscU auto-cleavage, resulting in enhanced affinity for the late effectors to be targeted [50], [73], [74].

Another model proposed regarding the mechanism that leads to EscU auto-cleavage regulation compromises the molecular ruler protein, EscP. The needle length is controlled from a protein that is partially secreted and is assumed to “measure” the length of the needle and filament structure, like a ruler or a tape. Protein EscP is proposed to interact with EscU with its C-terminal domain and the increasing needle with its N-terminal. Once the needle/filament structure reaches the correct length, presumably the extended EscP somehow promotes the auto-cleavage of the EscU [18], [75].

However, the fact that EscU non-cleavable mutants abolish secretion of T3SS for both translocators and effectors, and that purified EscU can cleave itself, without the presence of any interacting partners pin-point that the cleavage itself is not essential for secretion, but probably the conformational changes and the electrostatic surface

created upon cleavage is essential for secretion [18], [32], [42]. Thus, this model needs to be proven.

Apart from protein EscU and its auto-cleavage mechanism, there are more candidates that have been attributed as secretion regulation factors. Protein EscV, which forms a dodecameric ring and embraces the export apparatus, is a recently identified one. It has been recently shown that protein EscV can mediate protein secretion by interacting with chaperone-secretory protein complexes with its cytoplasmic C terminal domain. It has been proposed that the secretory protein-chaperone complexes are targeted to the ATPase of the system [55], [56]. After this first docking step, the secretory protein on its own, or still in complex with its chaperone can interact with EscV. In this model, the binding affinities that the cytoplasmic domain of EscV has for each complex somehow regulate the order of secretion [36], [62], [67], [76]. This model is proposed for flagellum regulation, but it needs also to be proven for T3SS as well.

Finally, SepL gatekeeper and SepD protein regulate somehow the hierarchy of protein secretion. In the absence of the SepL and/or SepD proteins, translocator proteins are not secreted while the effector proteins are being over-secreted, indicating the necessity of them for translocators' secretion [42], [59]. The mechanism however, is another debate in the field and still needs to be elucidated. Some studies, propose that the gate-keeper proteins are localized at the export apparatus and/or the C-ring. There, they can either "capture" the chaperone/effector protein complexes preventing their further association with the translocation pore[31], [40], [41], or interact with the translocator proteins and act like a sorting platform promoting the latter secretion [40], [42]. Recent data signified the existence of a signal sequence on the translocator proteins, downstream their signal peptide which could be recognized from the gate-keeper [42]. Therefore, it's possible that the translocator secretion is being promoted by interacting with the SepL or/and SepD proteins; however this is a pathway that needs to be determined

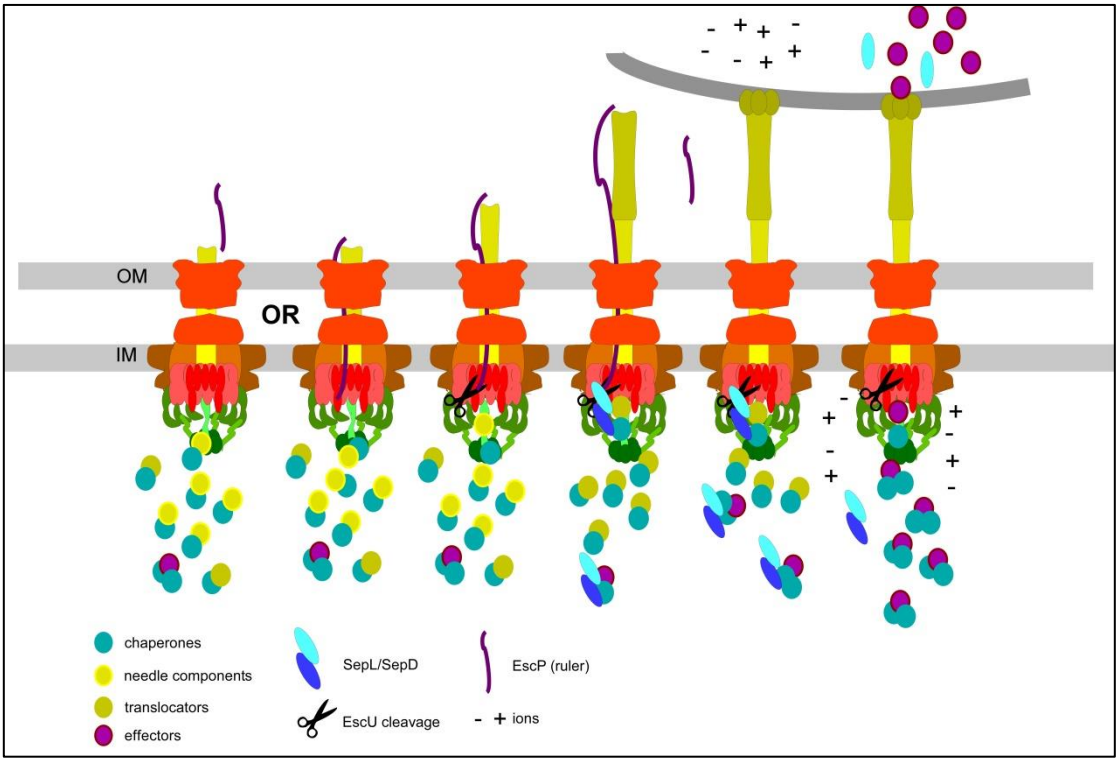

Figure 1-9: States of secretion and model of the events leading to substrate specificity switching. Secretion of early substrates leads to assembly of the needle filament until it reaches a specific length. Its length is controlled by the needle length regulator EscP, which is either secreted or anchored at the export apparatus. Once the needle/filament reaches the proper length, translocators are being secreted, upon EscU cleavage. The needle complex senses contact with the host cell membrane. The contact signal is transduced through the needle filament down to the cytoplasmic side of the base, where it leads to dislodging of the gatekeeper. This frees the way for secretion of late substrates and their subsequent injection into the host cell cytoplasm.

Chaperones mediate protein secretion

In addition to the secretion and translocation signal the secretory proteins through T3SS posse, several secreted proteins depend on cytoplasmic T3SS-chaperones for their efficient secretion. The main known role for the specialized chaperones of the system is to interact with the secretory proteins in the cytoplasm, upon expression, so to maintain them in a translocation competent state [48], [78], [79]. T3SS chaperones often interact as homo- or heterodimers with their cognate substrates and presumably promote the recognition of secreted proteins by components of the T3SS system [48], [49], [80].

Depending on their substrate specificities, T3SS chaperones have been categorized into different classes. Chaperones that are listed in Class I are divided in two sub-categories, class IA that are specific for one or several homologous effector proteins, while class IB that bind to different effectors with unrelated sequences [81].

Known class IB chaperones include many effector chaperones like CesT from EPEC [80]. Class I chaperones, are well studied and a great number of structures have solved. These chaperones are small molecules with basic features (pI 4-5) and their genes are almost always located next to the effectors' ones so to be expressed almost simultaneously [11]. They share an overall similar heart-shaped structure formed after association of two protomers that consists of a twisted β-sheet with two or three α helices [72] (Figure 10).

Class II and III chaperones interact with the needle or filament components and translocator proteins, respectively [79], [81], [82]. Translocator proteins have the tendency to self-associate and oligomerize, so the main role of class II chaperones in the bacterial cytosol is to prevent premature polymerization of the secretory proteins[48], [66], [78]. Chaperones of translocator proteins usually contain three tandem tetratricopeptide repeats (TPRs). TPR folds are characterized by two antipararrel α helices and are imperfect amino-acid repeats, also present in eukaryotic chaperones, that are often involved in protein-protein contacts, by recognition and binding of helical and stretched peptides [30], [82], [83]. Class II and III chaperones share the similar characteristics as far as structure and biochemical properties are concerned, with Class I (Figure 1-10).

A significant exception though is the chaperone CesAB of the filament protein EspA. CesAB is small molecule (13kDa) that it forms hodimers in solution, but in order to interact with the secretory protein EspA, the homodimer dissociates, so to form a heterodimer in a 1:1 molar ration with EspA. Apart from that, CesAB has pI is around 9.5 which is a quite uncommon biochemical property for a chaperone. Finally, and more interesting, although CesAB chaperone, is essential for EspA stability in solution and is not required for EspB translocator stability, but is essential for the secretion of both proteins. These specific biochemical and functional properties of CesAB chaperone should be further elucidated and perhaps CesAB should be classified in an another chaperone category [48], [55], [78].

In general, it is assumed that T3SS chaperones facilitate the binding of their cognate interaction partners to components of the secretion apparatus at the IM, such as the ATPase, or the IM components EscV or EscU. It has been hypothesized that the chaperones of the system facilitate the membrane targeting of the secretory protein or/and regulate the hierarchy of secretion by increasing the local concentrations of

secretion substrates at the base of the secretion apparatus or antagonize the same binding site in the export apparatus, thus promote their transport to the T3SS system, instead of the effector proteins [45], [55], [76], [80].

It has been proposed in many cases among different bacteria that chaperones facilitate an important role at the secretory protein docking procedure at the basal body of the injectisome, although the molecular mechanism behind the targeting process is not clear yet [45], [55], [56].

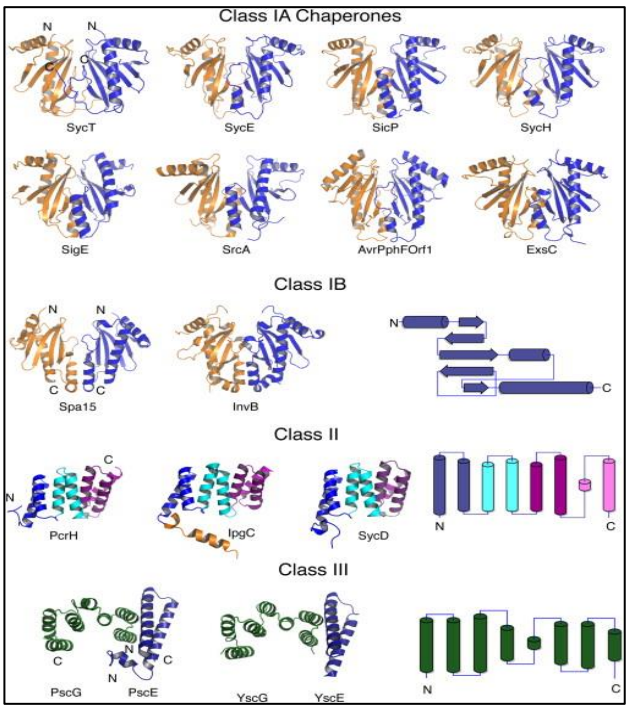

Figure 1-10: **A Gallery of T3SS Chaperones** Class IA and IB chaperones share a common overall heart-shaped structure, whereas class II and class III chaperones display TPR-like folds. In the latter class a smaller partner protein (blue) is required to stabilize the main chaperone (green). Depicted molecules in the gallery include SycT (2BSJ), SycE (1JYA), SicP (1JYO), SycH (1TTW), SigE (1K3S), SrcA, (3EPU), AvrPphF (1S28), ExsC (3KXY), Spa15 (1RY9), InvB (2FM8), PcrH (2XCB), IpgC (4GZ2), SycD (2VGX), PscG-PscE (2UWJ), and YscG-YscE (2P58). Figure was obtained from Izore et al, "*Biogenesis, Regulation, and targeting of the Type III secretion system"*, Review article, *Structure* vol.19, issue 5, 2011

Energy requirements for protein secretion

The export apparatus of EPEC T3SS is associated with a cytoplasmic ATPase, protein EscN. EscN, which is a member of the YscN protein family, forms homo-hexameric ring structures with an internal diameter of approximately 2.5 to 3 nm [32], [59], [84], [85]. However, it has been demonstrated that members of YscN family can form either homo-hexameric or dodecameric rings, like ATPase HrcN [85]. Oligomerization of the EscN ATPase leads to an increase of the ATPase activity, common characteristic to YscN family, which is assumed to provide the energy needed for the secretion process [58], [86]. Moreover, there is evidence that the

oligomerization procedure of ATPases can be induced upon binding of a T3SS chaperone, as shown for the multicargo T3SS chaperone SrcA from *Salmonella* sp, and the homologue from EPEC CesT [80], [87], [88]. Since the ATPases of T3SS can interact with secretory protein-chaperone complexes, they were proposed to be involved in T3SS substrate recognition [55]. It is believed that the ATPases of the system dissociate the secretory proteins from their cognate chaperones and contributes to the unfolding process of them prior to their entry into the secretion apparatus. This is probably important for efficient secretion, because the inner channel of the T3SS system has a diameter of 2 to 3 nm, which is too narrow for fully folded proteins to pass through [56].

Additionally, from crystal structure analysis of the ATPase EscN and the flagellar homologue, FliI, have been demonstrated structural similarity with the α/β subunits of F_oF_1-ATPases [32], [84]. F_oF_1-ATPases consist of a membrane-spanning F_o domain and a solvent-exposed F_1 domain that rotate in opposite directions. The F_1 domain is composed of a hexamer of α and β subunits arranged around a central stalk. A second peripheral stalk, which contains b and δ subunits, connects the F_o and F_1 domains [89]–[91]. After sequence and structure analysis, it has been shown that members of the YscL protein family (like protein EscL from EPEC) share sequence and structural homology with the protein component of the second stalk of the F_oF_1 ATPase complex. Proteins from YscL family can interact with the ATPase and are assumed to regulate both the oligomerization process and ATPase activity. It is assumed that protein EscL interacts with APTase EscN in the cytosol and prevents the premature oligomerization of the enzyme, so to avoid ATP hydrolysis, before docking of the enzyme to the translocation pore. Once the EscL-EscN complex is transferred to the bacterial membrane, EscN is stabilized by EscL interactions between EscN and SepQ, the basic component of the C ring [33], [57], [62], [92]. Moreover, similarities between the first stalk component and the stalk protein EscO have also been reported, and is assumed that it also somehow stabilizes the ATPase at the pore of the basal body of the system and regulates the ATPase hydrolysis of EscN [33], [36], [58] (Figure 1-11).

Conclusively, the docking of the ATPase and its enzymatic activity are important for T3SS, and undergo important regulation depending on protein-protein interactions.

However, it is probably not the only energy source of the T3SS protein secretion to occur. Experimental evidence suggests that protein secretion might be driven by the proton motive force (PMF) [93]. The PMF refers to the electrochemical potential difference of protons across a membrane and consists of the electrical potential difference (Δψ) and the proton concentration difference (ΔpH). PMF was shown to contribute to flagellar T3SS among different bacterial species, like *Salmonela* sp. or *Yersinia* sp., in the absence of the ATPase or its regulator protein [93]–[95]. It was therefore proposed that the PMF drives protein transport across both membranes, whereas the ATPase is required for the efficient initial docking of T3SS substrates to the secretion channel. In agreement with this assumption, recent publications revealed a contribution of FliJ protein to the export of flagellar T3SS substrates that probably depends on the interaction of FliJ (EscL homologue) with the cytoplasmic domain of the IM protein FlhA (EscV homologue). Additionally, the binding sites of FliJ in FlhA were shown to be required for the functioning of both proteins, and *vice versa*. The authors therefore proposed that FliJ alters the conformation of FlhA to activate Δψ-driven protein export [94], [95] (Figure 8). Although due to homology between the flagellum and the T3SS it has been hypothesized that PMF is also required for protein export through T3SS injectisome, there are no experimental data towards this direction, so this mechanism still needs to be proven for T3SS protein secretion.

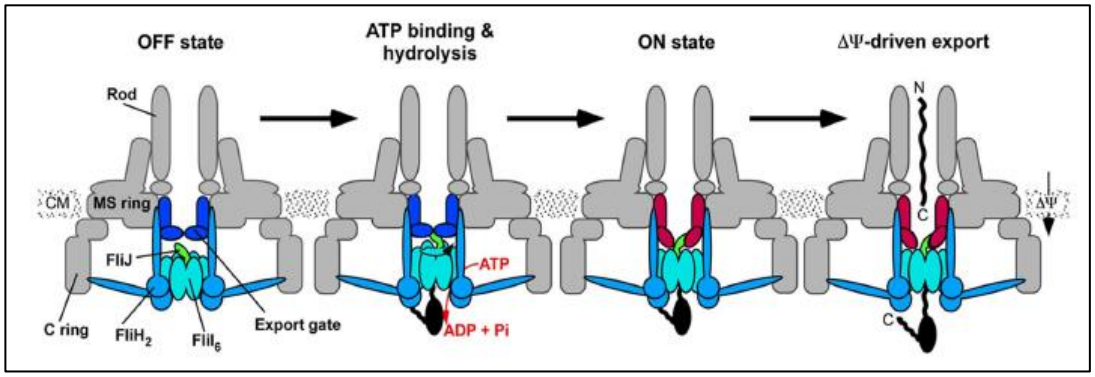

Figure 1-11: Energy requirements during flagellar protein export. ATP hydrolysis by the FliI6 ring (homologue to EscN) induces the FliJ rotation (EscL homologue) within the ring to cause a conformational change of the export gate so to activate it. The export gate then utilizes the membrane potential component (Δψ) of proton motive force across the cytoplasmic membrane to unfold and transport the substrates into the central channel. Figure was published in Minamino et al, "*The bacterial flagellar protein export apparatus processively transports proteins even with extremely infrequent ATP hydrolysis*", Scientific Reports 4, 7579,(2014)

2. Chapter: Determination of dynamic protein complexes formed during T3SS

The type III secretion system (T3SS) is a highly specialized bacterial protein secretory pathway. It plays an essential role in the pathogenesis of many Gram-negative bacteria including *Yersinia, Shigella, Salmonella, Bordetella, Pseudomonas*, and Enteropathogenic *E. coli* (EPEC) [82]. Although many studies have been published about the function of T3SS and its secreted effectors, the precise pathway proteins follow and their co-ordination in order to be secreted remain poorly understood. Very little is known about the regulation and hierarchy of secretion, the protein interactions that occur and the dynamic complexes that are formed from the cytosol to the membrane during secretion from T3SS.

In order to shed more light to the pathway the proteins follow in order to be secreted and the protein interactions that occur, we performed a comprehensive complexome analysis using Mass spectrometry (MS).

Identification of protein complexes using MS

Complexome analysis in wt EPEC as a function of time

In order to identify all the cytosolic protein complexes that are formed during protein secretion from T3SS, Enteropathogenic *E.coli* (EPEC) was used as a model organism. We performed a comprehensive complexome analysis using Size exclusion chromatography (SEC) and/or Native PAGE coupled with protein identification through high resolution MS.

In more detail, we cultured EPEC bacteria, under secretion permissive conditions, and collected culture samples as a function of time during bacterial growth. First, we have determined the time frame during bacterial growth where more proteins are being secreted and in the maximum quantity possible. Afterwards, we collected different samples before and after this time frame, during bacterial growth. From the collected samples, we separated the spare growth medium from the bacterial cells. The spare growth medium, in this case, contains the proteins that are being secreted

from the bacteria, which were also identified with MS, as a control of the secretion process.

The bacterial cells were lysed and the soluble fractions separated from the membrane ones, using ultracentrifugation. The soluble fractions, which in this case contain the majority of cytosolic proteins and the protein complexes that have been formed, were analysed using Native PAGE and SEC. The protein bands that were separated using Native PAGE, were stained with blue silver, excised from the gel and further processed by trypsin following in gel digestion protocol. As far as the SEC is concerned, again the same procedure was followed, and the fractions were collected and in solution digestion using trypsin was performed (Figure 2-1a, b).

All the samples were analysed using nano-LC MS/MS (LTQ Orbitrap-XL, Thermo Scientific). At least three biological and technical repeats of these procedures were performed so to validate the reproducibility of our technique and verify the identification of the proteins.

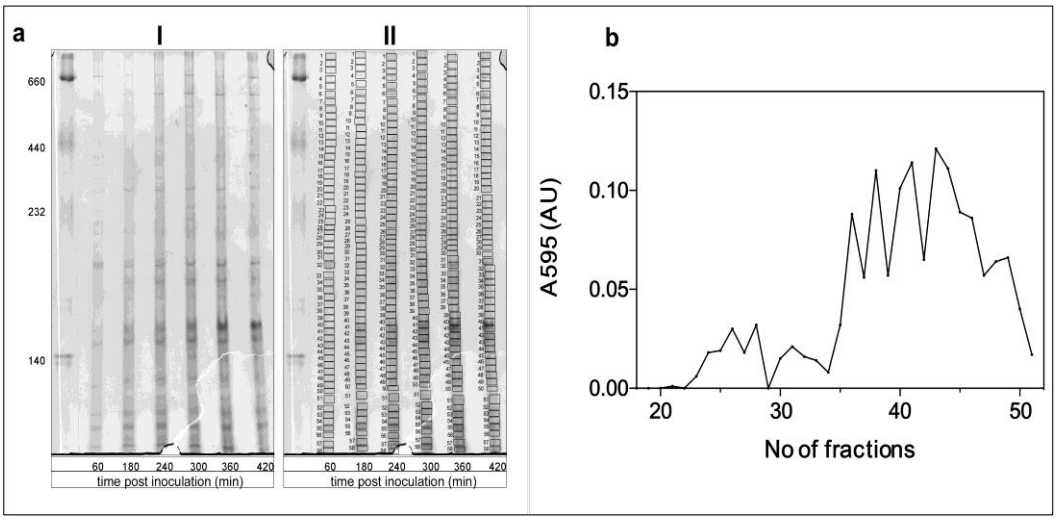

Figure 2-1: wt EPEC complexome analysis a) Protein complexes detected in wt EPEC as a function of time (I) and the bands that were excised from it to be analysed with MS (II), after separation by Native PAGE. Protein marker is indicated on the left (kDa), b) wt EPEC cytosolic fraction after analysis by SEC, indicating the number of fractions collected for MS analysis.

From the above analysis, we have extracted information about potential protein complexes that are formed during protein secretion through T3SS and the hierarchy proteins follow in order to be secreted.

More specific, the combination of the above approaches, in line with high accuracy mass spectrometry yielded the reliable identification of more than 1300

unique cytosolic proteins from EPEC cells. This corresponds to ~28% of its total theoretical proteome and ~50% of its predicted cytosolic proteome. The identified proteins represent a wide range of cellular processes as revealed from their GO annotations, which is required for a reliable and comprehensive subsequent complexome and protein network analysis (Figure 2a). Global complexome analysis determined more than 150 putative cytosolic protein complexes in EPEC including many previously reported complexes in laboratory strains of *E.coli*, providing validation for our approach (Figure 2-2b). Targeted cytosolic complexome analysis focused on the 54 predicted T3SS-related proteins (LEE and non-LEE encoded, membrane proteins are not included). Several T3SS pre-secretion protein complexes and interactions were thus identified in the EPEC cytosol against a background of the house-keeping complexome. More than 15 key cytosolic proteins of EPEC pathogenesis such as EspA, EspB, EspD, CesAB, CesD, Tir, CesT and Map [96]–[98] were identified as components of these protein complexes (Figure 2-2c,d).

The time-dependent complexome analysis of EPEC provided significant information about the dynamic formation of T3SS-related protein complexes. This information was correlated in a time-dependent manner to the secretion of more than 20 effectors identified in the extracellular milieu. For instance, the translocator protein, EspA and its cognate chaperone, CesAB were not present in the cytosol at the first time points during bacterial growth, while we were able to detect them as a complex, later on and in high amounts. The intra-cellular complexes detected, were in perfect agreement to the secretion profile of EspA, as a function of time (Figure 4). On the other hand, when the migration profile of the transcription factor, Ler [99], was followed, the protein was detected in high abundance as high oligomeric species very early during bacterial growth. Therefore, after combination of these findings, we were able to correlate the dynamics of the intracellular T3SS complexome with protein secretion as far as order, hierarchy and regulation is concerned. All the data derived from MS, were analysed and quantified from Dr. Michalis Aivaliotis.

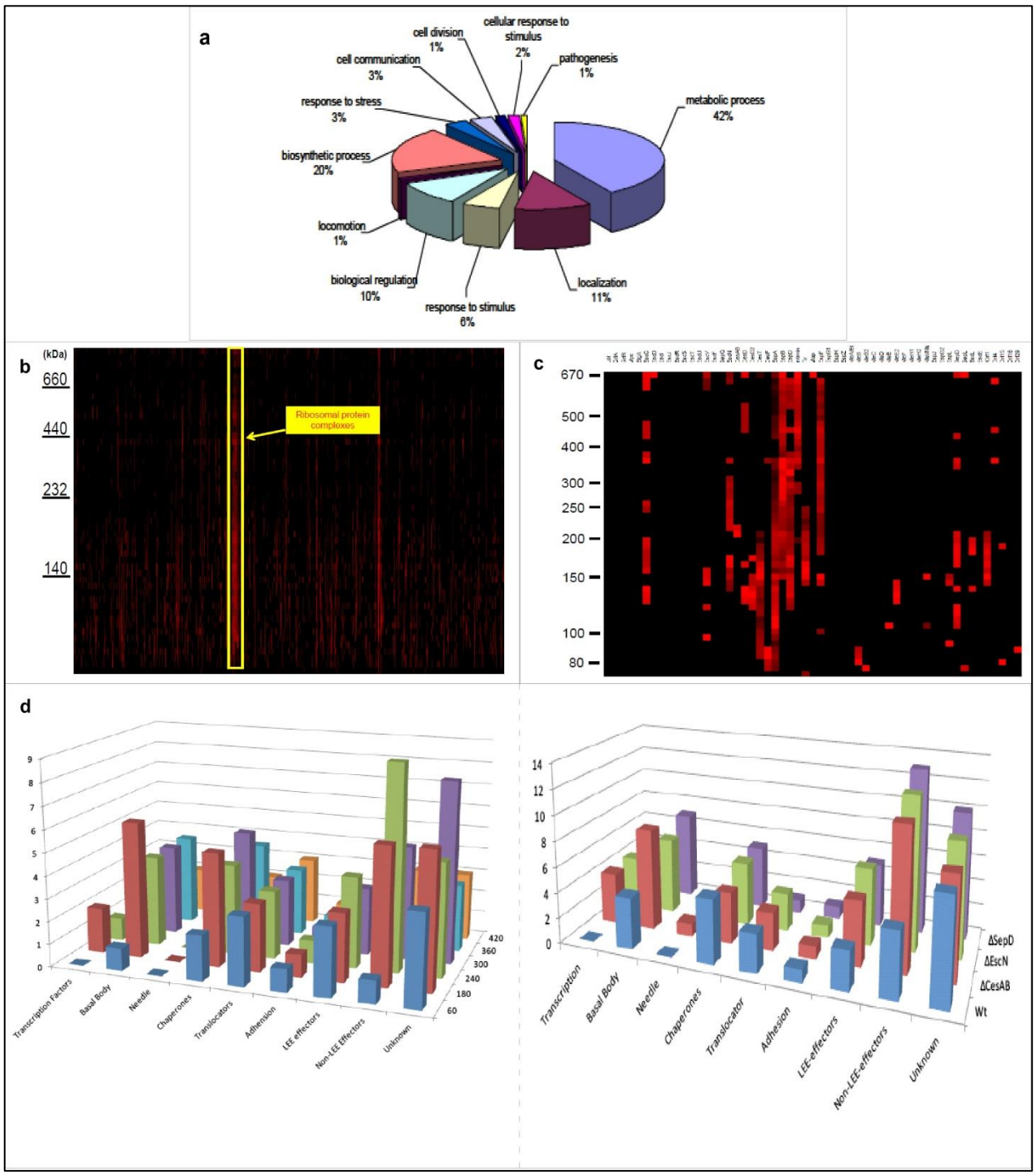

Figure 2-2: MS analysis of wt EPEC potential protein complexes. a) GO annotation of proteins identified, b) heat map representing migration profile of the total wt EPEC complexome, c) heat map representing migration profile of the T3SS-related wt EPEC complexome, as identified by MS. Quantification of the abundance of the proteins is represented with a colour scale from black to red, from the lower abundance to the highest respectively. Protein marker is shown in the left side (kDa). d) T3SS proteins identified by MS, categorized as far as their function is concerned. Their relative abundance in the samples was compared as a function of time during bacterial growth of wt EPEC (left bar graph) and between wt and deletion strains at the peak of secretion (right bar graph). All the data derived from MS, were analysed and quantified from Dr. Michalis Aivaliotis.

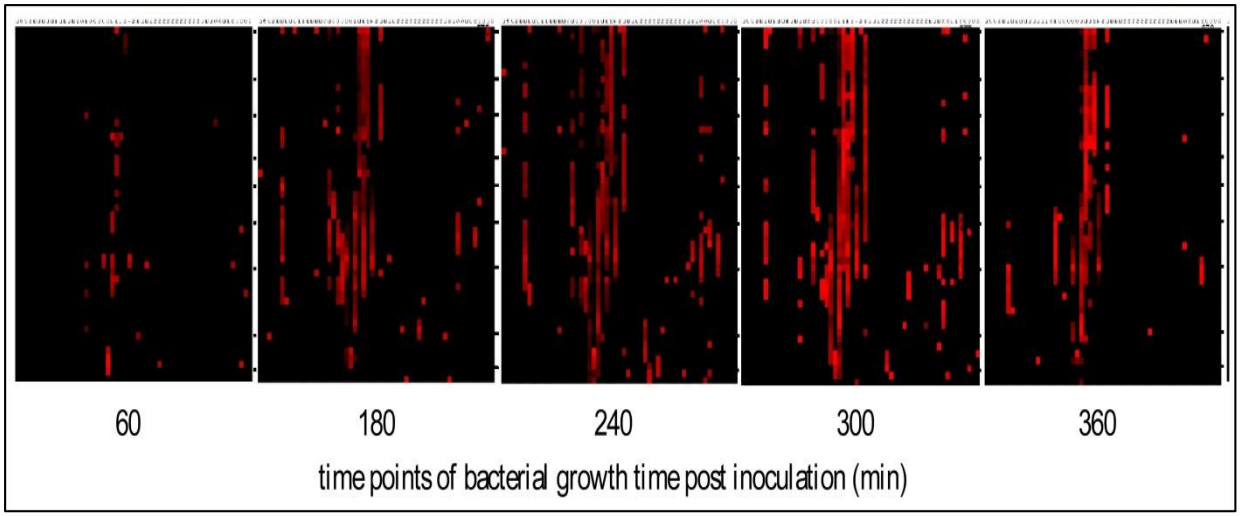

Figure 2-3 : EPEC compexome as function of time. Heat maps representing the migration profile of the T3SS- related wt EPEC complexome, as identified by MS, in different time intervals, during bacterial growth. Quantification of the abundance of the proteins is represented with a colour scale from black to red, from the lower abundance to the highest, respectively. The most protein complexes related to T3SS were identified in the bacterial cytosol at time point 240 and 300 min post inoculation. All the data derived from MS, were analysed and quantified from Dr. Michalis Aivaliotis

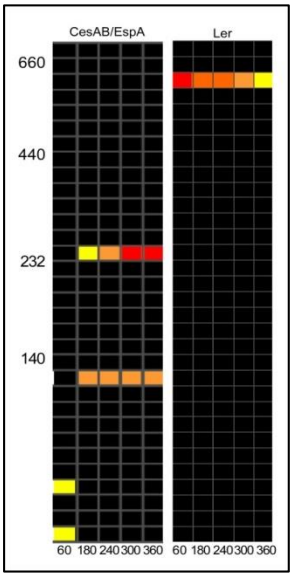

Figure 2-4: Protein complexes detected as a function of time, using MS. At heat maps the abundance of CesAB-Espa is represented with colors from yellow to red, from low to high, respectively, in a time dependent manner. Their migration profile is compared with the transcription factor, Ler, which is detected very early during bacterial growth. Time in minutes post inoculation is indicated. Protein marker is indicated in the left (kDa). All the data derived from MS, were analysed and quantified from Dr. Michalis Aivaliotis.

Validation of the MS findings

After the identification of the potential protein complexes in the wt EPEC cytosol, we performed a series of experiments, so to verify and to validate the physiological relevance of our findings. First, we analysed the protein complexes formed in the bacterial cytosol of different EPEC deletion strains and marked differences compared to the wt strain. Moreover, using specific antibodies, we followed the migration profile of the intra-cellular protein complexes formed from specific T3SS proteins,

and compared them with the MS findings. Finally, we purified protein complexes under Native conditions, using known T3SS proteins as bait.

Complexome analysis of EPEC Deletion strains

During the complexome analysis of wt EPEC cytosol, we had to exclude the possibility that the protein complexes that have been identified using MS analysis were artefacts of the method. Taking under consideration the fact that two proteins co-migrating in the same gel-band, or being eluted in the same fraction after SEC, does not make them protein partners in the same complex, we considered as an evanescence need to examine also the complexome profile from different EPEC deletion strains.

Towards this end we performed the same analysis, as above, for specific EPEC strains where the genes of essential proteins for the function of the system have been deleted. From a wide range of EPEC deletion strains that existed, we chose for this validation process the EPECΔcesAB, EPECΔescN, and EPECΔsepD. CesAB is the chaperone of the translocator EspA, and interacts with the secretory protein in order to keep it in a translocation competent state and unfolded in the bacterial cytosol. Otherwise, EspA has the tendency to self-polymerise and aggregate [48]. The ATPase, EscN, is essential for T3SS function due to the fact that produces the necessary energy by ATP hydrolysis, so that the secretory proteins will dissociate from their chaperones and enter the translocation pore of the system at the membrane [55], [56], [100]. Finally, as far as protein SepD is concerned, although little is known about its function, it is essential for the secretion of translocator proteins [77].

The procedure that was followed was the same as the one described above for the wt EPEC strain. In brief, the EPEC deletion strains were grown under the same secretion permissive conditions and samples were collected at the peak of secretion, as it was determined for the wt EPEC, due to the fact that these knock-out strains are unable to secrete any or less proteins through T3SS. Bacterial cytosolic extracts that were collected, were again analysed with Native–PAGE and SEC. Samples were digested using trypsin and proteins were identified using nano-LC MS/MS (LTQ Orbitrap-XL, Thermo Scientific).

After determination of the complexome profiles of these deletion strains, we compared them with the wt one. Many differences were detected, as far as protein-

complex formation and relative abundance of them are concerned. These differences could be correlated to the regulation, hierarchy and secretion processes that the deleted proteins are related with (Figure 2-2d). As expected, protein complexes containing these proteins detected in the wt complexome profile were not detected to the respective deletion strain.

A representative example, from this analysis is being shown in Figure 2-4. We compared the migration profile of EspA translocator in all the EPEC strains analysed. Only when CesAB chaperone was missing the main abundant oligomeric forms EspA was detected, were vanished in EPEC ΔcesAB strain (Figure 2-5). These results indicate that CesAB chaperone can form high oligomeric species with the translocator protein EspA, and the formation of these species is not affected from the absence of the APTase EscN, or the regulator factor, SepD. All the data derived from MS, were analysed and quantified from Dr. Michalis Aivaliotis.

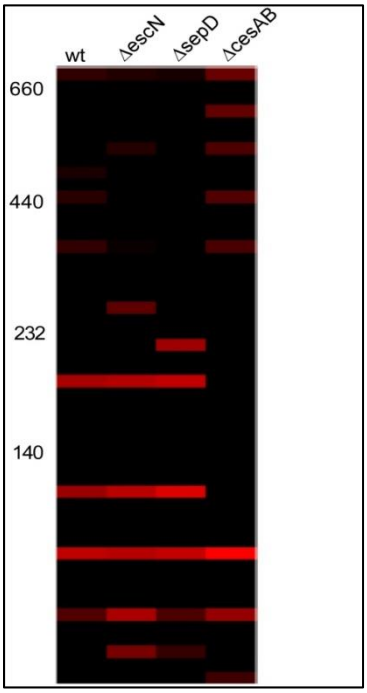

Figure 2-5: Heat map representing the migration profile of the translocator Espa in wt EPEC or EPEC deletion strains, as identified by MS. When the chaperone CesAB is missing (4th lane), the main oligomeric species detected at the wt, or other deletion strains are not formed (around 200 and 100 kDa respectively. Quantification of the abundance of the proteins is represented with a colour scale from black to red, from the lower abundance to the highest respectively. Protein marker is shown in the left side (kDa). All the data derived from MS, were analysed and quantified from Dr. Michalis Aivaliotis.

2.2 Validation of protein complexes using specific antibodies

As a more targeted approach to validate our MS results we have used specific antibodies against known T3SS proteins. Towards this end, wt EPEC were cultured under secretion permissive conditions, samples were collected and analysed as previously described, in a time-dependent manner. The protein complexes were

separated by Native-PAGE, and the migration profile of the proteins was detected using antibodies against them. In particular, when antibodies against CesAB or EspA were used to detect them, the migration profile derived was in agreement with the one determined after MS analysis for both proteins. These findings led us to conclude that not only the proteins migrate in the same fraction, forming macromolecular complexes in the bacterial cytosol, but also that these complexes are formed in a time dependent manner, which can be correlated with the EspA secretion to the external milieu (Figure 2-6). The outcome of this procedure was in complete agreement with the MS findings for the proteins that were analysed.

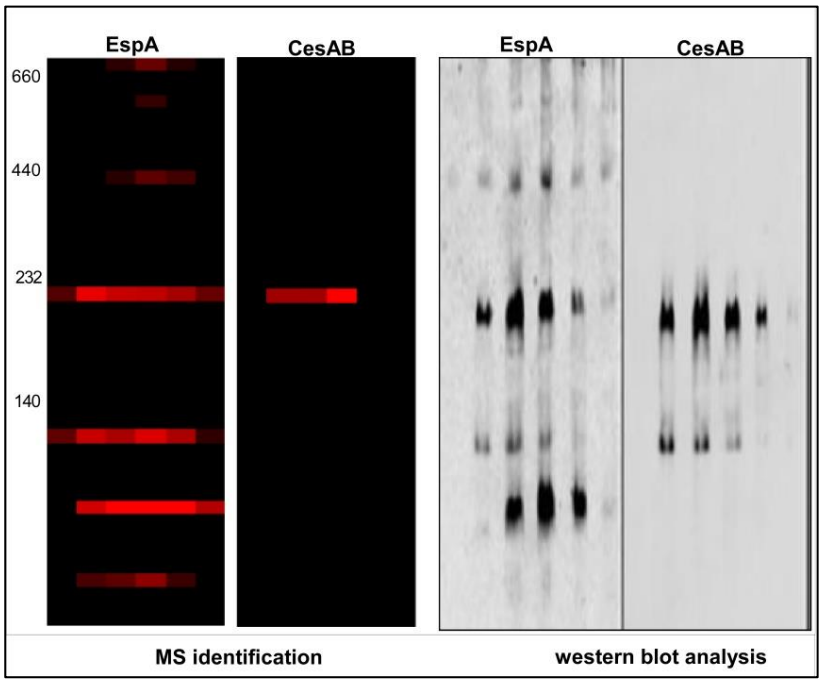

Figure 2-6: Comparison of the migration profile of protein complexes, as detected after MS analysis or western blot. At 1st and 3rd panel the migration profile of the translocator EspA is indicated, and at panels 2nd and 4th its cognate chaperone CesAB, in a time dependent manner. 1st and 2nd panels represent the MS findings and the abundance of the proteins is indicated with a colour scale from black to red, from lower to higher, respectively. 3rd and 4th panel indicates the migration profile detected after using poly-clonal antibodies for proteins EspA and CesAB, respectively.

Native purification of protein complexes

Additionally, also in a more targeted approach, His-tagged T3SS-related proteins were used as baits for the selective isolation of T3SS-related protein complexes. For this purpose EPECΔ*espA* or EPECΔ*cesAB* strains were complemented with plasmids carrying His-EspA or His-CesAB, respectively. First, we adjusted the amount of inducer used, anhydrous tetracycline, so to achieve low levels of protein-expression, comparable to the chromosomal ones. In that case we were able to avoid unspecific interactions related to over-expression of the genes. Afterwards, the strains were cultured under secretion permissive conditions and the bacteria were collected at the peak of secretion. From the cytosolic fraction, we purified the protein complexes that have been formed with His CesAB or His EspA, using Ni-NTA agarose beads, under native conditions. The elution fraction was further separated by Native-PAGE. The protein subunits of the complexes were analysed by nanoLC/MS or detected by specific antibodies against EspA or CesAB. In Figure 2-7, a representative result of this procedure is being shown, after His-EspA was used as bait. The high molecular weight protein complexes that were purified were in agreement with our initial MS findings from the wt EPEC strain.

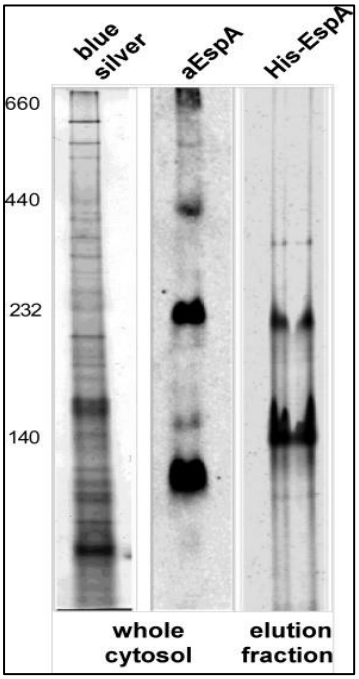

Figure 2-7: Protein complexes purified using His EspA as bait. 1st and 2nd lanes represent the typical outcome of the whole bacterial cytosol, seperated by Native PAGE stained with blue silver or probed with antibody against EspA protein. 3rd lane represents the elution fraction with protein complexes that are co-purified with His EspA.

3. Chapter: Structural determination of the CesAB- EspA interaction

Chaperones have particularly prominent and multiple roles in various protein transport and secretion pathways [101] . Specialized chaperones are important components of type III secretion (T3SS) systems wherein they assist with the assembly and operation of the entire machinery [39], [102].

CesAB is a chaperone for EspA in the enteropathogenic *Escherichia coli* (EPEC) [78].Translocator protein, EspA, once secreted, undergoes self-polymerization thereby forming a long extracellular filamentous extension that connects the needle to the translocation pore in the eukaryotic plasma membrane [68]. Because of its high tendency to self-oligomerize it is necessary for EspA to be captured in its monomeric state in the bacterial cytosol, a role served by the CesAB chaperone [49], [78].

Although the occurrence and the necessity of this interaction are known, the molecular mechanism that proteins follow in order to interact and how this interaction is being regulated was unknown. Therefore, we combined structural analysis tools (in solution NMR), biophysics tools (ITC, MALS) and biochemical ones (*in vivo* secretion and infection) to characterize in detail the chaperone complex on its own or in the presence of EspA.

CesAB exists as a loose dimer that structurally mimics the CesAB-Espa dimer

Structural analysis of CesAB homodimer

In order to gain a more structural insight of the chaperone CesAB, it was biophysically characterized using in solution Nuclear Magnetic Resonance NMR, Isothermal Titration Calorimetry (ITC) measurements and Multi Angle Laser light Scattering (MALS) analysis. The data acquired from this analysis showed that the protein CesAB can be divided in two domains, the N-terminal (N1-85) and the C-terminal (N 86-107). The N terminal domain of the protein can acquire a-helical secondary structure in solution, while the C-terminal region is a completely

disordered region, with no secondary structure elements. CesAB exists in solution as a homodimer (~27 kDa) with a dimer dissociation constant (K_d) of ~0.5 μM. This data analysis provided strong evidence that CesAB is a loosely packed, conformationally heterogeneous dimeric chaperone with molten-globule-like conformational properties.

CesAB adopts a four-helix bundle conformation. Each of the CesAB subunits adopts a "U" shape with an all-helical conformation, consisting of helices α1 (Arg8-Glu36), α2 (Gln50-Lys54) and α3 (Asp72-Thr84), with helices α1 and α2 connected by a hairpin. The C-terminal region (Ser86-Val107) is unstructured. Dimer formation is mediated by helical segments in both the N- and C-terminal regions, with helices α1 and α3 from each polypeptide chain packing together via extensive hydrophobic interactions to form a coiled-coil four-helix bundle (Figure 3-1)

Collectively, the data show that the CesAB homodimer adopts a molten-globule-like structure: a relatively compact helical bundle conformation, with regions of mixed folded and partially-folded secondary structure, but lacking extensive, specific tertiary side-chain packing characteristic of well folded structures. The above data analysis was performed from Dr Chen Li, under the supervision of Prof. Charalampos Kalodimos.

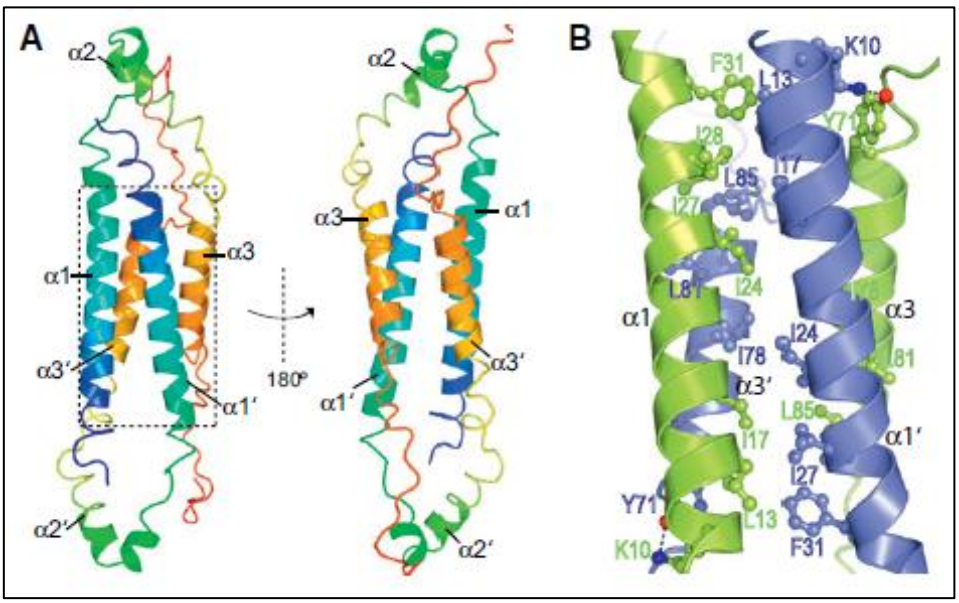

Figure 3-1: Structural Analysis of CesAB (A) Solution structure of the CesAB homodimer colored using a gradient scheme (blue to red, from the N to the C terminus) for each subunit. (B) The interface of the helical bundle (region in dashed box in (A) is dominated by hydrophobic residues and thus CesAB dimerization is primarily mediated by non-polar interactions. Hydrogen bonds are represented by black dashed lines. The two subunits are colored blue and green. NMR data analysis was performed from Dr. Chen Li

CesAB folds upon binding to the translocator EspA

The CesAB homodimer undergoes subunit exchange so to interact with its cognate substrate, the translocator EspA, and to form a 1:1 heterodimeric complex (Figure3-2a). NMR analysis showed that CesAB, which is poorly folded as a homodimer, acquires a well folded structure upon binding to EspA, in agreement with the crystal structure of a truncated form of the heterodimer [49]. In more detail, NMR analysis of the intact CesAB-EspA complex showed that CesAB forms three well-folded α helices (α1, residues 3-46; α2, residues 50-60; and, α3, residues 67-85), while EspA forms four α helices and a β sheet (α1, residues 37-58; α2, residues 77-92; α3, residues 132-144; α4, residues 149-188; β1, residues 96-102; β2, residues 123-130).

As revealed from NMR data, the CesAB protomer adopts a similar overall fold in the homo- and heterodimer. However, at the CesAB homodimer all three α helices are much shorter, largely unwound and dynamic, in contrast to the CesAB−EspA complex wherein they are well folded (Figure 3-2b, c).

Moreover, comparison between the two dimers, CesAB-CesAB and CesAB-EspA, indicated that CesAB homodimer has several unfavoured contacts (for instance: in close proximity two positive amino acids that will be opposed) resulting in "weak spots" formation at its helical bundle interface and overall low stability and poor packing. EspA counterbalance these "weak spots" by providing juxtaposed amino acids that can form favorable polar interactions in the heterodimer. In more detail, Arg174 on EspA forms a salt bridge with Glu20 on CesAB, and EspA Gln181 forms a hydrogen bond with CesAB Glu30. Additionally, while helices α1 and α3' in the CesAB homodimer are not properly packed because of the mismatch caused by Asp14 and Arg18, the residues at the corresponding positions in the heterodimer on EspA form optimal coiled-coil contacts with CesAB (Figure 3-2d).

Collectively, as far as the molecular mechanism of the interaction is concerned, NMR data revealed that EspA utilizes structural mimicry to form a complex with CesAB that has a similar fold to the homodimer. Furthermore, EspA exploits the sequence irregularities in CesAB and provides compensatory contacts that selectively stabilize the heterodimer over the homodimer.

All the NMR data analysis was performed from Dr Chen Li, under the supervision of Prof. Charalampos Kalodimos.

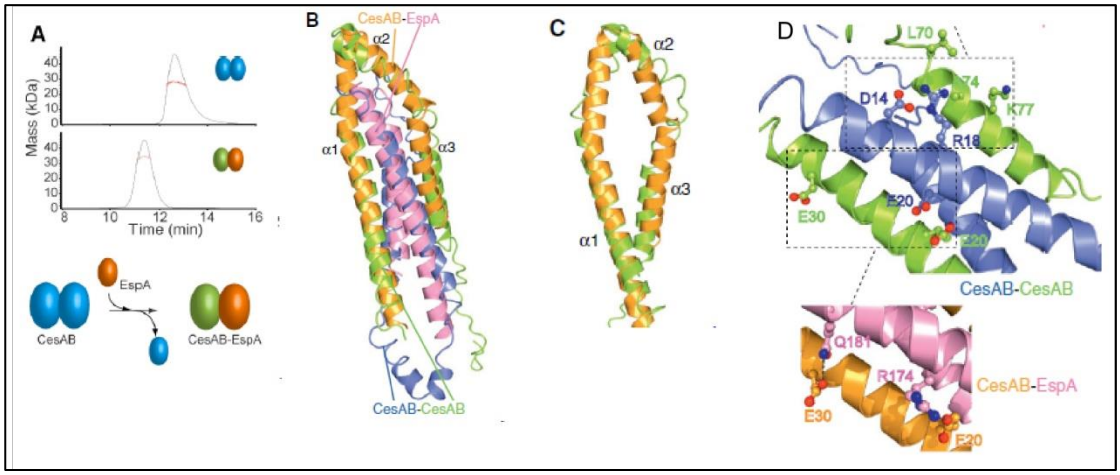

Figure 3-2: Folding of CesAB upon binding to EspA. A) MALS analysis of CesAB homodimer (top) and CesAB- EspA heterodimer (bottom). B) Superposition of the CesAB homodimer (subunits are colored green and blue) and the CesAB−EspA heterodimer (CesAB is in orange and EspA in magenta). C) CesAB and CesAB−EspA are superimposed as in (B) but the second CesAB subunit in the homodimer and EspA are not shown for clarity D) EspA binding to CesAB stabilizes and induces folding of the chaperone in the heterodimeric complex by providing compensatory contacts to CesAB residues that form unfavorable contacts in the homodimer. Hydrogen bonds/salt bridges are represented by black dashed lines. NMR data analysis was performed from Dr. Chen Li

The folding properties of CesAB regulates its function

Based on the results that derived from NMR data analysis, we wanted to elucidate the impact of the structural and dynamic properties of CesAB to its function, *in vivo*. Towards this end, we generated several mutations on CesAB gene that would introduce amino acids with favorable electrostatic charging state so to destroy "weak spots" on the overall structure, resulting in a more compact and stable homodimer, with a higher affinity. These mutants were expected not to interact with EspA in solution. Afterwards, we designed EspA mutants that would restore the biding interaction with the CesAB derivatives, by forming stable heterodimers, proving our hypothesis that the structure of CesAB regulates the interaction with EspA, therefore, its function as a chaperone.

The CesAB or EspA derivatives that were generated for this purpose were, CesAB_E20L/E30L, so to increase the a-helical propensity of CesAB, due to increased hydrophobicity, and CesAB_D14L/R18D, so to optimize packing of helices a1 and a3', by introducing a hydrophobic residue and a negatively charged one that would ulcerate the opposite ones and interact with them (Figure 3-2 d). Finally, the

triple mutant, CesAB_D14L/R18D/E20L (CesAB DRE) was designed to overall generate a very structured homodimer.

As far as EspA mutant is concerned, we generated the double mutant EspA_R174L/Q181L, which should interact with CesAB_E20L/E30L optimally, forming a very stable heterodimer, with very low dissociation constant.

The above CesAB and EspA derivatives, were characterized as far as structure was concerned, using in solution NMR, and Circular Dichroism analysis (CD). Furthermore, and as far as function of these mutants was concerned, they were tested biochemically, to elucidate their ability to interact *in vivo*, by following the secretion of EspA, and by determination of their ability to infect effectively HeLa cells, *in vivo*.

Structural characterization of CesAB folding-mutants

Indeed, sequence optimization by substituting Leu for Glu20 and for Glu30 (E20L/E30L) increased substantially the α-helical content and confers notable stabilization to the CesAB structure. Moreover, packing optimization between helices α1 and α3' in the CesAB homodimer by the D14L/R18D substitution, decreases drastically the CesAB affinity for EspA binding. Finally, the CesAB-D14L/R18D/E20L triple mutant, designed to correct the three most prominent sequence irregularities. Structure determination of CesAB-D14L/R18D/E20L showed the expected better folding of the triple CesAB mutant, although its overall structure is very similar to the structure of the wild-type CesAB (Figure 3-3).

As far as the EspA-R174L/Q181L, is concerned, that was designed to optimally juxtapose with CesAB-E20L/E30L, indeed, a stable heterodimeric complex was formed. However, this heterodimeric complex was not formed at all when the transient exposure of the α3 helix is suppressed by the double D14L/R18D substitution. The above data analysis was performed from Dr Chen Li, under the supervision of Pr. Charalampos Kalodimos, and Dr. Vassileia Balabanidou, under the supervision of Pr. Anastassios Economou.

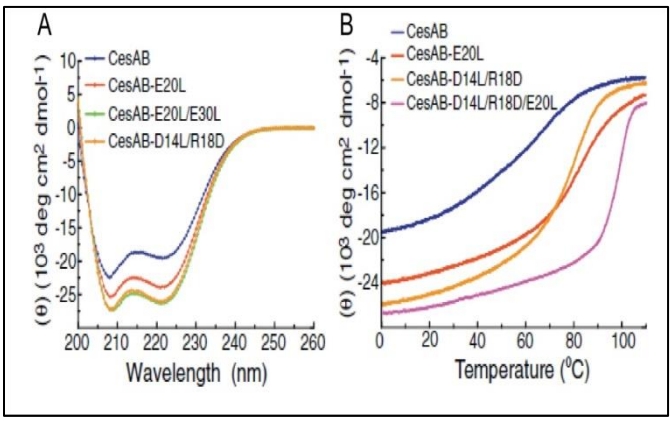

Figure 3-3: CesAB derivatives are more stable compared to the wt
A) Far-UV CD data of CesAB and variants show that the amino acid substitutions increase helicity.
B) Far-UV CD thermal denaturation data, monitored at 222 nm as a function of temperature, of CesAB and variants showing that the amino acid substitutions increase CesAB stability**.** Data analysis was performed from Dr. Chen Li and Dr. Vassileia Balabanidou

Biochemical characterization of CesAB folding-mutants, in vivo

In order to determine how the CesAB folding-mutants affect the function of the chaperone, we followed the secretion of EspA in a time dependent manner *in vivo*.

EspA is not secreted in the absence of CesAB, resulting in a non-functional T3SS at the EPECΔcesAB strain. For this reason, plasmids that were carrying the CesAB mutants were transformed in EPECΔCesAB strains, and their ability to complement the strains and rescue the phenotype was monitored. The gene expression of these mutants was under tight regulation, so to achieve low amounts of the derivative proteins that were produced. The cells, on one hand, were cultured under secretion permissive conditions and the secretion of EspA was monitored, in a time dependent manner, at the external milieu. On the other hand, the same strains were used to infect HeLa cells. In this case, both the secretion of EspA and the formation of actin pedestals were monitored, due to EPEC infection from T3SS secretion of effectors.

Moreover, we wanted to determine the impact on EspA secretion, when the stable heterodimer is being formed between the CesAB E20L/E30L and EspA R174L/Q181L. In order to perform the biochemical assays and monitor the secretion of EspA, we generated a double deletion strain, from which both *cesAB* and *espA* genes were deleted, using "One step Gene disruption technique" (see appendix) [103].

Additionally, in order to be able to co-express both genes *in trans* and complement the double deletion strain, EPECΔcesAB/ΔespA, we constructed double gene operons. In these cases, both *cesAB* and *espA* genes, wt and derivatives, were inserted in pASK IBA 7 plus vector (IBA, Germany), under the same promoter and a ribosome binding site between them, so to ensure the expression of both genes (see appendix).

Indeed, the packing–optimized mutants that were tested failed to complement EPECΔcesAB or EPECΔcesAB/ΔespA strains, regarding EspA secretion. Secretion of EspA was either vanished or dramatically compromised compared to the wt strain (Figure 3-4). Moreover, as far as the infection of HeLa cells is concerned, the amount of cells that were infected was decreased or there were no infected cells detected, indication that the T3SS system was not functional (Figure 3-5).

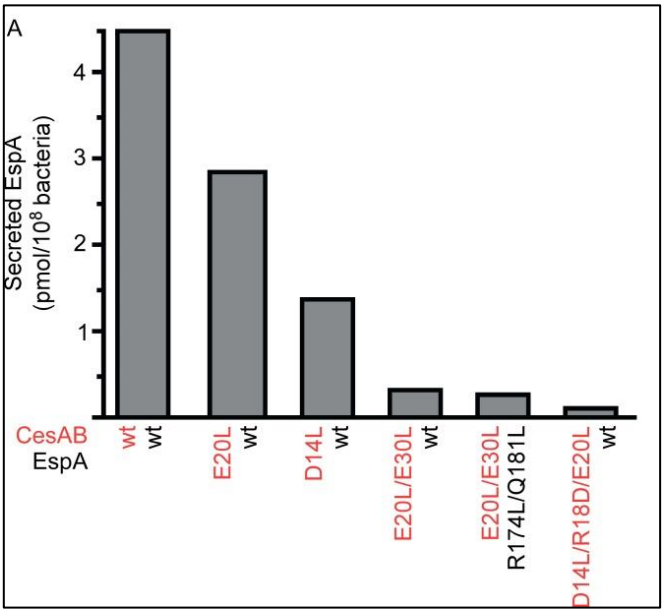

Figure 3-4: *In vivo* secretion of EspA. Bar graphs indicate the amount of EspA being secreted at the external milieu, at the peak of secretion. EspA was detected after Western blot analysis and antibody probing. The amount of the secreted EspA was quantified using Image J software. Data derived from at least three biological repeats.

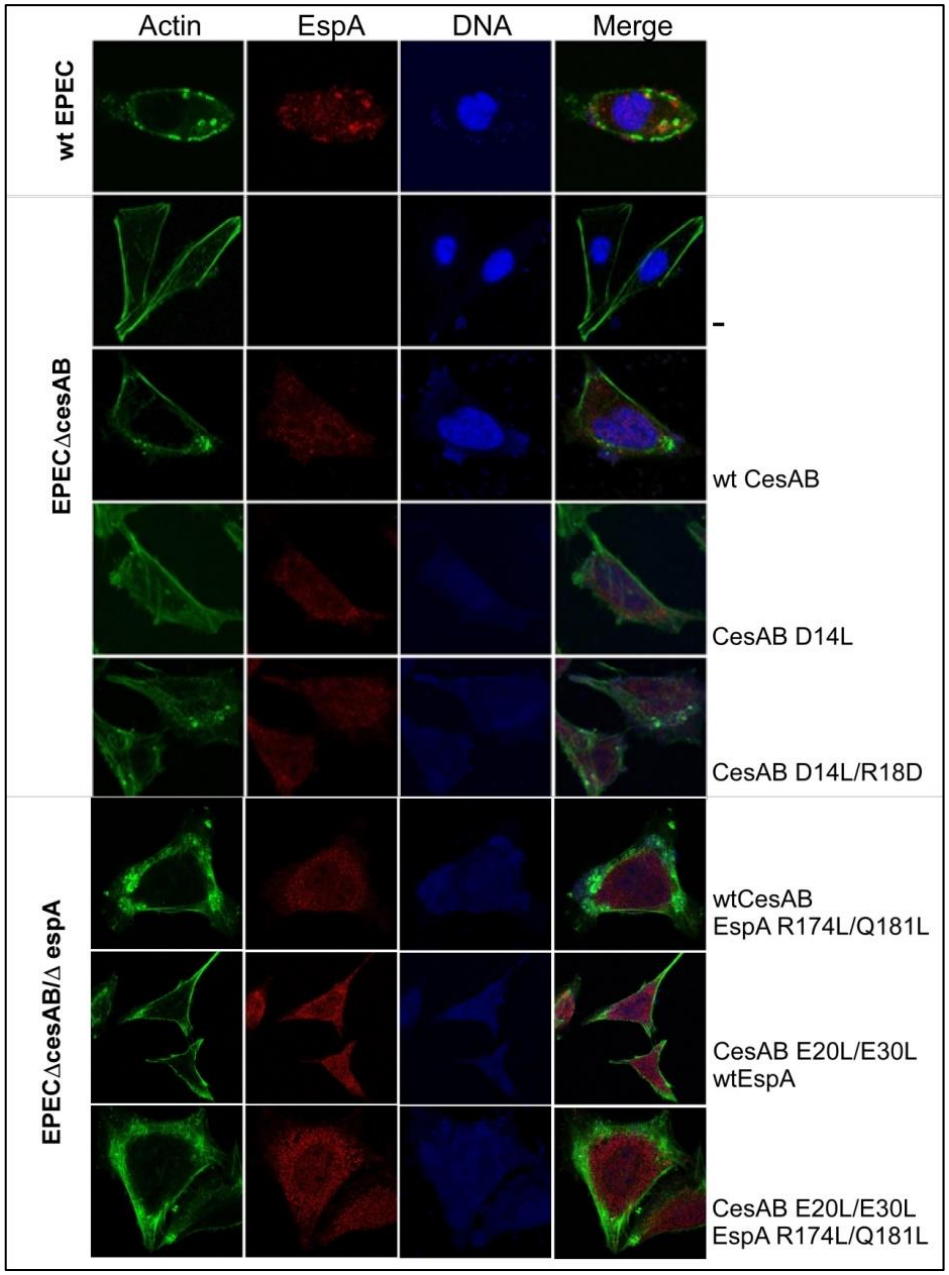

Figure 3-5 : Infected HeLa cells from EPEC wt or Deletion strains, complemented with cesAB or cesAB/espA genes, wt or mutants. Immobilized HeLa cells were incubated with EPEC cells for 2hrs and samples were probed with fluorescent antibodies and observed using fluorescence microscope (magnification: 100x). Green: actin, Red: EspA filaments, Blue: DNA/Nucleus

4. Chapter: Mapping the CesAB- EspA- EscN interaction

As already has been mentioned, T3SS is a multiprotein machinery from which, translocator and effector proteins are being secreted directly into the host cell [102]. Previous studies have demonstrated that the proteins that are going to be secreted from T3SS targeted to the cytoplasmic base of the injectisome and hierarchically secreted through the channel [82], [104]. Moreover, it has been shown that in the bacterial cytosol, T3SS secretory proteins interact with their cognate chaperones, forming stable protein complexes. The main role of the T3SS chaperones-secretory protein interaction is to maintain the secretory proteins soluble, unfolded and translocation competent, in the cytosol [39], [48], [87]. Moreover, it has been also implied from previous studies that chaperones could also carry signals for being targeted to the membrane and additionally, act as hierarchy-determining factors [7]–[9].

Finally, biochemical experiments have suggested that the T3SS chaperone-secretory protein complexes may be recognized and engaged by the ATPase of the system [56], [87]. The ATPase of the T3SS is a conserved protein, which forms oligomers and is localized at the cytoplasmic ring of the inner membrane, at the pore of the injectisome [30], [85], [100].

Although, the ATPases of the T3SS have been proposed as potential targeting elements at the T3SS pore for the chaperone-secretory protein complexes, the molecular mechanism of this interaction is completely unknown and needs to be elucidated.

Towards this end, as a model ATPase from T3SS, we used the ATPase EscN from EPEC [57], [100], and the chaperone-secretory protein complex CesAB-EspA that was previously characterized (see Thesis Chapter 3).

Biochemical characterization of T3SS ATPase, EscN, *in vitro*

The T3SS ATPases show high structural and functional homology with the F_1F_0 ATPases and previous studies have demonstrated that in order to become active, these molecules need to self-oligomerize and form hexamer or dodecamers, the formation of which and the overall activity of the enzymes is under tight regulation [58], [85], [100].

Purification of EscN

In order to characterize and map the interactions between the ATPase EscN, it was of high necessity to purify the protein and characterize it as far as the oligomeric state and the APTase activity of the protein were concerned.

Setting up the protocol of EscN purification was a challenging procedure, due to the fact that the protein was neither expressed in overwhelming levels from the bacteria, nor retained in a soluble conformation. Therefore, many parameters needed to be tested and different chromatography procedures were combined so to end up with purified EscN. The exact purification protocol that was set up for this protein is being described in detail at Thesis Chapter 7.

Briefly, in order to over-express the EscN gene and retain it as soluble as possible, we used an EscN derivative, where the EscN gene was fused at the C-terminal of Maltose-binding protein (MBP) and in between the two genes a Tobacco Etch Virus (TEV) cleavage site was inserted. After 60 hours of induction at 15^{o}C, BL21-19 (DE3) cells were harvested and lysed. The cytosolic fraction that contained the majority of His MPB TEV EscN was loaded on Ni-NTA agarose beads and "high salt purification" protocol was followed (see Thesis chapter 7). To the elution fraction size exclusion chromatography was performed, so to exclude some impurities from it. Afterwards, the fractions from SEC that contained the His MBP TEV EscN incubated with TEV protease for 12 hours, so to achieve the maximum cleaved EscN from His MBP TEV, in proportion to the lowest aggregated product. EscN had the tendency to aggregate upon TEV cleavage, presumably due to self-oligomerization. Afterwards, negative affinity chromatography was performed using Ni-NTA beads, so to purify the cleaved EscN population from the un-cut one. After negative affinity chromatography, anion exchange chromatography was performed and the different

oligomeric species EscN had formed were separated, due to different affinity on the Q resin that was used. These populations were kept separately so to be tested as far as oligomeric state and enzymatic activity is concerned. Data from this purification protocol can be found on Chapter 8: Appendix.

Biochemical characterization of EscN as an ATPase

Determination of the oligomeric state of EscN

Once the protein was purified, the oligomeric state and its ATPase activity was determined, so to characterize EscN biochemically.

In order to determine the oligomeric state of EscN in solution and elucidate how it is affected as a function of concentration, we performed Size exclusion chromatography (SEC) coupled with Multi laser light scattering (MALS). A set of experiments was performed in a wide range of EscN protein concentration. In each chromatogram that resulted, the elution time of the main peak and the molecular mass of it was determined, whenever that was possible. As derived from these results, EscN seemed to form oligomeric species upon increasing concentrations. In solution and in low concentration (below 10uM), the main population detected was the monomer. This population though, was converted to dimer, tetramer or hexamer in a concentration dependent manner. However, in the highest concentrations that could be reached using SEC-MALS, we were not able to shift the equilibrium of the oligomerization state towards the hexamer, so to end up with a homogeneous population, and the active state of EscN. Nevertheless, we assumed that EscN could form hexamers in solution in very high concentration (Figure 4-1).

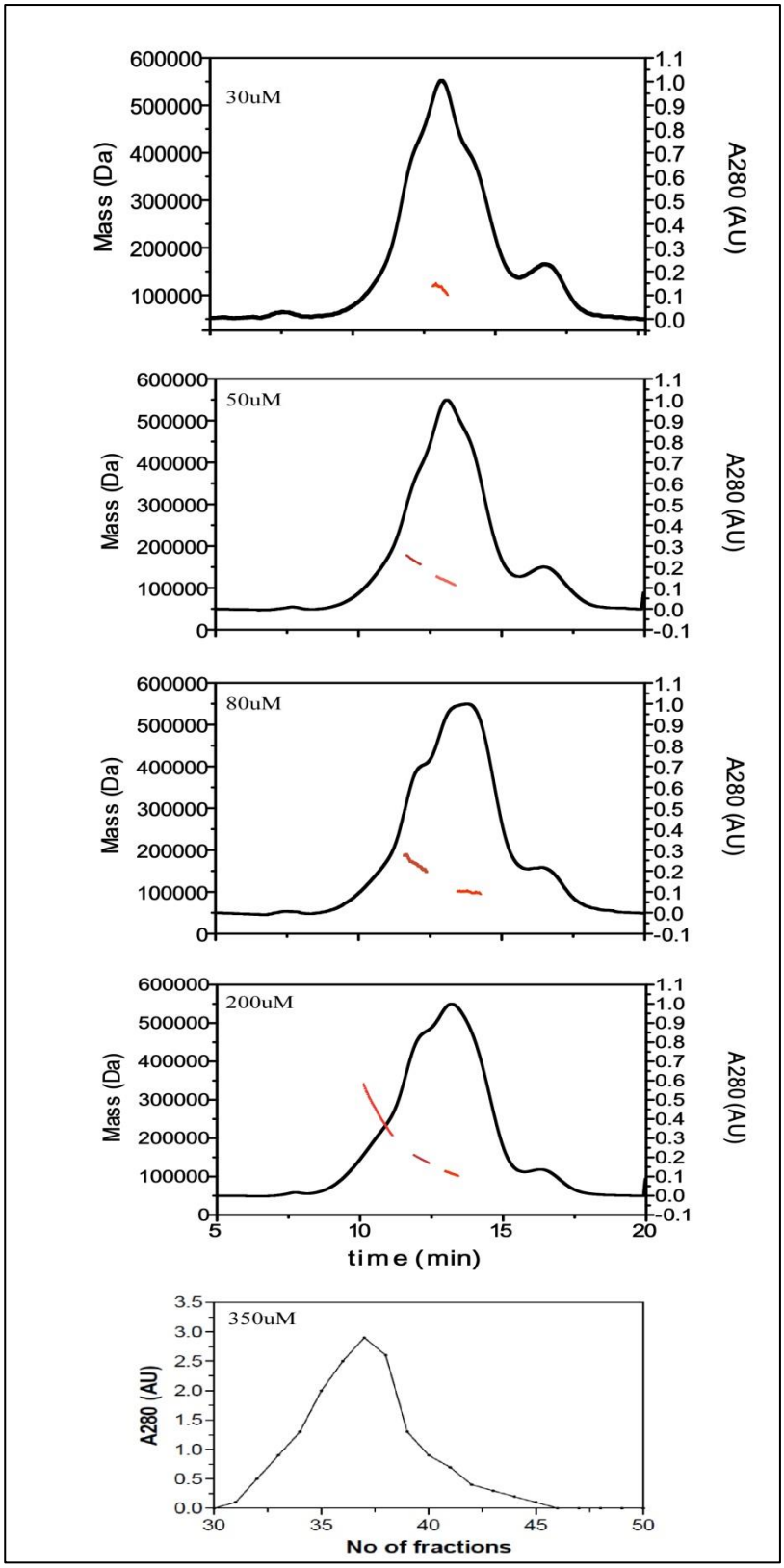

Figure 4-1: Oligomerization of EscN in a concentration dependent manner. SEC-MALS analysis to determine the EscN oligomeric state that was performed with different increasing concentrations. The elution profile of EscN was detected with UV absorbance at 280nm, and the molecular mass was measured with the best possible accuracy using MALS detector. Last panel, represents the chromatogram acquired after SEC that was performed without the MALS detector, due to high concentration of the loaded sample which out of the MALS detection limits.

Determination of enzymatic activity of EscN

In order to determine the ATPase activity of EscN we performed the ATP hydrolysis measurement assay (see Chapter 7). For the proper characterization of the enzymatic activity EscN has, we determined its activity under different conditions. First, the ATP hydrolysis was measured as a function of time and concentration (Figure 4-2). The amount of ATP that was hydrolyzed in the each reaction was quantified and was expressed as pmols ATP hydrolyzed per pmol EscN that was added. As derived from these results, EscN showed elevated ATP hydrolysis activity only in high concentrations.

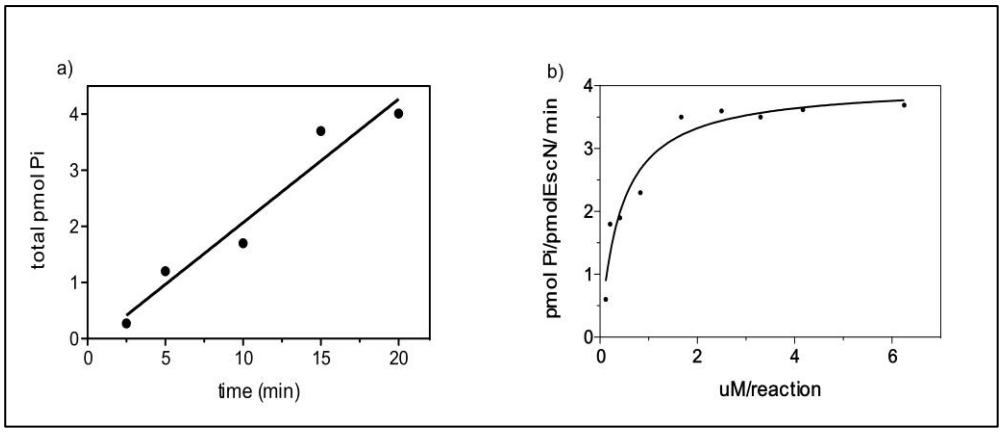

Figure 4-2: Enzymatic characterization of EscN, by ATP hydrolysis determination, as a function of time (a) and concentration of EscN (b). The hydrolyzed ATP was measured and transformed in pmol Pi per pmol EscN monomer used in each reaction (a) and per minute (b).

As described before, in high concentration EscN can form dimers, tetramers and hexamers (Figure 4-1). So, in order to determine the active oligomeric state of EscN, we combined SEC-MALS analysis with ATP hydrolysis measurements. Towards this end, SEC-MALS analysis was performed, fractions were collected so that the different oligomeric forms to be separated and the hydrolysis of ATP was measured in each fraction. Taking into account the oligomeric state of EscN as derived from SEC-MALS, the protein concentration as determined with Bradford assay and the amount of ATP that have been hydrolyzed in each fraction, we concluded that the active form of EscN is the hexameric one (Figure 3-3).

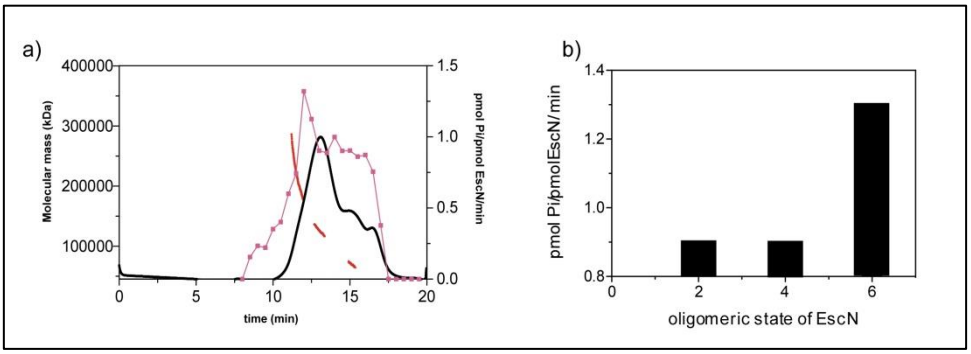

Figure 4-3 Determination of the active oligomeric state of EscN. a) SEC-MALS analysis of 250uM EscN (UV absorbance: black line) where fractions collected every 30sec so to separate the oligomeric forms of EscN. Mass measurments were determined using MALS detector (red lines). In each fraction hydrolyzed ATP was measured and transformed to pmols Pi/pmols EscN/min (magenta line). b) Simplified representation of a). Bar-graphs represent the fractions where the maximum ATP hydrolysis detected, in the different oligomeric states of EscN. For simplicity, the oligomeric state is mentioned instead of the number of fraction.

Finally, as far as temperature is concerned, we performed the same ATP hydrolysis assay, so to characterize the ATPase function of EscN, in a temperature dependent manner, both in low and high concentration. For this reason, the hydrolyzed ATP from EscN was quantified in a wide range of temperatures, from 4 ^{o}C up to 47 ^{o}C and in two different concentrations. As expected, the overall ATPase activity of EscN was less in low concentration compared to the high concentration (as also showed before), indicating that the formation of the active state of EscN is not promoted by temperature, but only from concentration. Moreover, EscN showed maximum ATPase activity, at 25 ^{o}C in low concentration, while in high concentration at 35 ^{o}C. This result, could be interpreted from the fact that EscN needs to be an active enzyme at the physiologically relevant temperature (37 ^{o}C is the optimal temperature for bacterial growth), only upon hexamer formation. The formation of this oligomeric state perhaps is regulated from other parameters, though (Figure 3-4).

Our findings were in agreement to what has already been proposed from previous studies. It has been demonstrated that T3SS ATPases are activated upon oligomerization, usually after formation of hexameric or dodecameric species. Moreover, optimal enzymatic activity is around 35 to 37 ^{o}C and other factors regulate the formation of the active species of the enzymes, in the bacterial cytosol or at the membrane [30], [56], [58], [85], [100].

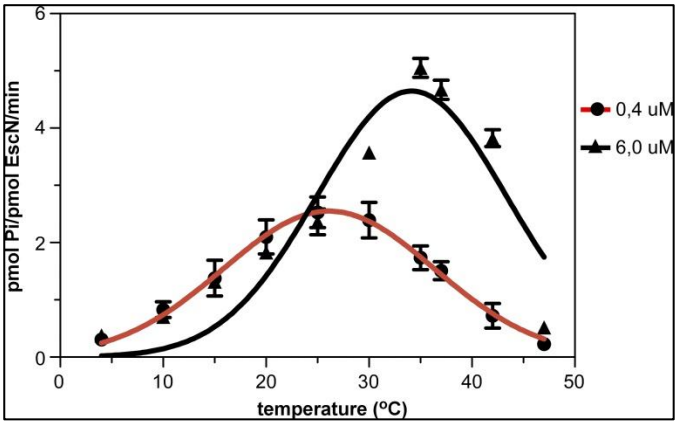

Figure 4-4: ATP hydrolysis measurements as a function of temperature. EscN in high concentration (black line) shows maximum activity at 35°C, while at low concentration at 25°C. Overall ATPase activity of EscN is increased in high concentration due to formation of hexamers, which are the active oligomeric state of EscN

Only CesAB-EspA complex can bind on EscN hexamer

Simultaneously with the biochemical characterization of the EscN ATPase and in collaboration with Prof. Charalampos Kalodimos' lab, the interaction between the EscN ATPase and the chaperone-secretory protein complex, CesAB-EspA, was mapped using in solution NMR.

As it has been described before (Thesis Chapter 3), in the absence of the secretory protein EspA, CesAB chaperone exists as a loosely packed, conformationally dynamic homodimer. Using NMR spectroscopy, so to be able to monitor transient binding interactions, we tested whether CesAB homodimer interacts with the ATPase EscN, in solution. The NMR data showed that none of the CesAB resonances is affected by the addition of EscN, demonstrating that there is no interaction between CesAB and EscN.

As it has been also described previously (Thesis Chapter 3), the CesAB dimer undergoes subunit exchange to interact with the secretory protein EspA, resulting the formation of a heterodimeric complex in 1:1 molar ration. Upon this complex formation CesAB acquires a well-folded structure. Again in solution NMR approach was used to determine the interaction between CesAB−EspA and EscN. As derived from NMR data analysis, addition of EscN causes a very significant effect to a large number of CesAB−EspA resonances indicating the formation of the ternary CesAB−EspA−EscN complex (Figure 4-5a).

The dissociation constant (K_d) of the ternary complex, that was determined by NMR line shape analysis, was ~3 μM. In the concentration that EscN was used for this analysis, according to previous results, the hexameric EscN was formed.

Moreover, no binding was observed between CesAB−EspA and an EscN variant, which even in high concentration existed in a monomeric state. Therefore, the heterodimeric chaperone−substrate complex can interact to the active hexameric state of the EscN ATPase

Collectively, NMR analysis revealed that the chaperone on its own cannot bind to the ATPase of the system. Only, the chaperone-secretory protein complex can interact to it. Additionally, EscN has to be in a functional oligomeric state in order to engage the chaperone−substrate complex. The NMR data processing was performed from Dr. Li Chen, under the supervision of Prof. Charalampos Kalodimos.

CesAB interacts with EscN due to conformational changes upon EspA binding

To determine the specific residues that mediate the interaction between CesAB−EspA and EscN, NMR differential line broadening analysis was used [105]. Due to the fact that EscN has a large molecular mass (~350 kDa), complex formation with labeled CesAB−EspA resulted in severe line broadening of the resonances. The broadening effect depends on the chemical shift difference of the CesAB−EspA resonances between the EscN-free and EscN bound. Thus, using this method the residues in CesAB−EspA that are most affected by the formation of the ternary complex with EscN can be identified. Interestingly, the NMR results indicated that the residues most affected by EscN binding are located on CesAB. These residues are located in helices α2 and α3 of CesAB and form a contiguous solvent-exposed surface in the heterodimer. The NMR data strongly suggest that this region forms the EscN-binding surface in CesAB−EspA. It was to our surprise that CesAB, and not EspA, appeared to be responsible for mediating the binding between CesAB−EspA and EscN, due to the fact that there was no binding observed when CesAB homodimer was used.

However, this was justified after comparison of the CesAB structures, on its own or with complex to EspA. Superposition of these structures showed that the EscN-binding region in CesAB was well formed in the heterodimer but extensively unfolded in the homodimer (Figure 4-5b, c,).

These results suggested that binding of EspA to CesAB poises CesAB to interact with EscN by eliciting a disorder-to-order transition that stabilizes the formation of a region that is specifically recognized by EscN.

To test the above hypothesis, we assessed the effect of a CesAB variant that was previously shown to mimic the EspA binding effect and stabilize a well-folded structure of the CesAB homodimer. Specifically, the CesAB-DRE mutant was used, in which substitutions of D14L, R18D and E20L optimized coiled-coil interactions at the CesAB helical bundle interface. The stabilized CesAB-DRE has NMR and CD features that are characteristic of a well folded protein (Thesis Chapter 3)

Structure analysis using NMR, showed that the CesAB-DRE structure is very similar to the structure that CesAB adopts in the CesAB−EspA heterodimer with all of the three helices well folded. Most importantly, though, the EscN-binding region was well formed (Figure 5-6).

We have used NMR to determine whether CesAB-DRE interacted with EscN. The results showed that there was indeed, a specific interaction between CesAB-DRE and EscN. Conclusively, the results showed that the triple amino-acid substitution in CesAB-DRE induced to CesAB an overall structure which was similar to the one induced by EspA binding. This conformational change resulted in EscN specific recognition and interaction with CesAB-DRE, in contrast to CesAB. All the above NMR data processing was performed from Dr. Li Chen, under the supervision of Pr. Charalampos Kalodimos.

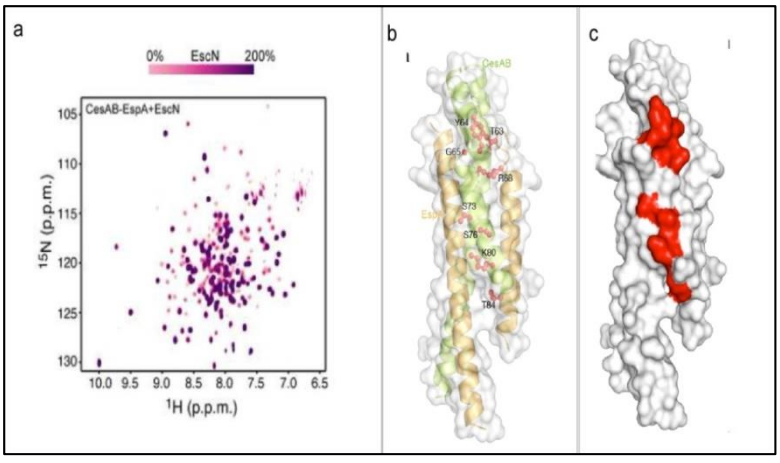

Figure 4-5: Interaction of CesAB−EspA with EscN. (a) Overlapped spectra labeled CesAB−EspA with unlabeled EscN. Addition of EscN results in gradual resonance broadening of the interacting residues in CesAB−EspA. (b) CesAB−EspA residues (red sticks) identified by NMR to be most affected upon binding to EscN. These residues are located in helices α2 and α3 in CesAB, (c) and form a contiguous solvent-exposed surface. Data were analyzed from Dr Chen Li.

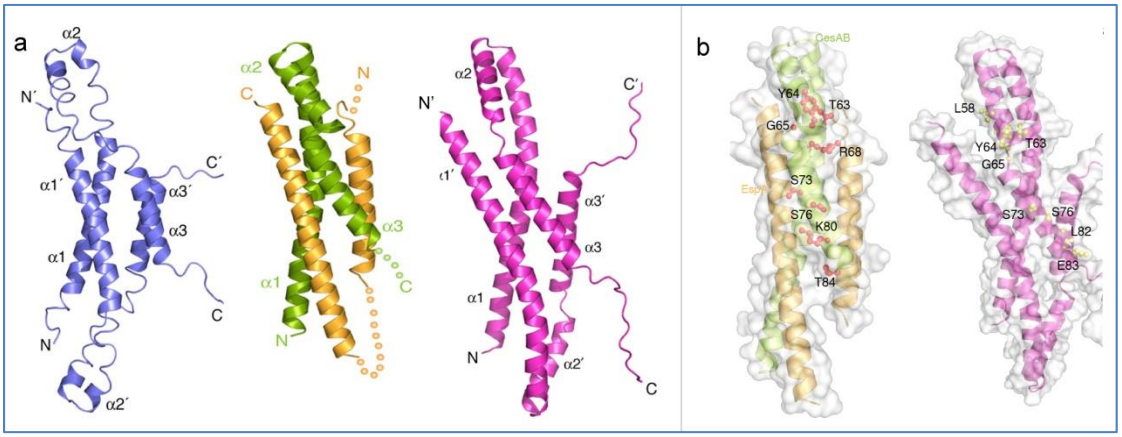

Figure 4-6 : Structural characterization and comparison of CesAB-DRE a) Solution structure of the homodimeric CesAB, crystal structure of the heterodimeric CesAB−EspA (Regions of the proteins that were not crystallographically resolved are represented as dotted lines) and solution structure of the CesABs DRE. b) Comparison of the EscN-binding interfaces in CesAB−EspA and CesAB-DRE. Residues identified by NMR to mediate the interaction of CesAB−EspA and CesABDREv with EscN.

The ternary complex formation between CesAB-EspA-EscN is essential for secretion

In order to validate the NMR results and verify the binding domain on CesAB mutants were generated, that should abolish the ternary complex formation. Amino acids in the region identified to mediate the interaction were mutated and their effect on the formation of the ternary complex was monitored by NMR. As expected, NMR data showed that substitutions at Glu60, Tyr64, Arg68 and Lys69 on CesAB decreased substantially the affinity of CesAB−EspA for EscN. All the above NMR data processing was performed from Dr. Li Chen, under the upervision of Pr. Charalampos Kalodimos.

These CesAB mutants were also characterized as far as their ability to complement EPECΔcesAB so that efficiently secrete EspA, *in vivo*. It was already known, but also determined in this thesis (Figure 4-7), that EscN ATPase is essential for T3SS secretion [30], [100]. Moreover, targeting to the ATPase of the secretory protein-chaperone complex has been hypothesized [87], [106]. So, in order to verify the targeting hypothesis and the necessity of the ternary complex formation *in vivo*, it was of evanescence need to determine the secretion profile of EspA.

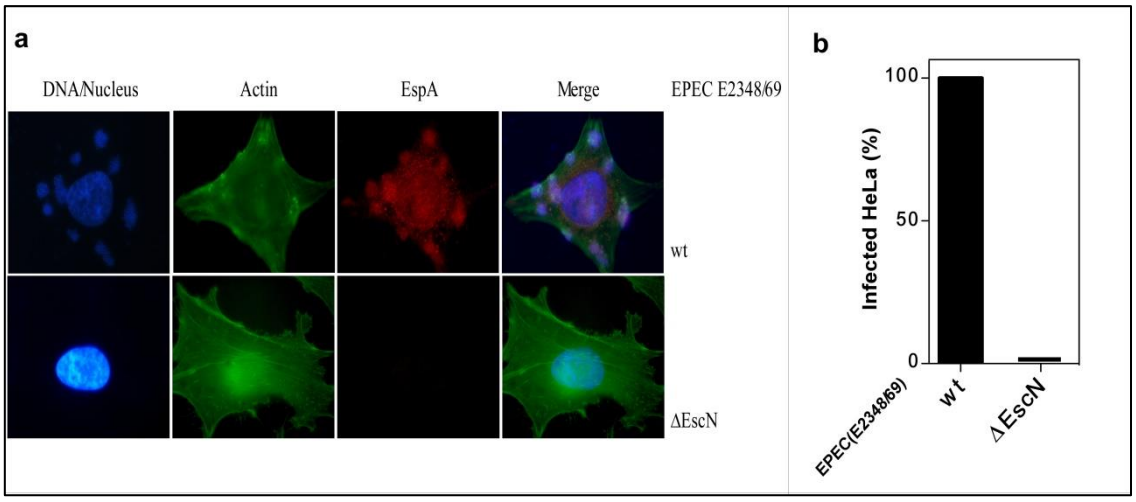

Figure 4-7: Infected HeLa cells from EPEC wt or ΔEscN. a) Immobilized HeLa cells were incubated with EPEC cells for 2hrs and samples were probed with fluorescent antibodies and observed under a fluorescence microscope (magnification: 100 x). Green: actin, Red: EspA filaments, Blue: DNA/Nucleus, b) Quantification of infection efficiency. The percentage of infected HeLa cells was determined after quantifying how many HeLa cells were infected compared to the non-infected ones, in each sample. Three biological repeats were performed, and for each biological repeat three technical ones were performed

Towards this end, plasmids that were carrying the CesAB mutants were transformed in EPECΔcesAB strains and their ability to complement the strains and rescue the phenotype was monitored. The gene expression of these mutants was under tight regulation, so to achieve low amounts of the derivative proteins that were produced. The cells, on one hand, were cultured under secretion permissive conditions and the secretion of EspA was followed, in a time dependent manner, at the external milieu. On the other hand, the same strains were used to infect HeLa cells. In this case, both the secretion of EspA and the formation of actin pedestals were monitored, due to EPEC infection from T3SS secretion of effectors, using fluorescence microscopy. Moreover, to the samples that derived from the infection assay, the ability of the strains used to infect HeLa cells, was quantified, so to acquire more accurate results as far as efficient infection is concerned (see Thesis Chapter 7).

As it was assumed from the NMR data, *in vivo* results showed that the secretion of EspA was reduced in a significant extent and the infection of HeLa cells from the EPEC strains was compromised, when the CesAB mutants that abolish interaction with EscN were used (Figures 4-8, 4-9).

Collectively, the combination of the above structural and functional data provides strong evidence that efficient targeting of CesAB−EspA to EscN is required for EspA secretion. At least in this biological system, it seems that this targeting signal is

encoded on the chaperone, upon conformational changes, which occur only upon binding to its cognate secretory protein.

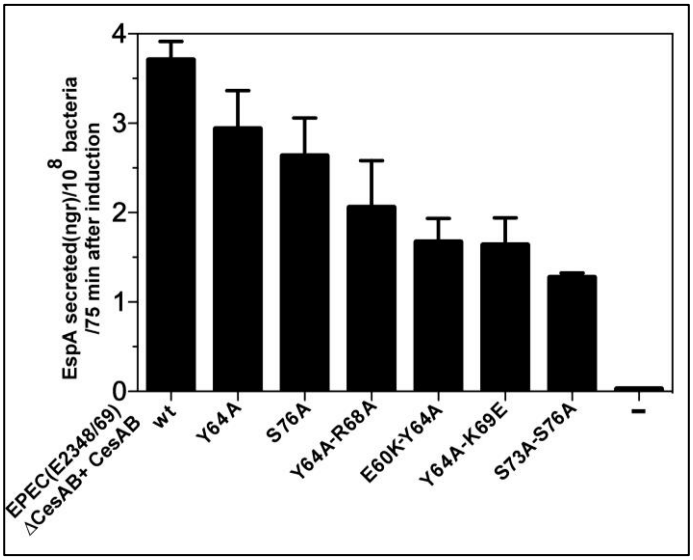

Figure 4-8: *In vivo* secretion of EspA. Bar graphs indicate the amount of EspA being secreted at the external milieu, at the peak of secretion. EspA was detected with Western blot analysis and antibody probing. The amount of the secreted EspA was quantified using Image J software. Data derived from at least three

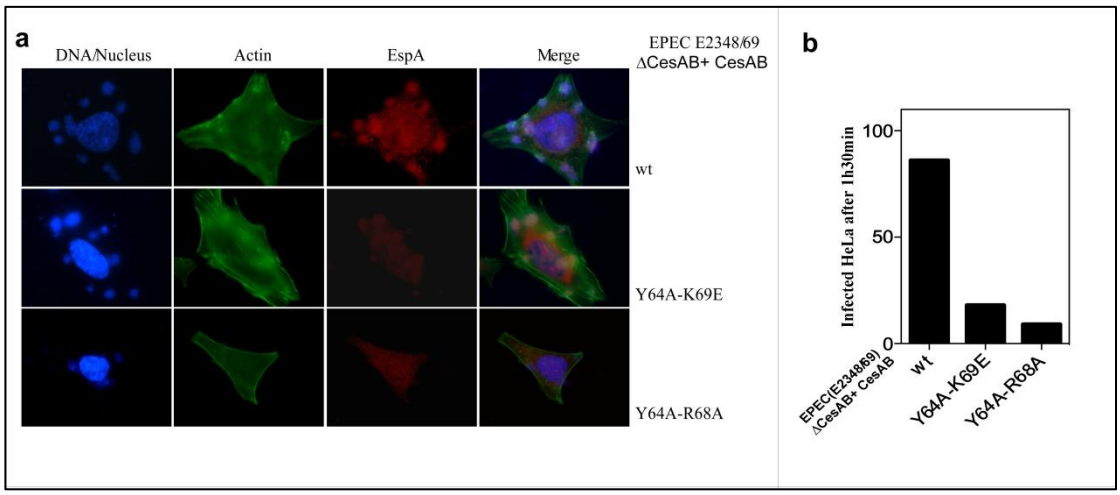

Figure 4-9 : Infected HeLa cells from EPECΔcesAB complemented *in trans* with plasmids carrying wt CesAB mutants. a) Immobilized HeLa cells were incubated with EPEC cells for 1.5 hrs and samples were probed with fluorescent antibodies and observed under a fluorescence microscope (magnification: 100 x). Green: actin, Red: EspA filaments, Blue: DNA/Nucleus, b) Quantification of infection efficiency. The percentage of infected HeLa cells was determined after quantifying how many HeLa cells were infected compared to the non-infected ones, in each sample. Three biological repeats were performed, and for each biological repeat three technical ones were performed

5. Chapter: Targeting to the membrane- a C-tail story

Although many studies have been published about the structure and function of T3SS, the precise mechanism of how proteins are being translocated is poorly understood. Very little is known about the pathway proteins follow from the cytosol towards the membrane and how they are being targeted to the T3SS basal body [36], [74].

To shed more light to the pathway proteins follow in order to be targeted to the bacterial membrane, we focused on one protein complex as a model, that of the translocator EspA and its chaperone CesAB [49], [78]. So far, we have monitored EspA and its interaction with CesAB (Thesis Chapter 3) [48]. Moreover, we have demonstrated that once the CesAB-EspA complex is formed in the cytosol, CesAB can interact with the ATPase of the system EscN (Thesis Chapter 4) [55].

Although, it has been so far demonstrated how proteins interact in solution, what happens at the membrane of the bacterium and what protein-protein interactions occur in order for the secretory protein to be targeted and eventually secreted to the external milieu, has to be elucidated.

CesAB C-tail is essential for EspA secretion

CesAB chaperone has two distinct domains

It has been demonstrated that EspA must interact with CesAB so to be retained unfolded and translocation competent and to be secreted [54], [78]. From the crystal structure of CesAB-EspA that was solved, the carboxyl tail (C-tail) of CesAB was missing [49]. From the biophysical analysis (NMR and CD) it has been demonstrated that CesAB is a simple, dimeric all-helical protein with an extended N-terminal domain and an unstructured C terminal domain. N-domain (N 1-85) consists of three a-helices, α1 (Ile3-Lys46), that is connected to two shorter helices, α2 (Gln50-Glu60)

and α3 (Glu67-Glu83). The C- tail of CesAB (N 86-107) consists of 22 amino acids, where most of them are either polar or charged and show no secondary structure formation (Figure 5-1). Preliminary, unpublished data from the lab, demonstrated that the C-tail is also flexible and disordered.

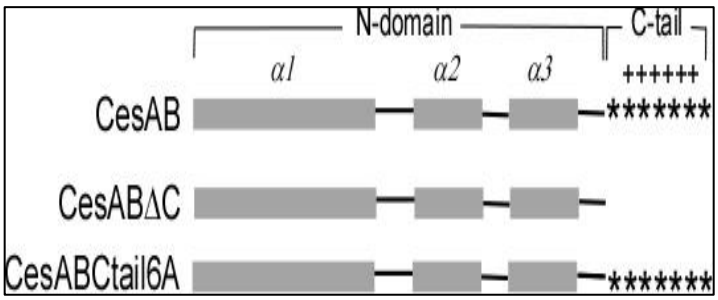

Figure 5-1 Schematic representation of the two CesAB domains. N terminal domain consists of three a- helices, while C domain shows no secondary structure. Two CesAB derivatives are also represented (ΔC, total deletion of the C-tail, and the Ctail 6A, total disruption of the charged amino acids)

C-tail is essential for secretion of EspA and EspB translocators

In order to elucidate the role of the C-tail during protein secretion, two CesAB derivatives were generated. The first one was a complete deletion of the last 22 amino acids, the CesABΔCtail (generated by Dr. Vassileia Balabanidou, Figure 5-1).

The second CesAB derivative was a total disruption of the charged load of the C-tail (Figure 5-1). All the charged amino acids at the C-tail were substituted in alanine. Specifically, four arginines and two lysines were mutated and the Ctail 6A derivative was occurred.

It has been demonstrated recently that apart from EspA translocator, CesAB is also important for the translocator protein EspB [78] as far as its secretion is concerned. It has been clearly demonstrated that EPECΔcesAB cells fail to secrete EspB, apart from EspA, although CesAB is not important for EspB stability on the cytoplasm [20], [78], [107].

The ability of the CesAB Ctail 6A to complement the secretion of the translocators EspA and EspB was monitored *in vivo*. Towards this end, EPECΔCesAB strains were complemented either with wt CesAB or CesAB Ctail 6A and the secretion of translocators was monitored as a function of time during bacterial growth. The secretion profile of the proteins was followed in the spare growth medium using specific antibodies against them (Figure 5-2). The amount of the proteins that was detected in the spare bacterial growth medium was quantified and

compared with the wt levels. Furthermore, the ability of these two CesAB derivatives to cause infection of HeLa cells was examined. Neither CesAB ΔC-tail nor CesAB Ctail6A, were able to complement efficiently EPECΔcesAB and no infected HeLa cells were detected, due to the fact that EspA was not secreted (Figure 5-3).

Collectively, the dramatic effect of these CesAB derivatives as far as EspA and EspB secretion is concerned, indicated, apart from the necessity of the C-tail, also the charging load of it is essential for its function and efficient secretion of translocators EspA and EspB.

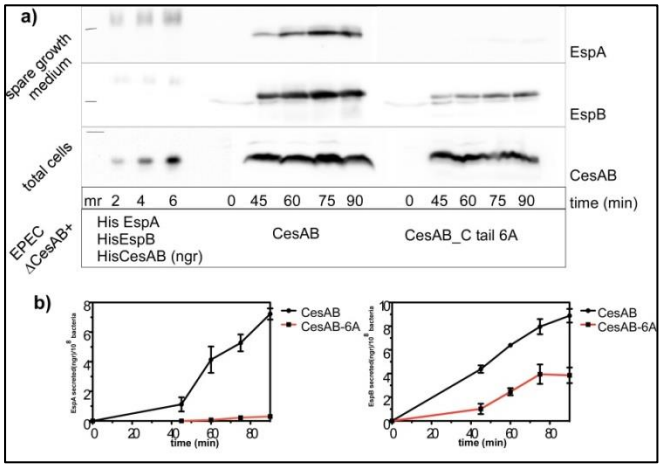

Figure 5-2 C-tail charges are essential for translocator secretion a) *In vivo* secretion of EspA and EspB from EPECΔ*cesAB* strains complemented with plasmid expressing wild-type or CesAB Ctail6A, as a function of time. Secreted EspA and EspB were detected in spare growth medium using specific antibodies against them. CesAB intracellular levels were detected so to ensure that both proteins are expressed equally. b) Quantification of the secreted proteins as a fuction of time, using Image J software, and known concentrations of purified proteins

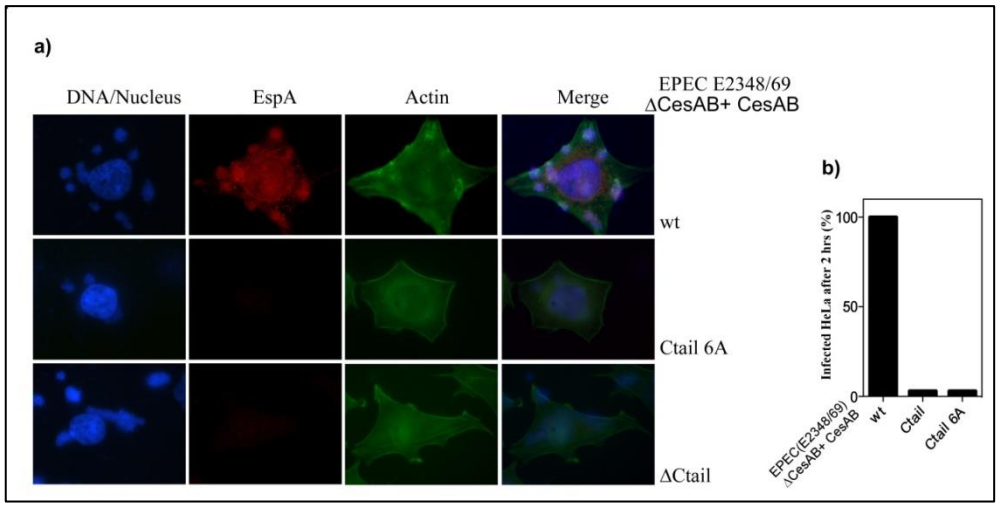

Figure 5-3: CesAB mutants fail to infect HeLa cells a) Immobilized HeLa cells were incubated with EPECΔcesAB cells complemented with wt or mutated CesAB for 2hrs and samples were probed with fluorescent antibodies and observed under a fluorescence microscope (magnification: 100 x). Green: actin, Red: EspA filaments, Blue: DNA/Nucleus, b) Quantification of infection efficiency. The percentage of infected HeLa cells was determined after quantifying how many HeLa cells were infected compared to the non-infected ones, in each sample. Three biological repeats were performed, and for each biological repeat three technical ones were performed

C-tail is not essential for CesAB-EspA complex formation

As already demonstrated in Thesis Chapters 3 and 4, the C-tail of CesAB, although essential for EspA secretion, is essential neither for CesAB-EspA complex formation nor for EscN interaction to occur. As NMR data analysis revealed, only the N-domain seems to interact with the translocator EspA, and the ATPase EscN.

To further validate these data, biochemical characterization of the CesABΔCtail-EspA complex, *in vitro*, was performed. First the proteins were co-expressed from the same vector, but only CesAB wt or mutant was His-tagged. Afterwards, co-purification of the two proteins was performed and the eluted complex was characterized with SEC-MALS analysis. This analysis revealed that CesABΔCtail can interact with EspA in solution so to form the heterodimer (Figure 5-4). As a consequence, the fact that EspA is not secreted is not due inability to interact with its chaperone that would result in aggregation of the secretory protein and therefore no secretion.

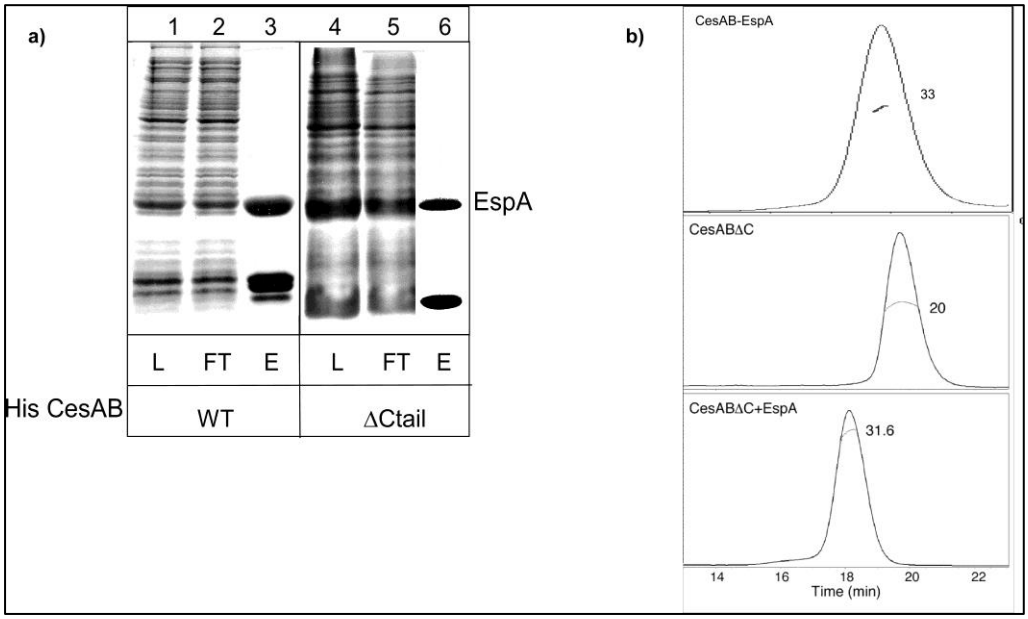

Figure 5-4: C-tail is not essential for CesAB- EspA complex formation a) Co-purification of His CesAB wt or ΔCtail with tag-less EspA. L=loading sample, FT= flow through, E= elution, b) SEC-MALS analysis of the complexes formed after co-purification. Mass measurements are also indicated in each chromatogram, as derived from MALS detector

C-tail is important for membrane targeting *in vivo*

As demonstrated above, the C-tail of the chaperone was not essential for the stability of the translocator EspA, but it was essential for the secretion of both EspA and EspB translocators. Specifically the charged amino acids on the C-tail are important for its function which could indicate electrostatic interactions between the chaperone's C-tail and other proteins, since substitution of the them with Alanines resulted so secretion of the translocation (CesABCtail6A mutant) . From these results, the hypothesis that was made was that the C-tail could play a role for the membrane targeting of the secretory proteins.

To address this question, we have performed sub-cellular fractionation assay. Briefly, EPECΔcesAB cells that were complemented with wt or C-tail mutants were cultured under secretion permissive conditions. The bacteria were harvested and cells were lysed, using sonication. After removal of the unbroken cells using a low spin centrifugation step, ultracentrifugation was performed of the total cell extracts so to separate the cytosolic fraction that contained the majority of soluble proteins, from the membrane fraction that contained the membrane proteins and the peripherally associated ones. The migration profile of the proteins was followed using specific antibodies against them.

Previous results from the lab have shown that indeed, there is no EspA or CesAB migrating at the membrane when the C-tail of CesAB was missing. Moreover, the amount of EspB detected at the membrane fraction had dramatically reduced. However, when these experiments, were repeated for the present thesis, the results were quite different. The amount of CesAB detected at the membrane showed no difference between the wt and the mutants. Moreover, the EspA translocator, although in reduced levels, was detected at the membrane fraction when the C-tail mutants were used for complementation (Figure 5-5).

From these results, and due to the discrepancies observed from the *in vivo* sub-cellular fractionation, although there were indications for not sufficient membrane targeting due to the absence of the C-tail, it was of evanescence need to reconstitute the system *in vitro*, so to elucidate the mechanism that proteins follow in order to be targeted at the membrane.

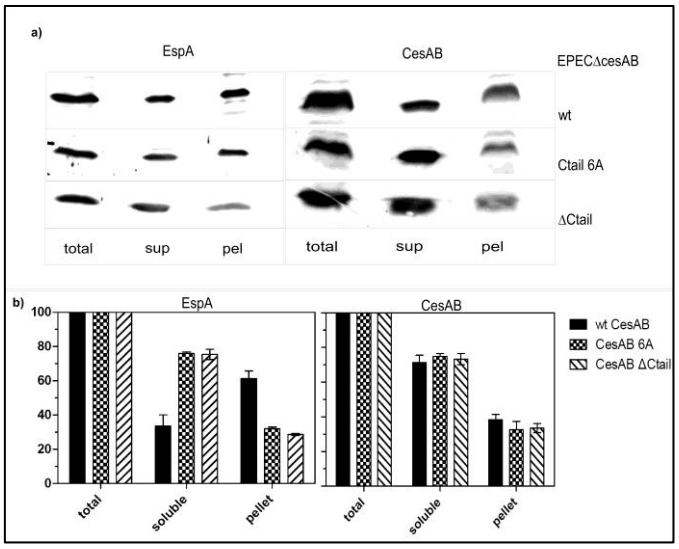

Figure 5-5: Sub-cellular localization of CesAB and EspA. a) Typical sub-cellular migration profile of wt CesAB, CesAB ΔCtail or Ctail 6A, and EspA. EPECΔcesAB cells that were complemented with CesAB wt or C-tail mutants were harvested and the migration profile of the chaperone and the translocator was detected using antibodies against them. b) Quantification of the detected amount in each fraction for each protein was performed using Image J software. The amount detected in each fraction, was normalized according the total amount of protein detected overall. Total= total cells, soluble= soluble fraction derived after cell lysis and ultracentrifugation, pellet= membrane fraction that derived after re-suspending the pellet from ultracentrifugation.

In vitro reconstitution of membrane targeting

Although it is of evanescence need the *in vitro* reconstitution of T3SS, so to elucidate the membrane interactions in the minimal background possible, it has never been tried before. According to the general idea in the field due to the high complexity of the system as far as protein composition and regulation is concerned, it is not possible to purify an intact and functional machinery and reconstitute the secretion process through it *in vitro*. However, we tried to do so, and managed to purify Inverted Membrane Vesicles (hereafter IMVs) that contain T3SS on them. Moreover, we have established an *in vitro* assay to follow membrane targeting of proteins.

Purification and characterization of IMVs from wt EPEC

In order to generate and purify IMVs from wt EPEC, we took into advantage the tendency bacterial membranes have to invert and form vesicles after cell lysis with high pressure [108]. Towards this end wt EPEC were cultured under secretion permissive conditions and harvested at the peak of protein secretion through T3SS.

Cells were lysed using high pressure and IMVs were separated from other membrane fragments using step-sucrose gradient. In general, IMVs are migrating in different sucrose density compared to inner or outer membrane fragments [108], [109]

In order to validate the success of the purification protocol that we established, we used *in vitro* assays that have already been published and are completely un-biased to the procedure followed and un-related to T3SS function. We examined whether the ATPase SecA can associate with the EPEC IMVs, by measuring the ATP hydrolysis activity that it has, in the presence of IMVs and in the presence of the secretory protein Alkaline Phosphatase (proPhoA). Moreover, we have detected the proPhoA being translocated into the IMVs, after performing *in vitro* translocation assays [110]. In parallel, with EPEC IMVs, IMVs from BL31 (a typical *E.coli* lab strain that is being used for such experiments) were used to compare our results. EPEC IMVs were functional as far as the SecA ATPase activity and proPhoA *in vitro* translocation were concerned (Figure 5-6).

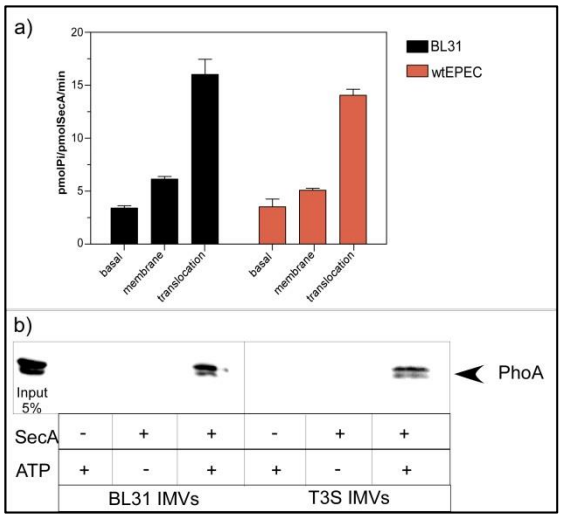

Figure 5-6: Characterization of EPEC IMVs using well-established assays. a) ATP hydrolysis activity stimulation from SecA ATPase, in the presence of IMVs from wt EPEC (red panels) or BL31 (black panels). Stimulated ATPase activity is detected when IMVS (membrane) or IMVs and secretory protein (translocation) is added in the reaction, compared to the one the enzyme has on its own in solution (basal). b) *in vitro* translocation of proPhoA. The secretory protein proPhoA can be detected in the IMVs, only in the presence of SecA and ATP, indicating an enzymatic procedure. Overall the results are comparable, indicating that EPEC IMVs are functional.

Additionally, to the functional assays described above that were used to verify the success of the purification protocol, it was of evanescence need to examine the existence of the T3SS injectisome on them. In order to do that, due to the fact that there was no assay related to our system, we used scanning electron microscopy (SEM) to observe the IMVs, and immune-gold staining coupled with negative staining to detect membrane proteins from T3SS on them. Towards this end, we overlaid on EM-grids EPEC IMVs and probed them with antibodies against the

transmembrane T3SS protein, EscV. EscV is a protein that has two distinct domains, a transmembrane domain that is localized in the inner membrane of the T3SS forming ring-like structure [33], and a cytosolic one that could be detected with antibodies, only if the IMVs were indeed inverted. As it was expected, from the EM data acquired, we verified on one hand the existence of T3SS on the isolated IMVs, and on the other hand the fact that the vesicles were inverted (Figure 5-7).

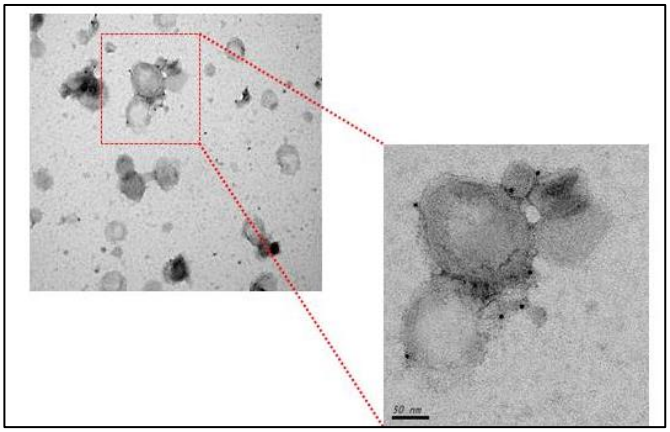

Figure 5-7: Immuno-staining of EPEC IMVs coupled with Electron microscopy. EPEC IMVs were immobilized on EM-grids and probed with antibodies against protein EscV and then with gold particles (5nm). Negative staining was performed and samples were observed using scanning electron microscopy (SEM). Gold particles were peripherally localized to the outer membrane, where EscV should be in T3SS.

In vitro reconstitution of membrane targeting in T3SS

Once IMVs from EPEC were characterised and the existence of the T3SS was verified, we established a binding assay to monitor the membrane targeting process of T3SS related proteins. To do that we took into advantage the fact that IMVs migrate to a specific sucrose concentration solution that is equal to their own density, once they were overlaid to a sucrose gradient. On the contrary, purified proteins do not enter the sucrose gradient, due to its high viscosity. However, if a protein or the protein complex is associated with the IMVs, it will migrate to the same sucrose concentration solution with them. As a result, using antibodies against specific proteins, we were able to detect whether cytosolic proteins co-migrate with IMVs at the same sucrose fraction which is a strong indication of membrane association of these proteins (Figure 5-8) [111].

Towards this end, we have purified the chaperone CesAB in complex with the tranclocator EspA and monitor their migration profile in the presence of EPEC IMVs, using antibodies against these proteins. According to these results, CesAB- EspA protein complex is associated with the membranes due to co-migration in the same sucrose fraction. The interaction detected is specifically related with T3SS membrane components, due to no interaction detected when IMVs derived from BL33(DH3) (no T3SS on them) has been used with CesAB-EspA complex (Figure 5-9).

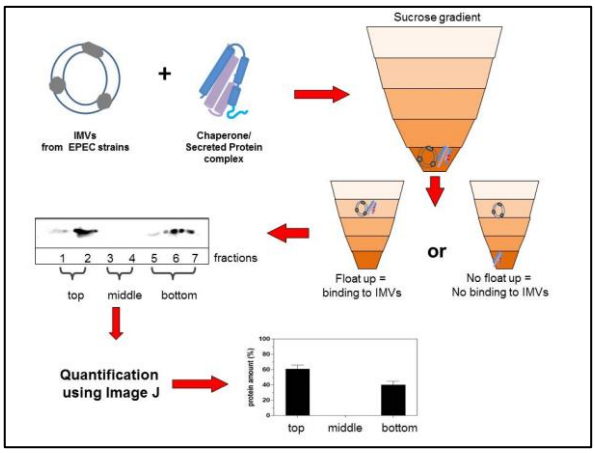

Figure 5-8: Schematic representation of the workflow followed in order to assay the membrane binding. Briefly, IMVs from various EPEC strains where mixed with purified CesAB- EspA or mutants and on top of them a sucrose gradient was formed. If the protein complex was to interact with the IMVS, it would be detected to the top fractions. Otherwise it would be unable to enter the gradient, and would be detected at the bottom fractions. The intensity of the signals, derived after immuno-detection was measured using Image J software. The amount of the protein detected in each fraction was normalized according to the total amount of protein detected in all fractions.

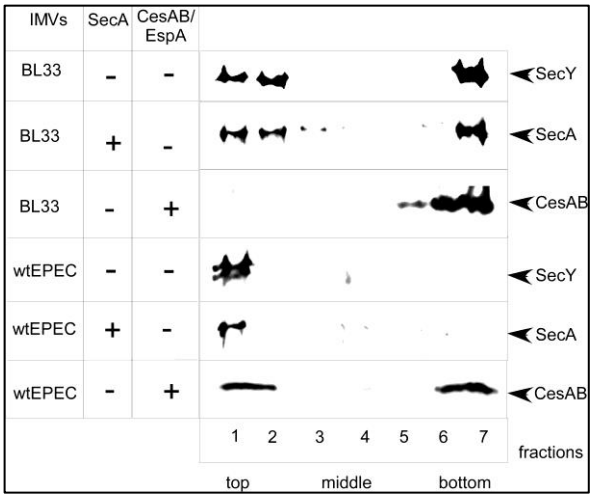

Figure 5-9: *in vitro* membrane binding of CesAB/EspA protein complex in EPEC IMVs. Migration profile of purified protein complex CesAB/EspA in the presence of IMVs derived from EPEC or BL33. Membrane association is detected only when the T3SS is present. As a control of the procedure SecA ATPase is shown, which is associated to *E coli* membranes at the SecYEG translocase. Immuno-blotting analysis was performed using antibodies against CesAB to detect the CesAB/EspA complex, against SecA and against SecY as a membrane protein to detect IMVs migration profile.

C-tail of CesAB is essential for membrane association of CesAB-EspA complex, interaction that is triggered by EspA.

From *in vivo* sub-cellular localization, it has been demonstrated that CesAB or EspA cannot migrate or migrate inefficiently to the membrane of the bacteria when

the C-tail of CesAB is missing. In order to determine whether the CesAB- EspA complex can be associated to the membranes also *in vitro*, and if the C-tail of the chaperone is essential for this interaction, we have used the membrane binding assay, described above (see also Thesis Chapter 7). First we have purified CesAB-EspA complex, wt, or CesAB-EspA complex where the C-tail of CesAB was deleted. These data resulted that when the C-tail was missing, the protein complex could not migrate to the same fractions where the membranes were. Moreover, the binding of CesAB on its own was also determined. Significantly reduced membrane binding was detected when the chaperone was on its own. Collectively, neither CesAB, nor CesABΔCtail-EspA was able to interact with the EPEC IMVs (Figure 5-10, see also APENDIX). From, these findings, we hypothesised that structural conformations on CesAB, occur upon binding to EspA (Thesis Chapter 3, [48]), leads to the exposure of the C-tail of the chaperone which can interact with the membrane protein components on IMVs.

To test the above hypothesis, we used a CesAB mutant, CesAB DRE that cannot interact with EspA but its structure is similar to the one CesAB acquires in a EspA-bound state [48], [55]. The CesAB DRE mutant was also detected to co-migrate with the membranes like the wild type complex, indicating a strong interaction. To verify, that the binding of CesAB DRE to the membranes was C-tail mediated also in that case, a CesAB derivative, the CesAB DREΔCtail was generated. From this CesAB mutant the C-tail was also deleted. As it was hypothesized, the CesAB DRE ΔCtail was not able to co-migrate to the sucrose fraction where the IMVs were (Figure 5-10, see also APENDIX).

Conclusively, from these experiments resulted that CesAB-EspA can be targeted to EPEC IMVs, via C-tail. However, this membrane binding is an EspA-driven interaction, perhaps due to allosteric exposure of the C-tail upon EspA binding to CesAB.

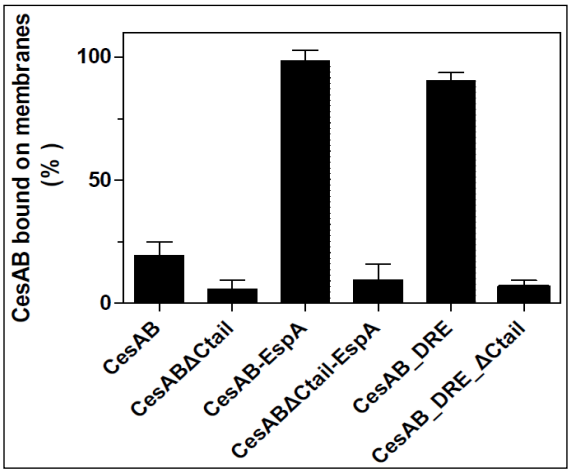

Figure 5-10: Membrane association of CesAB-EspA wt or derivatives. Bar graphs indicate the percentage of wt CesAB or CesAB derivatives, with or without the presence of EspA bound on wt EPEC IMVS. Migration profile of the proteins was detected using polyclonal antibodies against the chaperone CesAB in different fractions collected after ultracentrifugation of the sucrose gradient. The intensity of the signals was quantified using Image J software. Data were normalized after setting the amount of CesAB-EspA migrating to top fraction with IMVs as 100%

CesAB-EspA complex cannot be bound when specific T3SS membrane components are missing

Once we have determined that the targeting of CesAB-EspA complex to the membranes is being held via the C-tail of CesAB chaperone, upon binding to the translocator EspA, our next goal was to determine the protein receptor of the complex at the membrane. In order to do so, we used EPEC IMVs that derived from EPEC strains that essential genes for T3SS function have been deleted. T3SS is a very complicated and highly regulated system and many proteins are essential for its function, either by regulating the formation of the basal body of the system or by regulating the protein secretion [29], [30]. There are many proteins associated to the membrane and are essential for secretion through T3SS, which could also serve as potential protein-receptors for the CesAB-EspA complex at the membrane [30]. In order to elucidate the protein-receptor, we purified IMVs from all the EPEC deletion strains that fail to secrete EspA and the genes that are deleted are expressing proteins that are either inner membrane embedded, or peripherally associated to the membrane. The migration profile at the sucrose gradient of CesAB-EspA complex was followed when these IMVs were used.

Surprisingly, although all the proteins that were missing from the membranes are essential for EspA secretion *in vivo*, are not essential for membrane binding of the

chaperone-secretory complex (Figure 5-11, see also APENDIX). These results were the first indication that membrane targeting on T3SS basal body is a distinct process from protein secretion through the system.

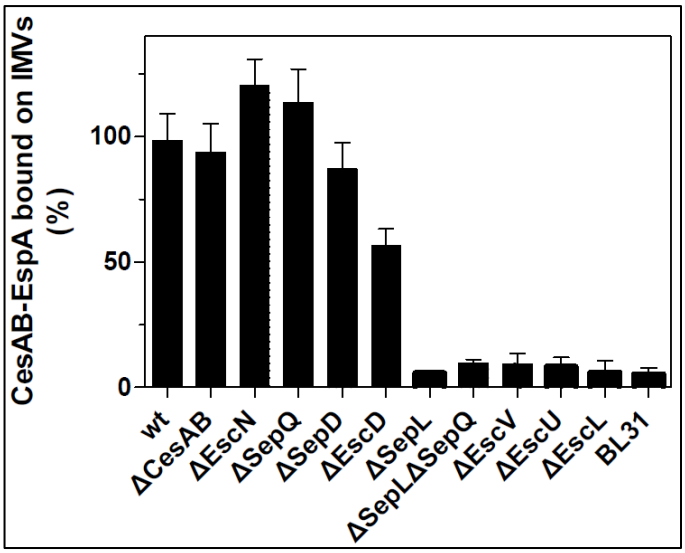

Figure 5-11: Membrane association of wt CesAB-EspA to IMVs derived from EPEC wt or deletion strains. Bar graphs indicate the percentage of wt CesAB-EspA protein complex bound on EPEC IMVS derived from EPEC wt or deletion strains that fail to secrete EspA, and the proteins that their genes have been deleted are localized to the cytosolic part of the inner membrane at the injectisome. Migration profile of the proteins was detected using polyclonal antibodies against the chaperone CesAB in different fractions collected after ultracentrifugation of the sucrose gradient. The intensity of the signals was quantified using Image J software. Data were normalized after setting the amount of CesAB-EspA migrating to top fraction with IMVs as 100%

Gate-keeper protein, SepL, is essential for membrane targeting of CesAB-Esp, but not the membrane-partner

The protein SepL acts as a "gate-keeper" and regulates the hierarchy of protein secretion [54], [77]. When the *sepL* gene has been deleted from the bacterial chromosome, only effector proteins (late secretory proteins) are being secreted from the system. This indicates that SepL is essential for protein secretion and somehow regulates the secretion of the translocators (early secretory proteins) [74].

When IMVs derived from EPEC ΔsepL strains were used to monitor CesAB-EspA protein complex binding, we detected no binding on them. Moreover, when the *sepL* gene was deleted from EPECΔsepQ stain, so the double EPEC ΔsepQ/ΔsepL was generated, again the membrane interaction of CesAB-EspA protein complex was vanished (Figure 5-11).

Furthermore, using radio-labelled CesAB-EspA protein complex, we measured the amount of CesAB- EspA that was bound on EPEC IMVs, in a wide concentration range. From these measurements, we estimated the affinity (K_d constant) of the complex for EPEC IMVs (see Thesis chapter 7, and APENDIX). The CesAB-EspA

Kd constant for wt EPEC IMVs was measured around 25 nM, while the save value could not be measured for EPECΔsepL IMVs, in the same concentration range. From these results, we have demonstrated that SepL is essential for the targeting of the CesAB-EspA complex to the membrane. But is protein SepL the protein receptor that we are looking for?

To answer the above question, we performed co-purification experiments. However, when the His-CesAB-EspA complex was immobilized on Ni-NTA beads we detected no SepL protein bound on them, at the eluted material. Moreover, using SEC- MALS, we failed to detect a ternary complex being formed (Figure 5-12). Furthermore, we used antibodies against protein SepL to detect and measure the protein concentration on EPEC IMVs. To our surprise, the amount of the protein on EPECΔsepQ IMVs was significantly reduced compared to the amount detected on the wt IMVs (Figure 5-12), although the binding of CesAB-EspA complex on these IMVs is at wt levels (Figure 5-11). Finally, according to preliminary quantification results there is no relevant stoichiometry between the amount of CesAB-EspA bound on IMVs and the amount of SepL detected on them. It appears to be one molecule SepL interacting with 10 molecules of CesAB-EspA complex.

Collectively, from the above results, although protein SepL presence at the EPEC IMVS is essential for CesAB-EspA membrane targeting, is not the protein receptor of the complex on the membrane.

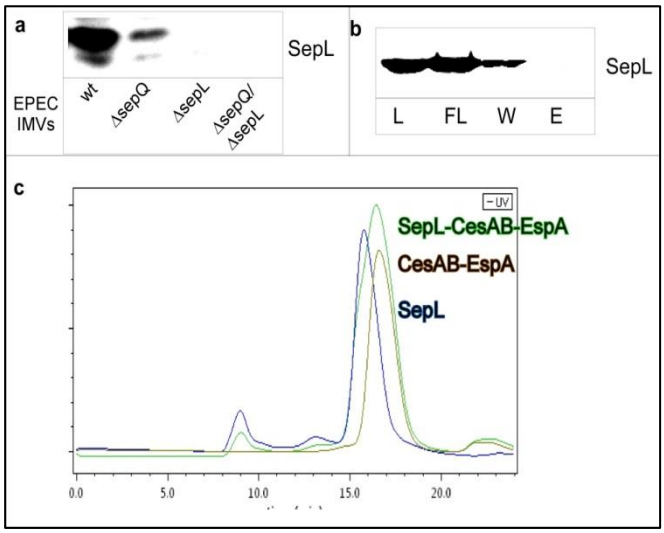

Figure 5-12: SepL does not interact with CesAB-EspA protein complex in solution. a) Amounts of SepL detected using specific antibodies against the whole protein, on IMVs derived from wt or EPEC Deletion strain. The amount of SepL is significantly reduced on ΔsepQ IMVs. b) Co-purification of SepL with His CesAB-EspA using Ni-NTA affinity chromatography under native conditions. No SepL protein was co-eluted with the CesAB-EspA complex, indication of no interaction in solution. L=loading, FT= flow through. W= wash, E= elution, c) Overlapped chromatographs that derived after SEC-MALS analysis. No complex formation detected between SepL- CesAB-EspA. Purified SepL (blue line), CesAB-EspA protein complex (brown line), and SepL-CesAB-EspA chromatograms (green line) are shown.

Potential receptors for SepL and/or CesAB- EspA complex could be either protein EscV or protein EscU.

EscU is a membrane protein, with a large cytoplasmic domain that has been showed to interact with T3SS components and is also essential for secretion. The cytoplasmic region of EscU is cleaved and this somehow regulates the protein secretion hierarchy, by causing conformational changes to the translocase that prevents or permits protein interactions with it [32], [42].

Protein EscV is also a transmembrane component, essential for secretion with a cytoplasmic domain that could serve as a platform for chaperone-secretory protein binding [112]. Using homologous proteins from other bacteria, it has shown to form a nonameric ring that surrounds the export aparratus of the system. Combination of data that have derived from the crystal structure, cryo-EM analysis and *in vivo* experiments, demonstrate that EscV ring needs to be formed and localized properly in order to have a functional system [33], [113] .

According to the literature, these two membrane proteins could be the missing partner for protein SepL and/or the protein complex CesAB-EspA at the membrane. To test this hypothesis, the membrane binding assay was performed in EPEC deletion strains, where the genes for proteins EscU or EscV was deleted.

When, we used IMVs derived from EPECΔescU or EPECΔescV, CesAB-EspA complex was not co-migrating with the membranes (Figure 5-11). These results pointed out the necessity of these two proteins to be localized at the membrane, so that the chaperone-secretory protein complex can be associated with the IMVs. Afterwards, the existence of protein SepL on the IMVs that derived from these deletion strains was examined. The protein levels of SepL that were detected using specific antibodies were significantly reduced, almost no SepL was detected at EPECΔescU or ΔescV IMVs (Figure 5-13).

Furthermore, we wanted to detect protein interactions between proteins SepL and/or the EscV or EscU. To do so, the cytoplasmic parts of these membrane proteins were cloned and purified using affinity chromatography. Afterwards, the purified proteins were used either for *in vitro* co-purification assays, or SEC-MALS analysis, to determine any protein interactions that could occur in solution.

When the cytoplasmic domain of protein EscV was used as a bait, the protein SepL was detected in the elution fraction, and no complex was formed when the proteins analyzed together using SEC-MALS. These results indicate that there is no strong interaction between protein SepL and the cytoplasmic domain of EscV in solution. However, these negative results could not explain the fact that SepL is absent from the EPECΔescV IMVs (Figure 5-13b). Further analysis is needed so to elucidate whether the protein EscV is the protein receptor for SepL and/or CesAB-EspA protein complex at the membrane. Our next goal will be to determine whether the CesAB-EspA protein complex can interact with protein EscV, in solution.

When EscU cytoplasmic domain was used as bait, a small amount of SepL was co-purified, indicating that these two proteins could interact. However, when SEC-MALS analysis was used to detect and characterize the interaction, no complex formation was detected between the protein SepL and the cytoplasmic domain of EscU. This was also true even when the CesAB-EspA protein complex was added in the reaction with EscU or with EscU and SepL (Figure 5-14).

Collectively, from the above data, it has been demonstrated that the basal body components, proteins EscV and EscU are essential for membrane targeting of CesAB-EspA protein complex and for SepL localization at the membrane. The molecular mechanism of this targeting procedure needs to be elucidated. Having in mind the complexity of the system and the transient nature of the membrane interactions, additionally to conformational changes that could occur upon membrane binding of all these proteins, perhaps the interactions that we want to map, is not easy to be demonstrated in solution. As a result, our next goal is also to determine whether the CesAB-EspA protein complex and/or SepL protein can interact with protein EscU on the membranes, using cross-linking experiments.

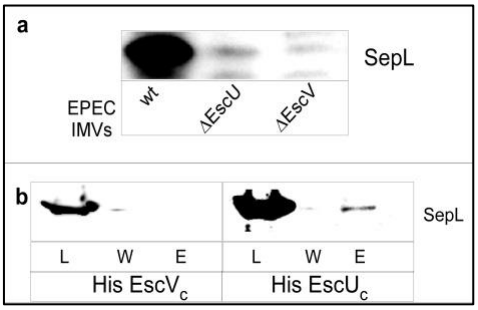

Figure 5-13 : SepL may interact with proteins EscV or EscU. a) Almost no SepL can be detected on IMVs derived from EPECΔescU or ΔescV, compared to the wt ones. b) SepL cannot be co-purified when the cytoplasmic domain of EscV(His EscV$_c$) was used, while a small amount of SepL was detected when the cytoplasmic domain of EscU (His EscU$_c$) was used. L=loading, W= wash, E= elution.

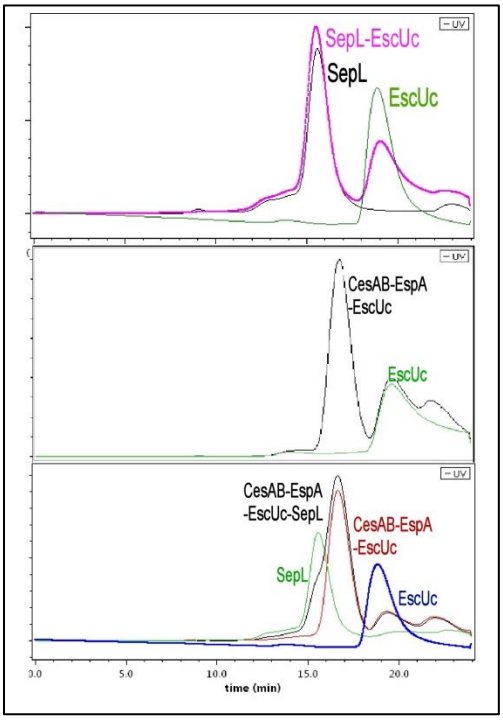

Figure 5-14: CesAB-EspA protein complex and/or SepL do not interact with EscUc. No complex formation detected after SEC-MALS analysis between proteins EscU, SepL and/or CesAB-EspA complex. Chromatograms represent the UV absorbance of the proteins analyzed alone or in the same reactions with other proteins. No complex formation was detected with EscUc and SepL proteins, neither between CesAB-EspA and EscU, nor when all the proteins were mixed together as indicated on each chromatogram. The molar ration in all the reactions was 1:1 per protein used.

6. Chapter: Discussion

Type III secretion system (T3SS) is a widespread virulence system, in many Gram negative bacteria. This specialized nano-machine is used to transport effector proteins directly from the bacterial cytosol into the eukaryotic host cell by spanning three membranes, two bacterial and one eukaryotic. In order for the system to become functional and active more than 50 proteins need to be co-ordinated so to the system be assembled and the proteins be secreted through it [41], [82]. Both processes undergo sophisticated regulation. Although recent structural and biochemical studies provide information about the assembly of the system, the understanding of the molecular mechanism behind the translocation process remains elusive. During this PhD thesis, we tried to determine the pathway proteins follow from the bacterial cytosol towards the membrane, so to be secreted through the system. We tried to map the protein-protein interactions that occur so that the secretory proteins be targeted to the membrane and how the specialized chaperones of the system mediate this procedure.

Enterophathogenic *E. coli* was used ss a model organism, and in a first global approach, we performed a comprehensive analysis of the protein complexes formed in the bacterial cytosol, during Type III protein secretion. In brief, cytosolic protein complexes were isolated and fractionated by two complementary approaches: Native polyacrylamide gel electrophoresis and size exclusion chromatography. Moreover, selected His-tagged T3SS-proteins were used as baits for the selective isolation of T3SS- protein interactors. Protein subunits of the complexes were identified by "bottom-up" proteomics using an LTQ-Orbitrap. Moreover, protein quantification was performed using label-free approaches, in order to quantify the abundance of the protein complexes in the bacterial cytosol as a function of time during bacterial growth and correlated with protein secretion through the system. Protein complexes identified from this analysis, were validated with immuno-detection using specific antibodies against known proteins of T3SS. Furthermore, single gene knock-out mutants were used and their complexome profile was also determined with MS and compared with the wt one to verify the formation of specific protein complexes and validate our initial findings.

The combination of the above approaches yielded the reliable identification of more than 1300 unique cytosolic proteins from EPEC cells. These proteins correspond to ~28% of its total theoretical proteome and ~50% of its predicted cytosolic proteome. The identified proteins represent a wide range of cellular processes as revealed from their GO annotations, which is required for a reliable and comprehensive subsequent complexome and protein network analysis. Global complexome analysis determined more than 150 putative cytosolic protein complexes in EPEC including many previously reported complexes in laboratory strains of *E.coli*, providing validation for our approach. Targeted cytosolic complexome analysis focused on the 54 predicted T3SS-related proteins (LEE and non-LEE encoded, membrane proteins are not included). Several T3SS pre-secretion protein complexes and interactions were thus identified in the EPEC cytosol after excuding the background of *E. coli* house-keeping complexome. More than 15 key cytosolic proteins of EPEC pathogenesis such as EspA, EspB, EspD, CesAB, CesD, Tir, CesT and Map were identified as components of these protein complexes. The time-dependent complexome analysis of EPEC provided significant information about the dynamics of T3SS-related chaperone-substrate protein complexes during type III protein secretion. This information was correlated in a time-dependent manner to the orderly secretion of more than 20 specific effectors identified in the extracellular milieu, thus correlating the dynamics of the intracellular T3SS complexome with specific secretion of individual effectors.

These data reveal a dynamic exchange between T3SS components depending on the secretion state of the EPEC cell. Our pipeline is generally applicable to the dissection of cellular sub-complexomes in any cell (Chapter 2, Aivaliotis, et al, in preparation).

In a more targeted approach, we focused on the secretory protein EspA and its cognate chaperone CesAB [78]. The secretory protein-chaperone complex was used as a model protein complex for T3SS, in order to map the pathway towards the membrane. Towards this end, we first characterized the protein complex formed when the chaperone is on its own in solution, afterwards, the one that is formed when the chaperone interacts with the translocator EspA, and finally the ternary complex formed between CesAB-EspA and the ATPase of the system, combining in solution NMR, biophysical tools and biochemical assays.

A generic feature among some T3SS systems is the co-transcription of the chaperone and substrate genes, so to form rapidly protein complexes, and prevent unspecific interactions in the cytoplasm. However, in EPEC, the *cesAB* and *espA* genes are located 25-kilobases apart and are thus not co-transcribed. From the structure of CesAB-EspA has been shown that the chaperone CesAB uses an extensive hydrophobic surface to bind to EspA[49]. After solving the structure of the CesAB chaperone with NMR alone, it was demonstrated that CesAB forms a homodimer in order to bury the hydrophobic surface and prevent aggregation. Moreover, the EspA-binding site is occluded in the homodimer and thus CesAB adopts an auto-inhibitory conformation.

Because EspA has a strong tendency to quickly self-oligomerize proper function of the T3SS system requires that CesAB rapidly capture EspA in the monomeric state. Because of the opposite charge of CesAB and EspA (pI is ~9.2 and 4.3, respectively), electrostatic steering could accelerate the association kinetics of complex formation. However, given the fact that CesAB exists in an auto-inhibitory conformation, fast and productive formation of the CesAB−EspA heterodimer can occur only if CesAB becomes somehow activated for EspA binding. Indeed, the activation mechanism is strongly stimulated by packing defects at the $\alpha1-\alpha3'$ interface originating in coiled-coil sequence irregularities. Generation of point-mutations that corrected these sequence irregularities suppressed the activation mechanism giving rise to no complex formation between the chaperone and the secretory protein, which resulted in a non-functional T3SS system, due to EspA self-oligomerization that causes aggregation.

Furthermore, coiled-coil sequence irregularities at the $\alpha1-\alpha1'$ interface on CesAB resulted in a rather unstable dimerization interface in CesAB, enhancing the efficiency of the partner exchange mechanism. Although the instability and dynamic nature of the $\alpha1-\alpha3'$ interface is crucial for the activation of CesAB, the $\alpha1-\alpha1'$ interface, which consists the main dimerization interface, is also important for the formation of a functional CesAB−EspA complex. However, on one hand, the low stability of the $\alpha1-\alpha1'$ interface ensures that all of the CesAB homodimer will dissociate so to form a complex with EspA. On the other hand, if the inter-subunit contacts at the $\alpha1-\alpha1'$ interface were optimal, the resulting heterodimer would have been more stable than the wild-type CesAB−EspA complex, and that would have prevented EspA secretion, presumably because the heterodimer is impossible to dissociate at the injectisome

base, thus resulting in a non-functional system (e.g. in the case of CesAB (E20L/E30L) – EspA (R174L/Q181L)).

Apparently, in order to carry out its function with maximum efficiency, the CesAB chaperone has evolved to adopt a partially folded, molten-globule-like conformation. Such a conformational state affords CesAB a significant regulatory capacity, resulting finely tune the structural and dynamic properties of both $\alpha 1-\alpha 1'$ and $\alpha 1-\alpha 3'$ interfaces simultaneously. Moreover, it is of particular interest that the translocator EspA makes use of structural mimicry to interact with the homodimeric CesAB chaperone, displace one of the subunits and form a stable heterodimeric complex (Thesis Chapter 3, [48]).

The targeting of the secretory proteins at the T3SS injectisome is the first crucial step for the efficient secretion of the translocator and effector proteins into the eukaryotic cell. The cytosolic basal structure of the injectisome is somehow capable in discriminating the T3SS secretory proteins from all the other bacterial proteins; yet, the molecular basis for this process remains poorly understood.

Several studies have focused on the determination of the so-called secretion signal. By secretion signal, studies referred to the region of the T3SS secretory protein that somehow regulates or catalyzes its secretion process [51]. The existing results have suggested, in certain cases, that specific sequences in the N-terminal region of the effector and translocator proteins play a role as a secretion signal [114], [115]. On the other hand, in other cases, it has been suggested that the secretion signal is encoded in the messenger RNA sequence [116]. The literature discrepancies and fuzziness are due to the complexity the whole secretion process from T3SS has and the lack of *in vitro* assays to determine it.

In order to shed more light in the targeting mechanism secretory proteins follow in order to be secreted from the T33SS, we first characterized the ternary complex between the ATPase and the secretory protein-chaperone complex, using in solution NMR. Afterwards, we established an *in vitro* membrane binding assay and mapped the membrane targeting pathway proteins follow in order to be secreted.

The T3SS ATPases are conserved among Gram negative bacteria with T3SS systems and share high structural and functional homology with the F_1F_0 ATPases. Previous studies have demonstrated that in order to become active, these molecules need to self-oligomerize and form hexamers or dodecamers, the formation of which

and the overall activity of the enzymes is under tight regulation [58], [85], [100]. T3SS ATPases are localized in the cytosolic domain of the injectisome and are essential for T3SS secretion possible in engaging T3SS secretory proteins [56], [102]. These features make the ATPase of the system a perfect protein- candidate for the targeting of the secretory protein to occur. To verify this hypothesis, first we performed biochemical characterization of the ATPase of T3SS in EPEC, EscN. Afterwards, we determined the interactions occurred between the ATPase of the system with the chaperone-secretory protein complex, CesAB-EspA, using in solution NMR.

Our biochemical results demonstrated that, the EscN ATPase functions as a hexamer and its oligomerization and enzymatic activity depends on concentration and temperature. Moreover, according to the binding interactions derived from NMR analysis, a ternary complex is being formed only between EscN and CesAB- EspA protein complex. EscN hexamer cannot interact with CesAB homodimer, and CesAB-EspA complex cannot interact with EscN monomer. After mapping the interactions occurred during the ternary complex formation, we have identified that the targeting signal for EscN binding is on CesAB. However, this signal is encoded in a conformational switch in the chaperone, CesAB, which is induced only upon the binding of the physiological substrate, EspA. These results suggested that binding of EspA to CesAB poises CesAB for interacting with EscN by eliciting a disorder-to-order transition state that stabilizes the formation of the region which is specifically recognized by EscN. Additionally, we have proven also *in vivo*, that the interactions between the chaperone- secretory complex with the ATPase of T3SS, is essential for the secretion of EspA, thus for the function of T3SS.

Collectively, having in mind that the targeting and secretion of the CesAB-EspA chaperone- substrate system are controlled by different signals (the targeting signal is encoded in the CesAB, while the secretion signal is located in the N-terminal region of EspA[107]) we concluded that the EscN ATPase can be served as the docking platform for chaperone-substrate complexes, and additional proteins of the cytosolic part of basal body of the injectisome could regulate downstream events during T3SS secretion pathway (Thesis Chapter 3, [55]).

Although, the identification of the targeting signals on CesAB to interact with the ATPase of the system was a significant indication of how the secretory protein-

chaperone complex is being targeted to the ATPase, presumably at the membrane, previous unpublished data could not be explained from this interaction, as far as secretion process is concerned. Having also in mind that the membrane targeting and the protein secretion are distinct procedures, our next goal was to determine the protein interactions at the membrane, and map downstream events during secretion process.

Although, the EscN-binding domain on CesAB main body is important for secretion, the C-tail of the chaperone is essential for translocator proteins secretion, and thus T3SS function. The C-tail of the chaperone CesAB, is a small domain, positively charged, natively disordered that shows no NMR resonances. As it has been clearly demonstrated *in vivo*, the C-tail of CesAB, and specifically the charging state of it, is essential for both EspA and EspB translocators' secretion process. From the data derived after the *in vivo* analysis of the CesAB C-tail mutants, although the chaperone can interact with the secretory proteins in solution, they cannot migrate at the membrane of the bacteria, efficiently. These results are indicating that the C-tail is somehow important from the targeting process of the secretory protein-chaperone complexes. However, from the NMR analysis of the EscN-CesAB-EspA complex, it was demonstrated that the C-tail of the chaperone does not play a role in this interaction; on the contrary, it stays unfolded.

The fact that, T3SS system is a very complex system as far as protein composition and secretion regulation are concerned, the necessity of developing an *in vitro* assay for membrane targeting was raised. Towards this end, we first purified and characterized Inverted Membrane Vesicles (IMVs) from EPEC strains, and afterwards we established an *in vitro* re-constitution assay to monitor membrane binding of the T3SS of protein complexes.

Using the membrane binding assay, we have demonstrated that the C-tail of the chaperone CesAB is essential for membrane targeting of the CesAB-EspA complex. According to the *in vitro* results that we obtained, the chaperone CesAB cannot be bound to the membrane on its own. However, once the chaperone is bound to the secretory protein EspA, the chaperone-secretory protein complex can then be targeted to the membrane of the bacterium, via the C-tail. We assumed then that conformational changes that occur on the structure of CesAB, upon binding to EspA, lead to the exposure of the C-tail, so that it can interact with the membrane

components. To verify this assumption, we used a CesAB variant, CesAB-DRE mutant, which mimics the structure CesAB acquires upon EspA binding. This gain of function mutant was able to interact with the IMVs, as efficiently as the wt CesAB-EspA complex. Furthermore, when the Ctail was also deleted from the CesAB-DRE variant, the binding was completely abolished.

Collectively, these data, also demonstrated that the targeting signal is encoded in a conformational switch in the chaperone, CesAB, which is induced only upon the binding of the physiological substrate, EspA. However, this signal is different from the EscN- binding one, due to the fact that the Ctail does not interact with the ATPase of the system in solution. Moreover, the wt EPEC IMVs that were used for the binding determination of the CesAB-EspA complex had no EscN bound on them, as derived from antibody analysis, Furthermore, efficient binding of the complex was measured when IMVs derived from EPEC ΔescN were used, indicating that the membrane receptor is another T3SS related protein. These findings lead us to hypothesize that the membrane targeting process is a two-step procedure.

Therefore, our next goal was to identify the protein receptor at the membrane that the protein complex interacts as a first targeting event. In this regard, we determine the association of the protein complex with IMVs derived from a variety of EPEC deletion strains using the *in vitro* membrane binding assay.

As derived from the our results, for this targeting event to occur the presence of the gate-keeper protein, SepL [77], [117], is essential, even in very low amounts. However, we were unable to detect any significant association of these proteins in solution. Moreover, no relevant complex- formation stoichiometry derived after determination of the amounts of SepL and CesAB-EspA that were detected bound to the membranes. Therefore, although the presence of SepL is essential for the protein complex to be targeted, we strongly believe that SepL could not be the direct receptor of the CesAB-EspA at the membrane.

As resulted from our data proteins EscV and EscU are also essential for membrane targeting of the complex. The membrane component EscU has been reported to be essential for protein secretion, and somehow regulates the process upon self-cleavage which leads to conformational changes and allosteric events at the basal body of the system [32], [42]. The other membrane component, protein EscV, upon self-association forms a nonamer ring which also could serve as a docking platform for the

chaperone-secretory complexes to bind [33], [39], [43]. Furthermore, these two proteins are essential for SepL migration and stabilization to the membrane, indicating an interaction between the gatekeeper and the membrane components. Although, the interaction between EscV and EscU with SepL and/or the CesAB-EspA secretory complex are not yet clarified, we are planning to demonstrate them using the membrane binding assay coupled with cross-linking and MS analysis.

If our assumptions are true, the targeting process to the membrane is a two-step procedure. During the first step, protein SepL should bind on the basal body of the injectisome, presumably by interaction with the cytoplasmic domain of EscU. This interaction will somehow cause conformational changes at the membrane so that CesAB-EspA can be bound to it, perhaps at the EscV nonamer, via the C-tail of the chaperone. In the next step, binding of the CesAB-EspA to the basal body will cause binding to the ATPase of the system, via the EscN-binding domain (Figure 6-1) (Thesis Chapter 5, Portaliou *et al*, in preparation).

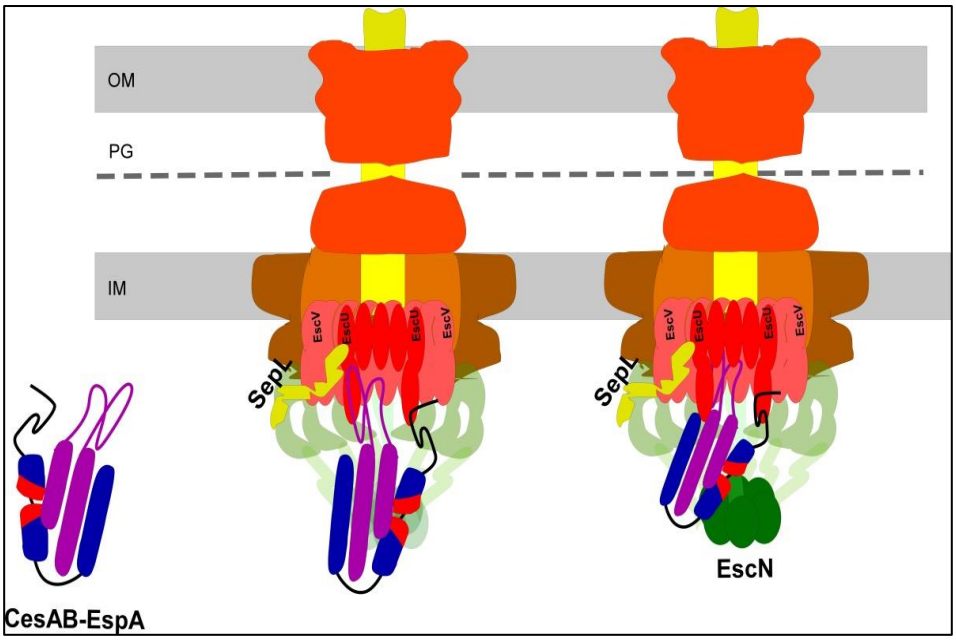

Figure 6-1 : Two-step targeting model. Once the basal body of the T3SS is formed, translocator proteins need to be targeted to the export apparatus of the system to be secreted. For this interaction to occur, the gate- keeper protein SepL is essential and possible associated with EscU and/or EscV cytoplasmic domain. CesAB-EspA complex is being targeted to the translocase via the C-tail of the chaperone (1st step). Once the CesAB- EspA protein complex is targeted to the translocase, the ATPase EscN, is able to interact with the main body of the chaperone CesAB (2nd step)

7. Chapter: Materials and Methods

Molecular Biology and Cloning Techniques

Plasmids constructed during this thesis

At the table below, all the genes that were constructed or mutated for the purpose of this thesis are listed. The primer numbers used, the plasmids and the restriction enzymes that were used for insertion of the gene of interest in specific vectors are indicated for each construct. All the vectors used carry ampicillin resistance genes.

Lab no	Vector	Construct Description	Primers (Forward/ Reverse)	Enzymes used (5'-3')
pIMBB1289	pASK IBA 7 plus	pASK-cesAB-espA	X1018/X1019	HindIII-HindIII
pIMBB1290	pASK IBA 7 plus	pASK-cesAB(E20L/E30L)-espA	X1018/X1019	HindIII-HindIII
pIMBB1291	pASK IBA 7 plus	pASK-cesAB-espA(R174L/Q181L)	X1018/X1019	HindIII-HindIII
pIMBB1292	pASK IBA 7 plus	pASK-cesAB(E20L/E30L)-espA(R174L/Q181L)	X1018/X1019	HindIII-HindIII
pIMBB1294	pASK IBA 7 plus	pASK-cesAB D14L-R18D-E20L		BamHI-HindIII
pIMBB1309	pASK IBA 7 plus	pASK-cesAB Y64A		BamHI-HindIII
pIMBB1377	pASK IBA 7 plus	pASK-cesAB Y64A-R68A	X1152/X1153	BamHI-HindIII
pIMBB1399	pASK IBA 7 plus	pASK-cesAB E60K-Y64A	X1158/X1159	BamHI-HindIII
pIMBB1236	pASK IBA 7 plus	pASK-cesAB D14L-R18L-E20L	X1000-X1001	
pIMBB1400	pASK IBA 7 plus	pASK-cesAB R68A	X1154/X1155	
pIMBB1401	pASK IBA 7 plus	pASK-cesAB Y64A- K69E	X1156/X1157	
pIMBB1407	pASK IBA 7 plus	pASK-cesAB S76A	X1180/X1181	
pIMBB1408	pASK IBA 7 plus	pASK-cesAB S73A-S76A	X118/X1183	

pIMBB1414	pASK IBA 7 plus	pASK-cesAB Y64A-K69E-S73A-S76A	X1180/X1181 X1231/X1232	
pIMBB1413	pASK IBA 7 plus	pASK-cesAB R68A-K91A-R99A-R101A-R104A-K105A (Ctail6A)	X1221/X1222 X1223/X1224 X1225/X1226	
pIMBB1421	pASK IBA 7 plus	pASK His CesAB-M96BpA	X1235/X1236	
pIMBB1420	pASK IBA 7 plus	pASK His CesAB-I106BpA-V107BpA	X1237/X1238	
pIMBB1419	pASK IBA 7 plus	pASK His CesAB- A88pA	X1233/X1234	
pIMBB1437	pASK IBA 7 plus	pASK His CesAB-L85BpA	X1251/X1252	
pIMBB1441	pASK IBA 7 plus	pASK His CesAB-Y71BpA	X1241/X1242	
pIMBB1442	pASK IBA 7 plus	pASK His CesAB-T63BpA- Y65BpA	X1239/X1240	
pIMBB1443	pASK IBA 7 plus	pASK His CesAB-A29BpA	X1245/X1246	
pIMBB1444	pASK IBA 7 plus	pASK His CesAB-K58BpA-L59BpA	X1249/X1250	
pIMBB1445	pASK IBA 7 plus	pASK His CesAB N1-86 (ΔCtaiL)		XbaI-HindIII
pIMBB1458	pET Duet1	pET Duet1 EscU Δ21-204	X1274/X1275 X1276/X1277	BamHI- PstI PstI- HindIII
pIMBB1459	pET Duet1	pET Duet1 EscV Δ21-509	X1278/X1279 X1280/X1281	BamHI- PstI PstI- HindIII
pLMB0006	pET Duet1	pET Duet1 MM-His CesAB N1-86-D14L-R18D-E20L	X1441/X431	NcoI-HindIII
pLMB0005	pET Duet1	pET Duet1 MM-His CesAB D14L-R18D-E20L	X1442/X346	NcoI-HindIII
pLMB0004	pET Duet1	pET Duet1 MM-His CesAB N1-86	X1442/X431	NcoI-HindIII
pLMB0008	pET Duet1	pET Duet1 MM-His CesAB N1-86/espA	X1442/X432	NcoI-HindIII
pLMB0003	pET Duet1	pET Duet1 MM-His CesAB	X1442/X346	NcoI-HindIII
pLMB0007	pET Duet1	pET Duet1 MM-His CesAB /espA	X1442/X347	NcoI-HindIII
pIMBB1307	pASK IBA 7 plus	pASK His EscL		XbaI-SalI
pIMBB1305	pASK IBA 7 plus	pASK His SepL		XbaI-XhoI
pIMBB1306	pASK IBA 7	pASK His CesT		XbaI-HindIII

	plus			
pIMBB1304	pASK IBA 7 plus	pASK His SepD		XbaI-XhoI
pIMBB1410	pET Duet1	pET Duet1 CesD2	X1186-X1187	BamHI-HindIII
pIMBB1411	pET Duet1	pET Duet1 TEV CesD2	X1186-X1187	BamHI-HindIII
pIMBB1415	pET Duet1	pET Duet1 EspD	X1229-X1230	BamHI- NotI
pIMBB1416	pET Duet1	pET Duet1 TEV EspD	X1229-X1230	BamHI- NotI
pIMBB1417	pET Duet1	pET Duet1 CesD2/ EspD	X1227-X1228	NdeI- KpnI
pIMBB1418	pET Duet1	pET Duet1TEV CesD2/ EspD		XbaI-BamHI

Table 1 Constructs made during this thesis. All the above plasmids have been made and used for the purposes of the present thesis. Vectors that were used provided ampicillin resistance to the strain that they were transformed in. Primers were made by Microchemistry lab, IMBB-FORTH. Enzymes were provided by Minotech, IMBB-FORTH, or Promega.

Primers	**Sequensce (5'-3')**
X1018	5' CCC AAG CTT TTA AGT ATA AGA AGG AGA TAT ACA TAT GGC 3'
X1019	5' CCC AAG CTT TTA TTT ACC AAG GGA TAT TCC TGA AAT AGT 3'
X1152	5' CACAGCGGGTGAAGAGGCGAAATTATATGATTCTGCC 3'
X1153	5' GGCAGAATCATATAATTTCGCCTCTTCACCCGCTGTG 3'
X1158	5' ACAAATTAATTAAGGGGTACACAGCGGGTG 3'
X1159	5' CACCCGCTGTGTACCCCTTAATTAATTTGT 3'
X1000	5' CTG AAA AAA ATA CTG TCA TTA ATT GAG GCG ATA AAA AAA 3'
X1001	5' TTT TTT TAT CGC CTC AAT TAA TGA CAG TAT TTT TTT CAG 3'
X1154	5' CACATATGGTGAAGAGGCGAAATTATATGATTCTGCC 3'
X1155	5' GGCAGAATCATATAATTTCGCCTCTTCACCATATGTG 3'
X1156	5' GGTGAAGAGCGAGAATTATATGATTCTGCCC 3'
X1157	5' GGGCAGAATCATATAATTCTCGCTCTTCACC 3'
X1180	5' GATTCTGCCCTAGCGAAGATTGAAAAACTAATAGAG 3'
X1181	5' CTCTATTAGTTTTTCAATCTTCGCTAGGGCAGAATC 3'
X1182	5' AGCGAAAATTATATGATGCGGCCCTAGCGAAG 3'
X1183	5' CTTCGCTAGGGCCGCATCATATAATTTTCGCT 3'
X1231	5’ CGA GAA TTA TAT GAT GCG GCC CTA GCG AAG ATT 3’
X1232	5’ AAT CTT CGC TAG GGC CGC ATC ATA TAA TTC TCG 3’
X1221	5’ GAG ACA CTG AGT CCA GCA GCA TCT GCA AGC CAA TCA ACA ATG AAT 3’
X1222	5’ ATT CAT TGT TGA TTG GCT TGC AGA TGC TGC TGG ACT CAG TGT CTC 3’
X1223	5’ CAA TCA ACA ATG AAT CAA GCG AAT GCA AAT AAT AGA AAA ATA GTA 3’
X1224	5’ TAC TAT TTT TCT ATT ATT TGC ATT CGC TTG ATT CAT TGT TGA TTG 3’

X1225	5’ CAA GCG AAT GCA AAT AAT GCA GCA ATA GTA TGA AAG CTT GAC CTG 3’
X1226	5’ CAG GTC AAG CTT TCA TAC TAT TGC TGC ATT ATT TGC ATT CGC TTG 3’
X1235	5’ AAA AGC CAA TCA ACA TGA AAT CAA CGG AAT AGA 3’
X1236	5’ TCT ATT CCG TTG ATT TCA TGT TGA TTG GCT TTT 3’
X1237	5’ AAT AGA AAT AAT AGA AAA TGA TGA TGA AAG CTT GAC CTG TGA 3’
X1238	5’ TCA CAG GTC AAG CTT TCA TCA TCA TTT TCT ATT ATT TCT ATT 3’
X1233	5’ GAG ACA CTG AGT CCA TGA AGA TCT AAA AGC CAA 3’
X1234	5’ TTG GCT TTT AGA TCT TCA TGG ACT CAG TGT CTC TAT 3’
X1251	5’ ATA TGT GTA CCC CTC AAT TCA TCA GTT TAA TTT TTC TGC CGC 3’
X1252	5’ AAA CTA ATA GAG ACA TGA AGT CCA GCA AGA TCT 3’
X1241	5’ GAA GAG CGA AAA TTA TGA GAT TCT GCC CTA AGT 3’
X1242	5’ ACT TAG GGC AGA ATC TCA TAA TTT TCG CTC TTC 3’
X1239	5’ AAA TTA ATT GAG GGG TAC TGA TGA GGT GAA GAG CGA AAA TTA 3’
X1240	5’ TAA TTT TCG CTC TTC ACC TCA TCA GTA CCC CTC AAT TAA TTT 3’
X1245	5’ GCG ATA AAA AAA ATA ATC TGA GAA TTT GAT GTC GTA AAA 3’
X1246	5’ TTT TAC GAC ATC AAA TTC TCA GAT TAT TTT TTT TAT CGC 3’
X1249	5’ GCG GCA GAA AAA TTA AAC TGA TGA ATT GAG GGG TAC ACA TAT 3’
X1250	5’ ATA TGT GTA CCC CTC AAT TCA TCA GTT TAA TTT TTC TGC CGC 3’
X1274	5’CGC GGA TCC G ATG AGT GAA AAA ACA GAA AAG CCC 3’
X1275	5’ AAAA CTG CAG TAC ATC GCC CTT CTT TTT TAG ATC 3’
X1276	5’ AAAA CTG CAG AAG CAT GAG GGA CTG AAG AAA ATG 3’
X1277	5’ CCC AAG CTT TTA ATA ATC AAG GTC TAT CGC AAT ACG 3’
X1278	5’ CGC GGA TCC G ATG AAT AAA CTC TTA AAT ATA TTT AAA AAA GCA 3’
X1279	5’ AAAA CTG CAG AGC CAG AAT AAG ATC GTG ATA TGA 3’
X1280	5’ AAAA CTG CAG CGC CAG CTT GGT TTG AGC AAA 3’
X1281	5’ CCC AAG CTT TCA TGC TCT GAA ATC ATT TAC CGT 3’
X346	CCCAAGCTTTCATACTATTTTTCTATTATTTCTATTCCG
X431	5’ CCCAAGCTTTCAACTCAGTGTCTCTATTAGTTTTTC 3’
X1442	5' CATG CCA TGG GC ATG ATG AGC AGC CAT CAC CAT CAT CAC 3'
X345	CGCGGATCCGATGAGTATTGTGAGCCAAACAAG
X1186	5’ CGC GGA TCC G ATG GTC GAT ACG TTT AAT GAT GAA GTG 3’
X1187	5’CCC AAG CTT TTA ACT ATT TAC GTT CAT TAC GAA CCA AAT TCC3’
X1229	5’ CGC GGA TCC G ATG CTT AAT GTA AAT AAC GAT ATC CAG 3’
X1230	5’ ATA AGA AT GCG GCC GC TTA AAC TCG ACC GCT GAC AAT ACG GAT 3’

X1227	5’ GGA ATT C CAT ATG CTT AAT GTA AAT AAC GAT ATC CAG TCT GTG 3’
X1228	5’ CGG GGT ACC TTA AAC TCG ACC GCT GAC AAT ACG GAT 3’

Table 2 Primers designed during this thesis. Primers were made by Microchemistry lab, IMBB-FORTH

Bacterial strains used in this thesis

At the table below, all the bacterial strains that were used for the purpose of this thesis are listed.

Lab no	Bacterial strain	Description (gene deleted in itailcs)	Reference/ person made it
B1030	E2348/69	Wild-type EPEC O127:H6	Levine et al, 1978
B1824	DF1358	E2348/69 *cesAB*	Creasey et al, 2003
B1823	CVD452	E2348/69 *escN*	Jarvis, K. G. et al, 1995
B2433	ICC305	E2348/69 *sepD*	Munera et al, 2010
B1827	UMD872	E2348/69 *espA*	Kenny *et al.*,1996
B2653	ΔcesT	E2348/69 *cesT*	Abe et al, 1999
B2602	ΔcesAB/ΔespA	E2348/69 cesAB/*espA*	this thesis / A. Portaliou
B2456	ΔescJ	E2348/69 *escJ*	Tomoaki et al., 2006
B2455	ΔescD	E2348/69 *escD*	Tomoaki et al., 2006
B2432	ΔsepL	E2348/69 *sepL*	Munera et al, 2010
B2917	ΔsepQ	E2348/69 *sepQ*	this thesis / K.Tsolis
B2997	ΔsepQ/ΔsepL	E2348/69 *sepQ/ sepL*	this thesis / K.Tsolis
B2915	ΔescU	E2348/69 *escU*	this thesis / K.Tsolis
B2916	ΔescV	E2348/69 *escV*	this thesis / K.Tsolis
B2918	ΔescL	E2348/69 *escL*	this thesis / K.Tsolis
B33	DH5a	E coli DH5a	Sambrook, J. 1989.
B88	BL21 (DH3)	E coli BL21 (DH3)	Studier, F.W., et al. (1986)
B137	BL21-19 (DH3)	E coli BL21-19 (DH3)	Davanloo, P. et al. (1984)

Table 3: List of all the bacterial strains used in this thesis. Last column indicates the reference paper of the strain or the person who made this strain, in case that the strain was made for the purpose of this thesis.

DNA manipulation techniques

For plasmid purification, the “Nucleo-Spin Plasmid- easy pure” kit was used from Macheney- Nagel. The protocol that was followed was provided by the company. For extracting DNA fragments from agarose gels, “QiA quick- Gel extraction” kit was used, from Qiagen. Also, the protocol followed was provided by the company.

The enzymes that were used for cloning purposes were provided by Minotech or Promega.

For generating mutation on genes, the protocol followed was the "Quick Change Mutagenesis Protocol" by Stratagene. The polymerase that was used was "Pfu Ultra High Fidelity Polymerase", by Roche.

The artificial operon that was generated was carrying the cesAB (B7UMC4_ECO27) and the *espA* (B7UM94_ECO27) genes in tandem, with a ribosomal binding site in between. For this reason, firstly, we introduced in pASK-IBA 7 plus vector (IBA, Germany) *cesAB* gene. Afterwards, the ribosomal binding site and the espA gene were amplified with PCR and a flanked Hind III restriction site was introduced. The PCR product was inserted in pASK-IBA 7plys vector, after the 3' end of the *cesAB* gene.

Preparation of Competent Cells using Rubidium Chloride

Bacteria were inoculated (1ml from overnight (O/N) culture into 100ml Psi-Broth Medium (1/100 dilution) and incubated at proper temperature with aeration until optical density reached 0.4-0.5. The culture was placed on ice and then the cells were pelleted with centrifugation at 3-5000g for 5min, at 4^{o}C. The bacteria were then, gently re-suspended in 0.4 culture volume of TFB1 buffer (30 mM KOAc, 100 mM RbCl2, 50 mM MnCl2, 15% Glycerol, pH = 5.8) and incubated on ice for 15 minutes. Then, again with centrifugation under the same conditions as above, bacteria were pelleted and re-suspended in 0.4 culture volume of TFB2 buffer (10 mM MOPS, 75 mM CaCl2, 10 mM RbCl2, 15% Glycerol, pH = 6.5). Finally, the bacterial re-suspension was incubated on ice for 30 minutes and then was either used immediately or was stored in aliquots at -80^{o}C.

Transformation of chemically competent bacteria

Usually, 100ul of chemically competent bacteria were incubated with 50ngr of plasmid, which was carrying the gene of interest, on ice for 20 minutes. Bacteria were shocked by heating at 42 ^{o}C, for 45 seconds and then transferred immediately on ice for two minutes. After addition of 900ul of LB medium, bacteria were transferred to

proper temperature in a shaking incubator for at least 60 minutes. Finally, all the sample or a small quantity of it was plated in LB- agar plates supplemented with proper antibiotics, mostly ampicillin (100ugr/ml) and left in a non-shaking incubator to grow for at least 15 hours, at proper temperature.

Preparation of electro-competent bacteria

From an O/N bacterial culture in LB Lennox (low salt concentration), a fresh culture was generated (Dilution 1/100 in 100ml LB Lennox) and bacteria were cultivated in proper temperature under gently shacking and proper aeration, until optical density at 600nm (OD_{600}) reached about 0.6 The culture was cooled down after incubation for 30min at 4^{o}C. Cells were harvested after low spin centrifugation (10min, 3,000g, at 4 ^{o}C). The bacteria were gently re-suspended after addition of half-culture volume of 15% pre-cooled glycerol. Afterwards, the cells were harvested again with low spin centrifugation and the washing step with 15% glycerol was repeated. Finally, the cell pellet was re-suspended gently, in 1 ml 15% pre-cooled Glycerol and were aliquoted, 100ul each. The competent cells were used either immediately, or stored at -80 ^{o}C, for a short period of time (maximum 5 days)

Transformation of electro-competent bacteria

At 100-120 μl of fresh electro competent bacteria 1-2ugr of linear DNA (PCR fragment) was added and the cells were transferred in proper electroporation cuvettes (0.2 cm electrode gap, Gene Pulser Cuvete, E coli Pulser cuvette, Cat No: 165-2086)

The Elecroporation procedure was performed at 300 Ω (Resistance), 25 μF (Contactivity), 2,5 V (Voltage). Immediately, after electroporation, the cells were transferred in proper tubes and incubated under constant shacking for minimum 2 hours and maximum O/N, at proper temperature.

Gene replacement from bacterial chromosome

The double deletion strain EPECΔcesAB-ΔespA was constructed with “one step Gene Disruption technique” (Datsenko and Wanner PNAS, 2000; 97(12): p6640-5) using λ red recombinase and a cassette containing the aminoglycoside 3’-phosphotransferase gene (aphT) in order to replace CesAB gene and introduce

kanamycin resistance to the deletion strain (Galan et al, Journal of Bacteriology, 1992; 174(13): p 4338-49). Briefly, we used as a mother bacterial strain EPECΔespA. Two primers were designed so to amplify the gene of aphT with flanking ends from *cesAB* gene. The reverse primer was designed using the 15 base pairs (bp) from the 3' end of the aphT gene followed from 30 bp from the 3' of the *cesAB* gene. The forward primer was designed using 30 bp from the 5' of the *cesAB* gene followed from 15 bp of the 5' of aphT gene. The AphT cassette was amplified with PCR and was introduced in EPECΔ*EspA* with electroporation. For the replacement of the cesAB gene we used the λ red recombinase and positive clones were selected using their ability to grow in the presence of kanamycin. The positive clones that were selected were further characterized using specific primers that amplified the inserted gene, on the bacterial chromosome. Moreover, specific antibodies used to verify the successful deletion of the gene in the protein level.

Protein handling and visualization techniques

Protein electrophoresis

Sodium dodecyl sulfate Polyacrylamide gel electrophoresis (SDS-PAGE)

Protein samples were analyzed by electrophoresis, and separated according to their molecular size using 12% or 15% polyacrylamide gels. The protein samples were first incubated with anionic detergent, SDS (sodium dodecyl sulfate) and reducing agent (β-mercaptoethanol) for 10 minutes at 100 ^{o}C. Electrophoresis procedure that was followed was according to Biorad protocols.

Polyacrylamide gel electrophoresis under native conditions

Protein samples were analyzed by electrophoresis and separated according to their native charge state and their hydrodynamic size.

Native charge state of a protein depends on the amino-acid content of the protein and post-translational modifications, a protein could have. It is affected from the pH of the buffer used during the electrophoresis. To the present thesis, native electrophoresis analysis was performed in neutral pH so to avoid dissociation of

protein complexes. Polyacrylamide gels were 7% and electrophoresis procedure was held at 4 ^{o}C, for 15 hours, at 30mA (constant Ampere).

Protein visualization techniques

Coomassie staining

Proteins that have been separated with gel electrophoresis were stained using Coomassie Brilliant blue, R-250 solution. During this procedure, polyacrylamide gels, are incubated in coomassie solution for at least 1 hour, at room temperature, with constant shacking, and then are de-stained using de-staining solution, under the same incubation conditions. The detection capacity of this procedure is above 0.5ugr of protein.

Blue silver staining

Proteins that have been analyzed in polyacrylamide gels and were to be analyzed with Mass Spectrometry were stained using Coomassie Brilliant Blue, G-250 solution. During this procedure, polyacrylamide gels, are incubated in coomassie solution for at least 1 hour, at room temperature, with constant shacking, and then are being destained using distilled water, under the same incubation conditions. The detection capacity of this procedure is above 0.1ugr

Western blot analysis

For Western blot analysis the Biorad protocol was followed. The antibodies that were used to detect T3SS proteins were polyclonal antibodies raised in rabbit (Davids Biotechnology, Germany) and purified using negative immuno-absorption. The secondary antibodies that were used were anti-rabbit IgGs with conducted Horseradish peroxidase, which by the oxidation of peracid salt, produces chemiluminescence light. The whole reaction was enhanced using an enhanced chemiluminescent substrate for detection of horseradish peroxidase (Thermo Scientific Pierce ECL Western Blotting Substrate).

Overexpression of recombinant proteins using pET or pASK vectors

pET Duet1 vector and pET system

For overexpression of recombinant proteins pETDuet1 vector (Novagen) and *E coli* BL21 (DH3) or BL21-19 (DE3) were used. Induction of expression was performed using Isopropyl β-D-1-thiogalactopyranoside (IPTG) (0,1mM, for 3 hours, unless otherwise indicated).

The pET expression system is one of the most widely used systems for expression of recombinant proteins. This is due to the high selectivity of the pET system's bacteriophage T7 RNA polymerase for its cognate promoter sequences, the high level of activity of the polymerase and the high translation efficiency mediated by the T7 gene 10 translation initiation signals.

Specifically, the pET Duet 1 vector contains two cloning sites and two T7 promoters, providing the cloning and co-expression of two proteins in parallel. Moreover, upstream the first cloning site it contains a 6x His Tag, so that once the proteins are over-expressed, to be co-purified as a protein complex.

Protein expression is achieved by IPTG induction of a chromosomally integrated cassette in which the T7 RNA polymerase is expressed from the *lacUV5* promoter. Due to the specificity of the T7 promoter, basal expression of cloned target genes is extremely low. Upon induction the highly active polymerase essentially out-competes transcription by the host RNA polymerase. This phenomenon, together with high-efficiency translation, achieves expression levels in which the target protein may constitute the majority of the cellular protein.

pASK IBA 7 plus vector, pASK system

In order to achieve low levels of protein expression of specific genes, for *in vivo* complementation experiments, the pASK IBA system was used. The pASK-IBA vectors work with the tightly regulated tetracycline (tet) promoter. Expression of the cloned gene is being strictly repressed until efficient chemical induction with a low concentration of anhydrotetracycline (AHT) is being performed**.** The levels of expression of the recombinant protein can controlled and they depend on the amount of the AHT added in the culture. In order to achieve low copies of the protein of

interest, similar to the chromosomal ones, different concentrations of AHT were used to induce the expression of each protein.

Protein purification using affinity chromatography

All the proteins of interest that were used in this thesis, had at the N-terminus 6x His-tag epitope and affinity chromatography using agarose beads with Ni-NTA was used in order to purify them.

Soluble purification using high concentration of salt

All the proteins of interest were carrying a His Tag at the N-terminus of their sequence. Harvested cells that the protein of interest was over-expressed, were re-suspended in the minimum volume possible in a high salt buffer (50mM Tris pH 8.0, 1M NaCl, 10% Glycerol, 5mM PMSF, 5mM Imidazole, and 5ugr/ml DNAse A) and the cells were lysed using mechanical pressure by French press (800psi, 5-7 repeats). The cell debris separated from the cytosolic fraction by ultracentrifugation (35min/ 100.000g/4^{o}C). The supernatant that contained the majority of the cytosolic proteins was loaded to a pre-equilibrated Ni-NTA Agarose (Qiagen) column, with the same buffer. If the protein of interest had cysteines, 5mM β'merkaptoethanol was added prior to loading. The Ni-NTA capacity was estimated for each protein and in general it was about 5-10 mgr protein /ml resin. Once loading was over, the column was washed with 10 column volumes with high salt buffer (50mM Tris pH 8.0, 1M NaCl, 10% Glycerol, 5mM Imidazole) and then with 5 column volumes of low salt buffer (50mM Tris pH 8.0, 50mM NaCl, 10% Glycerol, 5mM Imidazole). Proteins were eluted using 10 column volumes of high concentration of Imidazole buffer (50mM Tris pH 8.0, 50mM NaCl, 10% Glycerol, 300 mM Imidazole). The purified proteins were dialyzed against low salt buffer so to get rid of the high concentration of imidazole, and stored in 50% glycerol, at -20 ^{o}C.

Soluble purification using low concentration of salt (Native purification)

All the proteins of interest were carrying a His Tag at the N-terminus of their sequence. Harvested cells that the protein/ or proteins of interest were over-expressed,

were re-suspended in the minimum volume possible in a low salt buffer (50mM Tris pH 8.0, 50mM NaCl, 10% Glycerol, 5mM PMSF, 5mM Imidazole, and 5ugr/ml DNAse A) and the cells were lysed using sonication (75-80 pulse, 15-20 repeats using ethanol-dry ice bath to keep the samples at low temperature). The cell debris separated from the cytosolic fraction by ultracentrifugation (35min/100.000g/4^{o}C). The supernatant that contained the majority of the cytosolic proteins was loaded to a pre-equilibrated Ni-NTA Agarose (Qiagen) column, with the same buffer. The Ni-NTA capacity was estimated for each protein and in general it was about 5-10 mgr protein /ml resin. Once loading was over, the column was washed with 20 column volumes with low salt buffer (50mM Tris pH 8.0, 50mM NaCl, 10% Glycerol, 5mM Imidazole). Proteins or protein complexes were eluted using 3-5 column volumes of high concentration of Imidazole buffer (50mM Tris pH 8.0, 50mM NaCl, 10% Glycerol, 500 mM Imidazole). The purified proteins were either used immediately for further analysis, or dialyzed against low salt buffer so to get rid of the high concentration of imidazole, and stored in 50% glycerol, at -20 ^{o}C, for a few days (maximum 3-4 days, for protein complexes).

Purification of proteins with high concentration of chaotropic agent

All the proteins of interest were carrying a His Tag at the N-terminus of their sequence. Harvested cells that the protein of interest was over-expressed, were re-suspended in the minimum volume possible in a high salt buffer (50mM Tris pH 8.0, 1M NaCl, 10% Glycerol, 5mM PMSF, 5mM Imidazole, and 5ugr/ml DNAse A) and the cells were lysed using mechanical pressure by French press (800psi, 5-7 repeats). The cell debris separated from the cytosolic fraction by ultracentrifugation (35min/ 100.000g/4^{o}C). The pellet that was formed, which contained the majority of the inclusion bodies and membrane fragments, was re-suspended in high urea buffer (50mM Tris pH 8.0, 1M NaCl, 8M Urea, 10% Glycerol, 5mM Imidazole). After homogenizing of the pellet, the sample was again separated using ultracentrifugation (35min/ 100.000g/4^{o}C). At the Urea solubilized material (soluble fraction), Urea concentration was diluted down to 6M and the sample was loaded to a pre-equilibrated Ni-NTA Agarose (Qiagen) column, with the same buffer (50mM Tris pH 8.0, 1M NaCl, 6M Urea, 10% Glycerol, 5mM Imidazole). The Ni-NTA capacity was estimated for each protein and in general it was about 5-10 mgr protein /ml resin. If

the protein of interest had cysteines, 5mM β'merkaptoethanol was added prior loading. Once loading was over, the column was washed with 10 column volumes with high salt- urea buffer (50mM Tris pH 8.0, 1M NaCl, 6M Urea, 10% Glycerol, 5mM Imidazole) and then with 5 column volumes of low salt-urea buffer (50mM Tris pH 8.0, 50mM NaCl, 6M Urea, 10% Glycerol, 5mM Imidazole). Proteins were eluted using 10 column volumes of high concentration of Imidazole buffer (50mM Tris pH 8.0, 50mM NaCl, 6M Urea, 10% Glycerol, 300 mM Imidazole). The purified proteins were dialyzed against low salt Urea buffer so to get rid of the high concentration of imidazole, and stored in 50% glycerol, at -20 ^{o}C.

Protein purification using different kind of chromatography

Size exclusion chromatography

In order to separate protein samples using size exclusion chromatography, Superdex 75 HR 10/30 or Hi load^{TM} Superdex 200pg gel- filtration pre-packed columns (GE Healthcare) were used, regarding the amount of total protein need to be loaded. In Superdex 75 HR 10/30 every time 150 ugr of total protein samples were loaded, while in Hi load Superdex 200pg up to 150 mgr. Protein samples were loaded on the column which was pre-equilibrated with 50mM Tris-HCl pH8.0, 50mM NaCl, with a flow rate 0,4 ml/min. The column was connected with FPLC system from Pharmacia Biotech and a fraction collector, which collected fractions every minute. In all cases the running buffer was 50mM Tris-HCl pH8.0, 50mM NaCl and the temperature was 4^{o}C.

Size exclusion chromatography coupled with Multi Angle Laser Light Scattering (SEC- MALS)

Purified proteins (10-300uM; 200 μl loaded) were chromatographed on a Superdex 75 HR 10/30 or Superdex HR200 10/300 gel filtration pre-packed columns (GE Healthcare) equilibrated with 50 mM Tris-HCl, pH 8.0 and 50 mM NaCl buffer at a flow rate of 0.8 ml min^{-1}. Laser light scattering measurements were carried out online following gel permeation chromatography (GPC) and an HPLC system (LC10A-VP, Shimadzu) coupled to a quadruple detector scheme connected in series as follows: a photodiode-array detector (SPDM10AVP; Shimadzu) for UV monitoring

at 280 nm; an 18-angle MALLS detector (DAWN-EOS, Wyatt) using a K5-type cell and a laser wavelength of 690 nm; a QELS detector (Wyatt QELS; Wyatt) connected through an optical fiber to the MALLS instrument through laser detector 13; and a refractive index detector (RID- 10A; Shimadzu). MALLS and QELS data were collected, analyzed and plotted using the Astra v.5.0 software (Wyatt). All measurements were performed at 25 °C.

Anion exchange chromatography

Anion exchange chromatography relies on the charge-charge interactions between the protein of interest and the resin used. In order to purify proteins using anion exchange chromatography, Q Sepharose Fast flow resin was used (GE Healthcare). The resin capacity was estimated to be 50mgr of protein per 1ml resin. The protein samples were loaded on the column which was pre-equilibrated with in low salt buffer (50mM Tris-HCl pH8.0, 50mM NaCl, 10% Glycerol). Extensive washes (20 column volumes) were performed with medium salt buffer (50mM Tris-HCl pH8.0, 150mM NaCl, 10% Glycerol) and finally the protein was eluted from the column with 10 column volumes of high salt buffer (50mM Tris-HCl pH8.0, 0,5-1M NaCl, 10% Glycerol). The purified proteins were dialyzed against low salt buffer to get rid of the high concentration of salt, and stored in 50% glycerol, at -20 ^{o}C.

Protein quantification

Using Bradford assay

Quantification of purified proteins was performed using the Bradford assay. In brief, Biorad Protein Assay Dye reagent (Bradford reagent) was diluted 1:5. Bovine Serum Albumin (BSA, from Roth) protein at different concentrations (from 0 – 20 ugr) was diluted in 1ml of the Bradford reagent and the optical density of the samples was measured at 595 nm. From these measurements a standard concentration curve was made. Unknown protein concentration was determined after measuring the optical density of different volumes of the unknown samples at 595nm. The

concentration of the purified proteins was calculated from the standard concentration curve.

Using BCA assay

Quantification of the total protein concentration in an unknown sample (eg IMVs) was performed using BCA Protein Assay Kit (Pierce) and following the protocol provided by the company. In brief, reagent A was mixed with reagent B, 50:1. Different volumes of the unknown concentration samples were added in 1 ml of the mixed reagents and they were incubated for 20 minutes at 37^{o}C. Optical absorbance of the samples was determined at 563nm. The concentration of the total protein content of each sample was calculated from the standard concentration curve that was made using known concentrations of BSA.

Antibody negative immune-absorption

The serum that contained the polyclonal antibodies against T3SS proteins although the titer of the antibody was sufficient, un-specific protein signals were observed during Western blot analysis. For this reason all the antibody serums used in this thesis, were first negatively immune-absorbed. Towards this end, EPEC deletion strains, or DH5a cells were cultured and harvested when OD600 reached 1. The cells were lysed using sonication (75-80 pulse, 15-20 repeats using ethanol-dry ice bath to keep the samples at low temperature) and the membrane fragments were separated using ultracentrifugation. At the membrane fragments, the serum was added and incubated at 4^{o}C, under constant rotation. Every 4-6 hours, the membrane fragments were replaced with fresh ones. The procedure lasted for three days.

Purification of inverted membrane vesicles (IMVs)

EPEC wt or deletion strains were cultured in 15 liters of LB after 1/100 dilution from O/N culture, supplemented with antibiotics, when necessary. Cells were cultivated under secretion permissive conditions (incubation at 37^{o}C under constant shacking, 180rpm). Cells were harvested by centrifugation (5.000g, 15min, 4^{o}C) after 5 hours incubation, where the peak of secretion for T3SS proteins has been determined. The cell pellet was resuspended in the less volume possible in 50mM

Tris-HCl pH 8.0, 20% glycerol and the cells were lysed by applying mechanical pressure using French Press (800psi, 6-7 repeats). Unbroken cells were removed with low spin centrifugation (5.000g, 15min, 4 ^{o}C). The membrane fragments were separated from cytosolic fraction after ultracentrifugation using a fixed-angle rotor (140,000g/ 90min/at 4^{o}C). The pellet was resuspended in 50mM Tris-HCl pH 8.0, 20% glycerol, and homogenized using a Dounce homogenizer (Wheaton). The homogenized membranes were overlaid in a sucrose concentration gradient (1.9, 1.7, 1.5, 1.3, and 1.1, from bottom to top) and centrifuged for 16 hours, at 100,000g, at 4 ^{o}C, using a swing rotor. After the centrifugation was over, the second layer from the top of the sucrose gradient contained the majority of IMVs. The specific layer had a light brown colour and was distinct from the other more dark layers formed. The second layer was collected and diluted in 50mM Tris-HCl pH 8.0, 20% glycerol. The IMVs were pelleted after ultracentrifugation using fixed angle rotor, at 140,000g/ 90min/at 4^{o}C, so to get rid of sucrose. The pellet was resuspended in 6M urea, 50mM Tris-HCl pH 8.0 and samples were incubated on ice for 35 minutes, so that the peripherally associated proteins to be removed. Samples were loaded in equal volume of 0.2 M sucrose, 50mM Tris-HCl pH 8.0 and pelleted after ultracentrifugation using swing rotor, at 140.000g, for 90 min, at 4^{o}C. The pellet that derived was resuspended in 50mM Tris-HCl pH 8.0, 50mM KCl , 5mM $MgCl_2$ and homogenized using Dounce homogenizer (Wheaton). Finally, in order to achieve the same size of IMVs, the resuspended sample was passed through a lipid extruder (LiposoFast-Basic, 100nm, AVESTIN). The homogenized IMVs were aliquoted and stored in -80 ^{o}C [3], [108], [109].

In gel digestion of protein mixtures for MS analysis

The protein bands were excised from polyacrylamide gels and transferred in eppendorf tubes. Samples were washed with 50% acetonitrile and 50mM Ammonium bicarbonate (ABS), for 15 min each, by constant shacking. The washing step was repeated three times. Afterwards, 1mM DTT in 50mM ABS, was added and samples were incubated for 45 min at 56 ^{o}C. After removal of DTT, 55mM Iodoacetamide in 50mM ABS was added and samples were again incubated for 45 min, at room temperature, in the dark. Samples were washed again with 50% acetonitrile and 50mM Ammonium bicarbonate (ABS), for 15 min each, by constant shacking. The

washing step was repeated three times. Thereafter, 0.1mM of Trypsin (Promega) in 50mM ABS was added and samples were incubated for a minimum of 15 hours at 37^{o}C. The supernatants were transferred in new sterile plastic tubes and the gel bands were washed with double-distilled H_2O, by incubation at room temperature, for 20 min. Again supernatant was transferred in new tubes and two washes were performed at the gel slices, with 50% Acetonitrile and 0.1% TFA, 50% Acetonitrile respectively, for 20 minutes each. All the supernatants from the washing steps were collected as before and the total material that contained the peptides derived from trypsin proteolysis were lyophilized and stored at -20 for MS analysis.

In solution digestion of protein mixtures for MS analysis

Samples with 10 ugr of total protein content were diluted to 200ul of Urea Buffer, to achieve final Urea concentration 6M in 50mM Ammonium bicarbonate (ABS). Afterwards, 1mM DTT in 50mM ABS, was added and samples were incubated for 45 min at 56 ^{o}C. After removal of DTT, 55mM Iodoacetamide in 50mM ABS was added and samples were again incubated for 45 min, at room temperature, in the dark. Thereafter, 50 ngr of Trypsin (Promega) in 50mM ABS was added and samples were incubated for a minimum of 15 hours at 37^{o}C. Then, the samples were diluted 2x in double-distilled H_2O and acidified with TFA. Finally, liquid samples were de-salted by passing through home-made C-34 columns, which binds the peptides and the salt passes through them. The purified salt-free peptides were lyophilized and stored at -20 for MS analysis.

Biochemical assays

Sub-cellular fractionation of proteins or protein complexes

In order to follow the sub-cellular localization profile of the proteins of interest, EPEC bacteria were cultivated in the secretion-permissive conditions, and samples were collected after 3h incubation with tetracycline. Cells were harvested using low spin centrifugation (5,000g/ 15min/ 4 ^{o}C). The cell pellet was resuspended in 50 mM Tris-HCl, pH 8.0, 50mM NaCl, 5mM EDTA and cells were lysed with sonication (75-80 pulse, 15-20 repeats using ethanol-dry ice bath to keep the samples at low temperature). After removal of unbroken cells with low speed centrifugation, the

soluble fraction was centrifuged at high speed (300.000g/30 min/4^{o} C). The supernatant from this centrifugation contained the majority of the soluble proteins, while the pellet contained the membrane embedded or peripherally associated with the membrane proteins. Samples were separated by 15% SDS-PAGE or 7% Native PAGE, transferred onto nitrocellulose membrane and analyzed by immunoblotting using specific antibodies against T3SS proteins.

In vivo secretion of proteins from EPEC strains

In vivo secretion was induced by incubation of EPEC wt or deletion strain cultures at 37°C in LB or DMEM medium, after 1/100 back dilution of a thick O/N bacterial culture, supplemented with antibiotics when necessary. All genes of interest were cloned downstream from the Tet promoter and the expression of these genes was induced by addition of 0.1 μg mL^{-1} of anhydrous tetracycline (IBA, Germany) to the culture when OD_{600} reached 0.3. Cells and supernatant fractions from different time intervals, were separated by centrifugation for 10 min at 4,000 x g at 4 ºC. Proteins in the spare growth medium were precipitated with trichloroacetic acid (20 % w/v; 30 min; 4 ºC) followed by two ice-cold acetone washes (15 min at -20^{o}C). The precipitated proteins were pelleted between steps by centrifugation for 35 min, 20,000g, at 4 ^{o}C. Finally the secreted polypeptides were analyzed by 15% SDS-PAGE and immunoblotting using rabbit polyclonal antibodies against EspA. Protein signals in each sample were quantified using a CCD camera (LAS 3000, FujiFilm) and Image J open software (version 64, available on-line at http:// rsbweb.nih.gov/ij download. html) and a standard curve of purified proteins.

In vivo infection of HeLa cells with EPEC strains

Bacterial cultures of EPEC strains were grown for 18 h in LB medium, and then were diluted 100-fold in DMEM medium and allowed to grow for another 3 h at 37 ºC, 5% CO_2 without shaking for the priming of bacteria. The sub-confluent lawns of HeLa cells, which had grown on glass coverslips inside a 24-well tissue culture dish (approximately 40,000 cells per well), were infected for 2 h, unless otherwise indicated, with the primed bacterial cultures (~3.5 x 10^{7} bacteria were inoculated in

each well). The non-adhered bacteria were removed with sequential gentle washes with 1 x PBS solution and the cells were fixed with 3% Paraformaldehyde (PFA) for 30 min. After removal of PFA, cells were permeabilized with 0.1% TRITON X-100. After incubation with a polyclonal α-EspA antibody (500-fold dilution; 30 min), cells were rinsed 3 times and the EspA filaments were stained with a donkey α-rabbit (200-fold dilution; Cy3-labeled, Jackson Immunoresearch). In parallel, the eukaryotic actin was detected with phalloidin (Cy2-labeled, Invitrogen) and both DNA bacterial and eukaryotic DNAs were stained with 1/1000 TOP-RO-3 solution (Invitrogen). The Coverslips were mounted on slides using Prolong Gold anti-fade reagent (Invitrogen) and were examined with an Axio Imager M1 Microscope (Carl Zeiss MicroImaging GmbH, Germany). Finally the images were acquired using an AxioCam MRm monochrome camera and computer processed using Axiovision software (Carl Zeiss MicroImaging GmbH Germany).

Membrane binding assay

In order to detect the bound CesAB- EspA protein complex on IMVs we performed ultracentrifugation sedimentation experiments as described before [111], but with some modifications to acquire maximum floatation. In brief, purified CesAB-EspA protein complex (100 ngr) was mixed with IMVs (15ngr total protein concentration) in Buffer B until final volume reached 8ul, and incubated on ice for 20 min. Afterwards, 15ul of 2,4 M sucrose were added in the reaction so to achieve 2M final sucrose concentration and deposited over 15μl of 2.4M sucrose . Samples were overlaid with one layer (30μl) of 1.7M sucrose and two consecutive layers, (75μl) of 1.4M and (20μl) of 1M sucrose in buffer B. Samples were separated with ultracentrifugation which was carried out in a bench-top ultracentrifuge (Optima^{TM}MAX-XP; TLA100 rotor; Beckman coulter), using polypropylene tubes (0.2ml). Seven fractions of 25ul were collected, analyzed by SDS-PAGE, and visualized by immunostaining using antibodies against SecA, CesAB and SecY. The protein signals intensities were quantified using Image J software, and expressed in percentage of complex bound on IMVs, compared to the wt CesAB-EspA complex bound.

In vitro protein translocation assay

During *in vitro* translocation assay, the secretory protein Alkaline phosphatase (proPhoA) was monitored to be transferred into the membrane lumen, reaction that depends on ATP hydrolysis from ATPase SecA [110], [111]. The secretory protein proPhoACys$^-$ (8.5 μM) and SecA-N6-901 (0.6μM) were incubated for 15 minutes, in the presence of EPEC IMVs or BL31 IMVs (1,2μM SecY), in Buffer B (50mM Tris-HCl, pH:8, 50mM KCl, 5mM $MgCl_2$; 1mg/ml BSA; 1mM DTT; 1mM ATP) at 37°C. Proteinase K was added (1mg/ml; 30min; 4°C). Proteins were TCA-precipitated (15%), washed with acetone, analyzed by 12% SDS-PAGE, immuno-stained (α-PhoA), visualized by a CCD camera (LAS3000, GE).

ATP hydrolysis measurement

During ATP hydrolysis measurement assay, the amount of the released Pi after ATP hydrolysis was determined using Malachite green. Routinely, the hydrolyzed ATP was measured in Buffer B (50mM Tris-HCl, pH: 8, 50mM KCl, 5mM $MgCl_2$; 1mg/ml BSA; 1mM DTT; 1mM ATP). For basal ATPase activity determination SecA (0.4 μM) or EscN in different concentrations were used and their ATPase activity in solution was measured.

Membrane ATPase activity: EPEC IMVs or BL31 IMVs (0,8 μM SecY) were added in the basal reaction. In the presence of SecY protein, SecA can be bound on the membrane and has a stimulated ATPase activity, basal/membrane which is determined around 1,3 folds of stimulation.

Translocation ATPase activity: proPhoACys$^-$ (3μM) was further added to the above reaction. In the presence of the secretory protein, SecA which was bound on SecY hydrolyzes ATP so that the secretory protein to be translocated into the lumen, resulting ATPase stimulation activity minimum 5 times more compared with the membrane one. Released Pi was estimated in all cases by measuring the optical absorbance of Malachite Green at 660nm. From these measurements the K_{cat} (mol Pi/mol SecA or EscN protomer/min) was determined.[110], [118]

Membrane binding affinity measurement

CesAB-EspA protein complex binding on IMVs derived from EPEC wt or ΔSepL was measured using titrations of ^{35}S labeled proteins against bound mass values [111], [118]. In brief, in order to produce ^{35}S-labbeled proteins the TNT Quick kit (Promega) was used and the protocol from the company was followed. All the genes of interest were inserted downstream to a T7 promoter and in the *in vitro* transcription/ translation reaction 3ul of ^{35}S-methionine (10μCi) was added. Once the protein synthesis was completed, the ^{35}S-labbeled proteins were purified using Sephadex™ G50 Fine resin (Renner GmbH), which captured the free ^{35}S-methionine.

Afterwards, CesAB-EspA complex was serially diluted in buffer B reactions (20μl; 50mM Tris-HCl pH:8.0; 50mM KCl, 5mM MgCl2; 1mg/ml BSA) containing EPEC IMVs (10ugr total protein content, as estimated by BCA assay), in order to achieve a 10-200nM CesAB-EspA concentration range. [35S]-CesAB-EspA was added as tracer (2μl) to all reactions. Samples were incubated on ice, for 20 min, overlaid with an equal volume of sucrose cushion (0.2M sucrose in buffer B) and ultracentrifuged (320,000xg; 30min; 4^{o}C). The membrane bound material was resuspended in buffer B and immobilized on a nitrocellulose membrane using a vacuum manifold (Bio-Rad). [35S]-signals were visualized on the phosphorimager (Storm, GE), quantified using Image J and then extrapolated to the amount of CesAB-EspA bound to IMVs taking into account that, each signal represented : x concentration of non-labeled CesAB-EspA (10-250nM)+2μl [^{35}S]-CesAB-EspA. Bound protein complex to IMVs was plotted (y axis) against total protein complex concentration used in the reaction (x axis). Fitting of the hyperbolic curves was done by nonlinear regression, for one binding site; K_D was determined using Prism software (Graph Pad).

8. Appendix

His MBP TEV EscN purification

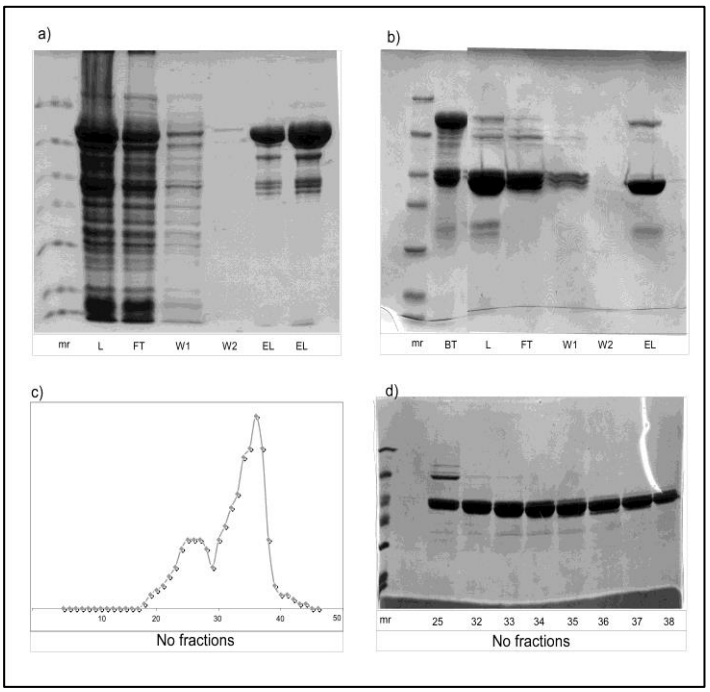

Figure 8-1: His MBP TEV EscN Purification procedure. a) SDS-PAGE analysis of high salt soluble purification steps after affinity chromatography. MR= marker, L=loading, FT= flow through, W1=first wash, W2= second wash. EL=elution fractions. b) Negative purification after TEV cleavage. The majority of His MPB TEV EscN is being cleaved after 14 hrs incubation at 4°C. FL and W1 fractions were collected. BT= before incubation with TEV protease, L=after Tev cleavage/loading sample, FT= flow through, W1=first wash, W2= second wash. EL=elution fractions. c) SEC analysis of the EscN material derived after TEV cleavage to get rid from impurities due to unspecific binding on the Ni-NTA column. d) SDS-PAGE analysis of the peak fractions derived from c). Fractions 32-38 were collected and stored for further analysis. Related to Chapter 3

Membrane binding affinity measurement

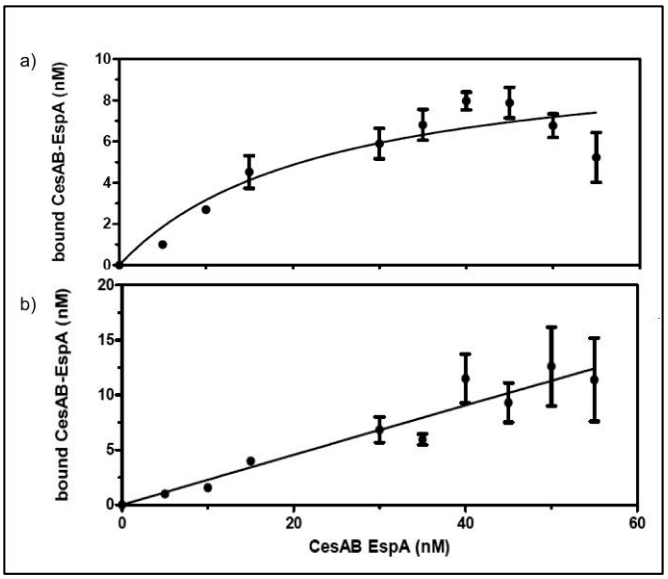

Figure 8-2 : Membrane binding affinity measurement. The hyperbolic curves derived after quantification of the radio-labeled protein signals bound on IMVs. On the x-axis the total amount of protein complex used is plotted while on the y-axis the amount detected bound on IMVs. The curves were done by nonlinear regression, for one binding site; K_D values were determined using Prism software (Graph Pad). A) wt IMVs, K_d approximately 24nM (+/- 9), b) ΔSepL IMvs, K_d non measurable. Related to chapter 5

Membrane binding of CesAB-EspA wt or mutants on wt EPEC IMVs

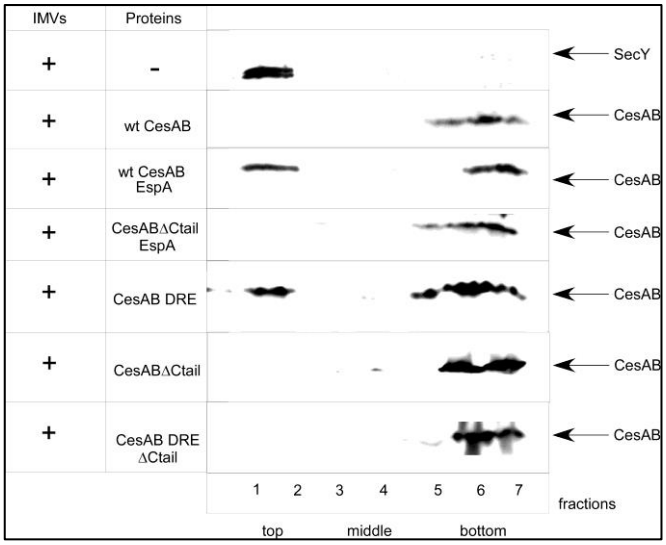

Figure 8-3 : Migration profile of wt or mutated CesAB, alone or in complex with EspA in the presence of wt EPEC IMVs. Fractions analyzed in SDS-PAGE and probed with antibodies against CesAB to detect the protein migration and SecY as membrane protein marker. Antibody signals were quantified using Image J software and normalized according to CesAB-EspA complex migration at top fraction (1-2 fractions). Related to Chapter 5

Membrane binding of CesAB-EspA complex to IMVs derived from EPEC Deletion strains

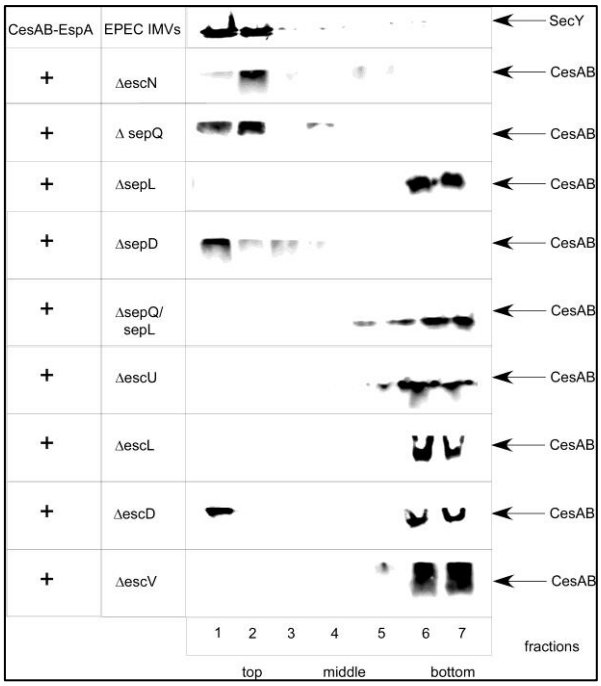

Figure 8-4: Migration profile of CesAB-EspA complex with in the presence of IMVs derived from wt or Deletion strains. Fractions analyzed in SDS-PAGE and probed with antibodies against CesAB to detect the protein migration and SecY as membrane protein marker. Antibody signals were quantified using Image J software and normalized according to CesAB-EspA complex migration at top fraction (1-2 fractions). Related to Chapter 5

Cell Reports
Report

Substrate-Activated Conformational Switch on Chaperones Encodes a Targeting Signal in Type III Secretion

Li Chen,[1] Xuanjun Ai,[1] Athina G. Portaliou,[2] Conceicao A.S.A. Minetti,[1] David P. Remeta,[1] Anastassios Economou,[2,3] and Charalampos G. Kalodimos[1,*]

[1]Center of Integrative Proteomics Research and Department of Chemistry & Chemical Biology, Rutgers University, Piscataway, NJ 08854, USA

[2]Institute of Molecular Biology & Biotechnology and Department of Biology, University of Crete, FORTH, PO Box 1385, GR-71110, Iraklio, Crete, Greece

[3]Rega Institute, Katholieke Universiteit Leuven, Molecular Bacteriology Laboratory, Minderbroedersstraat 10, B-3000 Leuven, Belgium

*Correspondence: babis@rutgers.edu

http://dx.doi.org/10.1016/j.celrep.2013.02.025

SUMMARY

The targeting of type III secretion (TTS) proteins at the injectisome is an important process in bacterial virulence. Nevertheless, how the injectisome specifically recognizes TTS substrates among all bacterial proteins is unknown. A TTS peripheral membrane ATPase protein located at the base of the injectisome has been implicated in the targeting process. We have investigated the targeting of the EspA filament protein and its cognate chaperone, CesAB, to the EscN ATPase of the enteropathogenic *E. coli* (EPEC). We show that EscN selectively engages the EspA-loaded CesAB but not the unliganded CesAB. Structure analysis revealed that the targeting signal is encoded in a disorder-order structural transition in CesAB that is elicited only upon the binding of its physiological substrate, EspA. Abrogation of the interaction between the CesAB-EspA complex and EscN resulted in severe secretion and infection defects. Additionally, we show that the targeting and secretion signals are distinct and that the two processes are likely regulated by different mechanisms.

INTRODUCTION

stabilizing factors for TTS substrates. It has been hypothesized that chaperones may also act as signals for targeting and hierarchy-determining factors (Birtalan et al., 2002; Lilic et al., 2006; Rodgers et al., 2010; Lara-Tejero et al., 2011).

A key protein in TTS systems is the ATPase (Woestyn et al., 1994; Pallen et al., 2005), a peripheral membrane protein located at the entrance of the injectisome. Biochemical experiments have provided evidence that the TTS ATPase protein, which is ubiquitous to all TTS systems, may serve to recognize and engage the TTS proteins at the injectisome (Gauthier and Finlay, 2003; Akeda and Galán, 2005; Thomas et al., 2005; Boonyom et al., 2010; Cooper et al., 2010). The ATPase is located at the cytoplasmic base of the injectisome and forms a ring structure (Müller et al., 2006) that resembles the F_1F_0-ATPase (Pallen et al., 2006; Imada et al., 2007; Zarivach et al., 2007). The molecular basis for the targeting of TTS substrates to the ATPase remains completely unknown.

We studied this targeting process in enteropathogenic *E. coli* (EPEC), the archetype of a group of pathogens that adhere to host enterocytes via the formation of attaching and effacing lesions and cause extensive host cell cytoskeletal rearrangements (Dean and Kenny, 2009). When secreted, EspA undergoes self-polymerization, thereby forming a long extracellular filamentous extension that coats the needle and connects it to the translocation pore in the eukaryotic plasma membrane, and most likely acts as a molecular conduit for TTS protein translocation (Knutton et al., 1998). EspA has a high tendency to self-oligomerize and, thus, is retained in a monomeric, soluble state in the cytoplasm by forming a complex with the CesAB chaperone

Please cite this article in press as: Chen et al., Structural Instability Tuning as a Regulatory Mechanism in Protein-Protein Interactions, Molecular Cell (2011), doi:10.1016/j.molcel.2011.09.022

Molecular Cell
Article

Structural Instability Tuning as a Regulatory Mechanism in Protein-Protein Interactions

Li Chen,[1] Vassilia Balabanidou,[4,5] David P. Remeta,[1] Conceição A.S.A. Minetti,[1] Athina G. Portaliou,[4] Anastassios Economou,[4,5] and Charalampos G. Kalodimos[1,2,3,*]
[1]Department of Chemistry & Chemical Biology
[2]Department of Biomedical Engineering
[3]BioMaPS Institute for Quantitative Biology
Rutgers University, Piscataway, NJ 08854, USA
[4]Institute of Molecular Biology and Biotechnology, Foundation for Research & Technology–Hellas (FORTH), P.O. Box 1385, GR-71110 Iraklio, Crete, Greece
[5]Department of Biology, University of Crete, 71409 Iraklio, Crete, Greece
*Correspondence: babis@rutgers.edu
DOI 10.1016/j.molcel.2011.09.022

SUMMARY

Protein-protein interactions mediate a vast number of cellular processes. Here, we present a regulatory mechanism in protein-protein interactions mediated by finely tuned structural instability and coupled with molecular mimicry. We show that a set of type III secretion (TTS) autoinhibited homodimeric chaperones adopt a molten globule-like state that transiently exposes the substrate binding site as a means to become rapidly poised for binding to their cognate protein substrates. Packing defects at the homodimeric interface stimulate binding, whereas correction of these defects results in less labile chaperones that give rise to nonfunctional biological systems. The protein substrates use structural mimicry to offset the weak spots in the chaperones and to counteract their autoinhibitory conformation. This regulatory mechanism of protein activity is evolutionarily conserved among several TSS systems and presents a lucid example of functional advantage conferred upon a biological system by finely tuned structural instability.

INTRODUCTION

Protein-protein interactions mediate a vast number of regulatory pathways and are, thus, central to cell physiology (Kuriyan and Eisenberg, 2007; Yu et al., 2008). Formation of protein complexes often is precisely regulated to control protein activity and prevent premature and undesirable interactions among cellular components (Kobe and Kemp, 1999; Schlessinger, 2003).

The multiple roles of chaperones are particularly prominent in various protein transport and secretion pathways (Cross et al., 2009; Waksman and Hultgren, 2009). Specialized chaperones are important components of type III secretion (TTS) systems, wherein they assist with the assembly and operation of the entire machinery (Birtalan et al., 2002; Cornelis, 2006; Feldman and Cornelis, 2003; Galán and Wolf-Watz, 2006; Parsot et al., 2003). The TTS apparatus is exquisitely engineered molecular machinery that has evolved specifically to deliver bacterial virulence proteins directly into eukaryotic cells (Cornelis, 2006; Galán and Wolf-Watz, 2006). Loss of a TTS chaperone generally results in rapid degradation, aggregation, or reduced secretion of its cognate secretion substrate(s) (Feldman and Cornelis, 2003; Parsot et al., 2003).

CesAB is a chaperone for EspA in the enteropathogenic *Escherichia coli* (EPEC) (Creasey et al., 2003). EPEC, the archetype of a group of pathogens that adhere to host enterocytes via the formation of attaching and effacing (A/E) lesions, causes extensive host cell cytoskeletal rearrangements (Dean and Kenny, 2009). Once secreted, EspA undergoes self-polymerization, thereby forming a long extracellular filamentous extension that connects the needle to the translocation pore in the eukaryotic plasma membrane and likely acts as a molecular conduit for TTS protein translocation (Knutton et al., 1998). Because of its high tendency to self-oligomerize, it is necessary to capture EspA in its monomeric state in the bacterial cytosol, a role served by the CesAB chaperone (Creasey et al., 2003; Yip et al., 2005).

Here, we show that CesAB, in contrast to typical chaperones, exists as a loosely packed, conformationally dynamic homodimer in solution. CesAB adopts an autoinhibited conformation to prevent self-aggregation but undergoes a subunit exchange mechanism to form a stoichiometric complex with EspA. By transiently exposing part of the binding site in a mechanism that is facilitated by packing defects at its homodimeric coiled-coil subunit interface, CesAB rapidly becomes poised for EspA binding.

9. References

[1] G. Orfanoudaki and A. Economou, "Proteome-wide subcellular topologies of E. coli polypeptides database (STEPdb)," *Mol. Cell. Proteomics MCP*, vol. 13, no. 12, pp. 3674–3687, Dec. 2014.

[2] E. Papanikou, S. Karamanou, and A. Economou, "Bacterial protein secretion through the translocase nanomachine," *Nat. Rev. Microbiol.*, vol. 5, no. 11, pp. 839–851, Nov. 2007.

[3] R. Lill, K. Cunningham, L. A. Brundage, K. Ito, D. Oliver, and W. Wickner, "SecA protein hydrolyzes ATP and is an essential component of the protein translocation ATPase of Escherichia coli," *EMBO J.*, vol. 8, no. 3, pp. 961–966, Mar. 1989.

[4] J. T. Harries, "The problem of bacterial diarrhoea," *Ciba Found. Symp.*, no. 42, pp. 3–25, 1976.

[5] Y. M. Rho and J. E. Josephson, "Epidemic enteropathogenic Escherichia coli, Newfoundland, 1963: autopsy study of 16 cases," *Can. Med. Assoc. J.*, vol. 96, no. 7, pp. 392–398, Feb. 1967.

[6] M. Soleimani, A. Morovvati, S. Z. Hosseini, and M. R. Zolfaghari, "Design of an improved multiplex PCR method for diagnosis of enterohaemoraghic *E.coli* and enteropathogic *E.coli* pathotypes," *Gastroenterol. Hepatol. Bed Bench*, vol. 5, no. 2, pp. 106–111, 2012.

[7] J. Liu, F. Kabir, J. Manneh, P. Lertsethtakarn, S. Begum, J. Gratz, S. M. Becker, D. J. Operario, M. Taniuchi, L. Janaki, J. A. Platts-Mills, D. M. Haverstick, M. Kabir, S. U. Sobuz, K. Nakjarung, P. Sakpaisal, S. Silapong, L. Bodhidatta, S. Qureshi, A. Kalam, Q. Saidi, N. Swai, B. Mujaga, A. Maro, B. Kwambana, M. Dione, M. Antonio, G. Kibiki, C. J. Mason, R. Haque, N. Iqbal, A. K. M. Zaidi, and E. R. Houpt, "Development and assessment of molecular diagnostic tests for 15 enteropathogens causing childhood diarrhoea: a multicentre study," *Lancet Infect. Dis.*, vol. 14, no. 8, pp. 716–724, Aug. 2014.

[8] A. B. Vulcano, M. Tino-De-Franco, J. A. Amaral, O. G. Ribeiro, W. H. K. Cabrera, M. A. Bordenalli, C. B. Carbonare, E. P. Álvares, and S. B. Carbonare, "Oral infection with enteropathogenic Escherichia coli triggers

immune response and intestinal histological alterations in mice selected for their minimal acute inflammatory responses," *Microbiol. Immunol.*, vol. 58, no. 6, pp. 352–359, Jun. 2014.

[9] R. Stephan, N. Borel, C. Zweifel, M. Blanco, and J. E. Blanco, "First isolation and further characterization of enteropathogenic Escherichia coli (EPEC) O157:H45 strains from cattle," *BMC Microbiol.*, vol. 4, p. 10, Mar. 2004.

[10] K. Creuzburg, B. Middendorf, A. Mellmann, T. Martaler, C. Holz, A. Fruth, H. Karch, and H. Schmidt, "Evolutionary analysis and distribution of type III effector genes in pathogenic Escherichia coli from human, animal and food sources," *Environ. Microbiol.*, vol. 13, no. 2, pp. 439–452, Feb. 2011.

[11] F. Goffaux, B. China, L. Janssen, V. Pirson, and J. Mainil, "The locus for enterocyte effacement (LEE) of enteropathogenic Escherichia coli (EPEC) from dogs and cats," *Adv. Exp. Med. Biol.*, vol. 473, pp. 129–136, 1999.

[12] C. C. Gruber and V. Sperandio, "Global analysis of post-transcriptional regulation by GlmY and GlmZ in enterohemorrhagic E. coli (EHEC) O157:H7," *Infect. Immun.*, Jan. 2015.

[13] F. A. Salvador, R. T. Hernandes, M. A. M. Vieira, A. C. Rockstroh, and T. A. T. Gomes, "Distribution of non-LEE-encoded type 3 secretion system dependent effectors in enteropathogenic Escherichia coli," *Braz. J. Microbiol. Publ. Braz. Soc. Microbiol.*, vol. 45, no. 3, pp. 851–855, 2014.

[14] F. T. Romão, R. T. Hernandes, D. Yamamoto, L. Osugui, A. Popi, and T. A. T. Gomes, "Influence of environmental factors in the adherence of an atypical enteropathogenic Escherichia coli strain to epithelial cells," *BMC Microbiol.*, vol. 14, no. 1, p. 299, Dec. 2014.

[15] A. Mora, M. Blanco, D. Yamamoto, G. Dahbi, J. E. Blanco, C. López, M. P. Alonso, M. A. M. Vieira, R. T. Hernandes, C. M. Abe, R. M. F. Piazza, D. W. Lacher, W. P. Elias, T. A. T. Gomes, and J. Blanco, "HeLa-cell adherence patterns and actin aggregation of enteropathogenic Escherichia coli (EPEC) and Shiga-toxin-producing E. coli (STEC) strains carrying different eae and tir alleles," *Int. Microbiol. Off. J. Span. Soc. Microbiol.*, vol. 12, no. 4, pp. 243–251, Dec. 2009.

[16] B. Spira, G. M. Ferreira, and L. G. de Almeida, "relA enhances the adherence of enteropathogenic Escherichia coli," *PloS One*, vol. 9, no. 3, p. e91703, 2014.

[17] J. Flores-Kim and A. J. Darwin, “Regulation of bacterial virulence gene expression by cell envelope stress responses,” *Virulence*, vol. 5, no. 8, pp. 835–851, Nov. 2014.

[18] J. Monjarás Feria, E. García-Gómez, N. Espinosa, T. Minamino, K. Namba, and B. González-Pedrajo, “Role of EscP (Orf16) in injectisome biogenesis and regulation of type III protein secretion in enteropathogenic Escherichia coli,” *J. Bacteriol.*, vol. 194, no. 22, pp. 6029–6045, Nov. 2012.

[19] M. P. Singh, R. K. Shaw, S. Knutton, M. J. Pallen, V. F. Crepin, and G. Frankel, “Identification of amino acid residues within the N-terminal domain of EspA that play a role in EspA filament biogenesis and function,” *J. Bacteriol.*, vol. 190, no. 6, pp. 2221–2226, Mar. 2008.

[20] W. Luo and M. S. Donnenberg, “Interactions and predicted host membrane topology of the enteropathogenic Escherichia coli translocator protein EspB,” *J. Bacteriol.*, vol. 193, no. 12, pp. 2972–2980, Jun. 2011.

[21] A. J. Blocker, J. E. Deane, A. K. J. Veenendaal, P. Roversi, J. L. Hodgkinson, S. Johnson, and S. M. Lea, “What’s the point of the type III secretion system needle?,” *Proc. Natl. Acad. Sci. U. S. A.*, vol. 105, no. 18, pp. 6507–6513, May 2008.

[22] B. A. Vallance and B. B. Finlay, “Exploitation of host cells by enteropathogenic Escherichia coli,” *Proc. Natl. Acad. Sci. U. S. A.*, vol. 97, no. 16, pp. 8799–8806, Aug. 2000.

[23] S. Michgehl, G. Heusipp, L. Greune, C. Rüter, and M. A. Schmidt, “Esp-independent functional integration of the translocated intimin receptor (Tir) of enteropathogenic Escherichia coli (EPEC) into host cell membranes,” *Cell. Microbiol.*, vol. 8, no. 4, pp. 625–633, Apr. 2006.

[24] S. E. Battle, M. J. Brady, S. K. Vanaja, J. M. Leong, and G. A. Hecht, “Actin pedestal formation by enterohemorrhagic Escherichia coli enhances bacterial host cell attachment and concomitant type III translocation,” *Infect. Immun.*, vol. 82, no. 9, pp. 3713–3722, Sep. 2014.

[25] E. Nieto-Pelegrin, E. Meiler, J. M. Martín-Villa, M. Benito-León, and N. Martinez-Quiles, “Crk adaptors negatively regulate actin polymerization in pedestals formed by enteropathogenic Escherichia coli (EPEC) by binding to Tir effector,” *PLoS Pathog.*, vol. 10, no. 3, p. e1004022, Mar. 2014.

[26] S. Knutton, T. Baldwin, P. H. Williams, and A. S. McNeish, “Actin accumulation at sites of bacterial adhesion to tissue culture cells: basis of a new diagnostic test for enteropathogenic and enterohemorrhagic Escherichia coli,” *Infect. Immun.*, vol. 57, no. 4, pp. 1290–1298, Apr. 1989.

[27] A. R. C. Wong, J. S. Pearson, M. D. Bright, D. Munera, K. S. Robinson, S. F. Lee, G. Frankel, and E. L. Hartland, “Enteropathogenic and enterohaemorrhagic Escherichia coli: even more subversive elements,” *Mol. Microbiol.*, vol. 80, no. 6, pp. 1420–1438, Jun. 2011.

[28] P. Dean and B. Kenny, “The effector repertoire of enteropathogenic E. coli: ganging up on the host cell,” *Curr. Opin. Microbiol.*, vol. 12, no. 1, pp. 101–109, Feb. 2009.

[29] A. Diepold and S. Wagner, “Assembly of the bacterial type III secretion machinery,” *FEMS Microbiol. Rev.*, vol. 38, no. 4, pp. 802–822, Jul. 2014.

[30] D. Büttner, “Protein export according to schedule: architecture, assembly, and regulation of type III secretion systems from plant- and animal-pathogenic bacteria,” *Microbiol. Mol. Biol. Rev. MMBR*, vol. 76, no. 2, pp. 262–310, Jun. 2012.

[31] C. K. Yip, T. G. Kimbrough, H. B. Felise, M. Vuckovic, N. A. Thomas, R. A. Pfuetzner, E. A. Frey, B. B. Finlay, S. I. Miller, and N. C. J. Strynadka, “Structural characterization of the molecular platform for type III secretion system assembly,” *Nature*, vol. 435, no. 7042, pp. 702–707, Jun. 2005.

[32] R. Zarivach, W. Deng, M. Vuckovic, H. B. Felise, H. V. Nguyen, S. I. Miller, B. B. Finlay, and N. C. J. Strynadka, “Structural analysis of the essential self-cleaving type III secretion proteins EscU and SpaS,” *Nature*, vol. 453, no. 7191, pp. 124–127, May 2008.

[33] P. Abrusci, M. Vergara-Irigaray, S. Johnson, M. D. Beeby, D. R. Hendrixson, P. Roversi, M. E. Friede, J. E. Deane, G. J. Jensen, C. M. Tang, and S. M. Lea, “Architecture of the major component of the type III secretion system export apparatus,” *Nat. Struct. Mol. Biol.*, vol. 20, no. 1, pp. 99–104, Jan. 2013.

[34] L. J. Worrall, M. Vuckovic, and N. C. J. Strynadka, “Crystal structure of the C-terminal domain of the Salmonella type III secretion system export apparatus protein InvA,” *Protein Sci. Publ. Protein Soc.*, vol. 19, no. 5, pp. 1091–1096, May 2010.

[35] A. Kawamoto, Y. V. Morimoto, T. Miyata, T. Minamino, K. T. Hughes, T. Kato, and K. Namba, “Common and distinct structural features of Salmonella injectisome and flagellar basal body,” *Sci. Rep.*, vol. 3, p. 3369, 2013.

[36] J. Radics, L. Königsmaier, and T. C. Marlovits, “Structure of a pathogenic type 3 secretion system in action,” *Nat. Struct. Mol. Biol.*, vol. 21, no. 1, pp. 82–87, Jan. 2014.

[37] O. Schraidt and T. C. Marlovits, “Three-dimensional model of Salmonella’s needle complex at subnanometer resolution,” *Science*, vol. 331, no. 6021, pp. 1192–1195, Mar. 2011.

[38] A. Gauthier, J. L. Puente, and B. B. Finlay, “Secretin of the enteropathogenic Escherichia coli type III secretion system requires components of the type III apparatus for assembly and localization,” *Infect. Immun.*, vol. 71, no. 6, pp. 3310–3319, Jun. 2003.

[39] A. Diepold, M. Amstutz, S. Abel, I. Sorg, U. Jenal, and G. R. Cornelis, “Deciphering the assembly of the Yersinia type III secretion injectisome,” *EMBO J.*, vol. 29, no. 11, pp. 1928–1940, Jun. 2010.

[40] M. Kudryashev, M. Stenta, S. Schmelz, M. Amstutz, U. Wiesand, D. Castaño-Díez, M. T. Degiacomi, S. Münnich, C. K. Bleck, J. Kowal, A. Diepold, D. W. Heinz, M. Dal Peraro, G. R. Cornelis, and H. Stahlberg, “In situ structural analysis of the Yersinia enterocolitica injectisome,” *eLife*, vol. 2, p. e00792, 2013.

[41] C. Berger, G. P. Robin, U. Bonas, and R. Koebnik, “Membrane topology of conserved components of the type III secretion system from the plant pathogen Xanthomonas campestris pv. vesicatoria,” *Microbiol. Read. Engl.*, vol. 156, no. Pt 7, pp. 1963–1974, Jul. 2010.

[42] J.-L. Thomassin, X. He, and N. A. Thomas, “Role of EscU auto-cleavage in promoting type III effector translocation into host cells by enteropathogenic Escherichia coli,” *BMC Microbiol.*, vol. 11, p. 205, 2011.

[43] N. Hartmann and D. Büttner, “The inner membrane protein HrcV from Xanthomonas spp. is involved in substrate docking during type III secretion,” *Mol. Plant-Microbe Interact. MPMI*, vol. 26, no. 10, pp. 1176–1189, Oct. 2013.

[44] N. Barison, J. Lambers, R. Hurwitz, and M. Kolbe, “Interaction of MxiG with the cytosolic complex of the type III secretion system controls Shigella

virulence," *FASEB J. Off. Publ. Fed. Am. Soc. Exp. Biol.*, vol. 26, no. 4, pp. 1717–1726, Apr. 2012.

[45] M. Kinoshita, N. Hara, K. Imada, K. Namba, and T. Minamino, "Interactions of bacterial flagellar chaperone-substrate complexes with FlhA contribute to co-ordinating assembly of the flagellar filament," *Mol. Microbiol.*, vol. 90, no. 6, pp. 1249–1261, Dec. 2013.

[46] T. Fujii, M. Cheung, A. Blanco, T. Kato, A. J. Blocker, and K. Namba, "Structure of a type III secretion needle at 7-Å resolution provides insights into its assembly and signaling mechanisms," *Proc. Natl. Acad. Sci. U. S. A.*, vol. 109, no. 12, pp. 4461–4466, Mar. 2012.

[47] L. D. B. Evans, S. Poulter, E. M. Terentjev, C. Hughes, and G. M. Fraser, "A chain mechanism for flagellum growth," *Nature*, vol. 504, no. 7479, pp. 287–290, Dec. 2013.

[48] L. Chen, V. Balabanidou, D. P. Remeta, C. A. S. A. Minetti, A. G. Portaliou, A. Economou, and C. G. Kalodimos, "Structural instability tuning as a regulatory mechanism in protein-protein interactions," *Mol. Cell*, vol. 44, no. 5, pp. 734–744, Dec. 2011.

[49] C. K. Yip, B. B. Finlay, and N. C. J. Strynadka, "Structural characterization of a type III secretion system filament protein in complex with its chaperone," *Nat. Struct. Mol. Biol.*, vol. 12, no. 1, pp. 75–81, Jan. 2005.

[50] M. D. Lefebre and J. E. Galán, "The inner rod protein controls substrate switching and needle length in a Salmonella type III secretion system," *Proc. Natl. Acad. Sci. U. S. A.*, vol. 111, no. 2, pp. 817–822, Jan. 2014.

[51] L. J. Mota, L. Journet, I. Sorg, C. Agrain, and G. R. Cornelis, "Bacterial injectisomes: needle length does matter," *Science*, vol. 307, no. 5713, p. 1278, Feb. 2005.

[52] A. Diepold, M. Kudryashev, N. J. Delalez, R. M. Berry, and J. P. Armitage, "Composition, Formation, and Regulation of the Cytosolic C-ring, a Dynamic Component of the Type III Secretion Injectisome," *PLoS Biol.*, vol. 13, no. 1, p. e1002039, Jan. 2015.

[53] M. Lara-Tejero, J. Kato, S. Wagner, X. Liu, and J. E. Galán, "A sorting platform determines the order of protein secretion in bacterial type III systems," *Science*, vol. 331, no. 6021, pp. 1188–1191, Mar. 2011.

[54] D. Wang, A. J. Roe, S. McAteer, M. J. Shipston, and D. L. Gally, “Hierarchal type III secretion of translocators and effectors from Escherichia coli O157:H7 requires the carboxy terminus of SepL that binds to Tir,” *Mol. Microbiol.*, vol. 69, no. 6, pp. 1499–1512, Sep. 2008.

[55] L. Chen, X. Ai, A. G. Portaliou, C. A. S. A. Minetti, D. P. Remeta, A. Economou, and C. G. Kalodimos, “Substrate-activated conformational switch on chaperones encodes a targeting signal in type III secretion,” *Cell Rep.*, vol. 3, no. 3, pp. 709–715, Mar. 2013.

[56] Y. Akeda and J. E. Galán, “Chaperone release and unfolding of substrates in type III secretion,” *Nature*, vol. 437, no. 7060, pp. 911–915, Oct. 2005.

[57] E. Biemans-Oldehinkel, N. Sal-Man, W. Deng, L. J. Foster, and B. B. Finlay, “Quantitative proteomic analysis reveals formation of an EscL-EscQ-EscN type III complex in enteropathogenic Escherichia coli,” *J. Bacteriol.*, vol. 193, no. 19, pp. 5514–5519, Oct. 2011.

[58] M. Romo-Castillo, A. Andrade, N. Espinosa, J. Monjarás Feria, E. Soto, M. Díaz-Guerrero, and B. González-Pedrajo, “EscO, a functional and structural analog of the flagellar FliJ protein, is a positive regulator of EscN ATPase activity of the enteropathogenic Escherichia coli injectisome,” *J. Bacteriol.*, vol. 196, no. 12, pp. 2227–2241, Jun. 2014.

[59] T. Ibuki, K. Imada, T. Minamino, T. Kato, T. Miyata, and K. Namba, “Common architecture of the flagellar type III protein export apparatus and F- and V-type ATPases,” *Nat. Struct. Mol. Biol.*, vol. 18, no. 3, pp. 277–282, Mar. 2011.

[60] F. Van Gijsegem, C. Gough, C. Zischek, E. Niqueux, M. Arlat, S. Genin, P. Barberis, S. German, P. Castello, and C. Boucher, “The hrp gene locus of Pseudomonas solanacearum, which controls the production of a type III secretion system, encodes eight proteins related to components of the bacterial flagellar biogenesis complex,” *Mol. Microbiol.*, vol. 15, no. 6, pp. 1095–1114, Mar. 1995.

[61] T. Kubori, Y. Matsushima, D. Nakamura, J. Uralil, M. Lara-Tejero, A. Sukhan, J. E. Galán, and S. I. Aizawa, “Supramolecular structure of the Salmonella typhimurium type III protein secretion system,” *Science*, vol. 280, no. 5363, pp. 602–605, Apr. 1998.

[62] L. D. B. Evans, C. Hughes, and G. M. Fraser, “Building a flagellum outside the bacterial cell,” *Trends Microbiol.*, vol. 22, no. 10, pp. 566–572, Oct. 2014.

[63] O. Poyraz, H. Schmidt, K. Seidel, F. Delissen, C. Ader, H. Tenenboim, C. Goosmann, B. Laube, A. F. Thünemann, A. Zychlinsky, M. Baldus, A. Lange, C. Griesinger, and M. Kolbe, “Protein refolding is required for assembly of the type three secretion needle,” *Nat. Struct. Mol. Biol.*, vol. 17, no. 7, pp. 788–792, Jul. 2010.

[64] K. Yonekura, S. Maki-Yonekura, and K. Namba, “Building the atomic model for the bacterial flagellar filament by electron cryomicroscopy and image analysis,” *Struct. Lond. Engl. 1993*, vol. 13, no. 3, pp. 407–412, Mar. 2005.

[65] S. J. Daniell, E. Kocsis, E. Morris, S. Knutton, F. P. Booy, and G. Frankel, “3D structure of EspA filaments from enteropathogenic Escherichia coli,” *Mol. Microbiol.*, vol. 49, no. 2, pp. 301–308, Jul. 2003.

[66] J.-P. Demers, B. Habenstein, A. Loquet, S. Kumar Vasa, K. Giller, S. Becker, D. Baker, A. Lange, and N. G. Sgourakis, “High-resolution structure of the Shigella type-III secretion needle by solid-state NMR and cryo-electron microscopy,” *Nat. Commun.*, vol. 5, p. 4976, 2014.

[67] P. Abrusci, M. A. McDowell, S. M. Lea, and S. Johnson, “Building a secreting nanomachine: a structural overview of the T3SS,” *Curr. Opin. Struct. Biol.*, vol. 25, pp. 111–117, Apr. 2014.

[68] T. Ogino, R. Ohno, K. Sekiya, A. Kuwae, T. Matsuzawa, T. Nonaka, H. Fukuda, S. Imajoh-Ohmi, and A. Abe, “Assembly of the type III secretion apparatus of enteropathogenic Escherichia coli,” *J. Bacteriol.*, vol. 188, no. 8, pp. 2801–2811, Apr. 2006.

[69] T. G. Kimbrough and S. I. Miller, “Assembly of the type III secretion needle complex of Salmonella typhimurium,” *Microbes Infect. Inst. Pasteur*, vol. 4, no. 1, pp. 75–82, Jan. 2002.

[70] S. Wagner, L. Königsmaier, M. Lara-Tejero, M. Lefebre, T. C. Marlovits, and J. E. Galán, “Organization and coordinated assembly of the type III secretion export apparatus,” *Proc. Natl. Acad. Sci. U. S. A.*, vol. 107, no. 41, pp. 17745–17750, Oct. 2010.

[71] A. P. Tampakaki, V. E. Fadouloglou, A. D. Gazi, N. J. Panopoulos, and M. Kokkinidis, “Conserved features of type III secretion,” *Cell. Microbiol.*, vol. 6, no. 9, pp. 805–816, Sep. 2004.

[72] E. D. Brutinel and T. L. Yahr, “Control of gene expression by type III secretory activity,” *Curr. Opin. Microbiol.*, vol. 11, no. 2, pp. 128–133, Apr. 2008.

[73] N. Sal-Man, W. Deng, and B. B. Finlay, “EscI: a crucial component of the type III secretion system forms the inner rod structure in enteropathogenic Escherichia coli,” *Biochem. J.*, vol. 442, no. 1, pp. 119–125, Feb. 2012.

[74] Y. Cherradi, L. Schiavolin, S. Moussa, A. Meghraoui, A. Meksem, L. Biskri, M. Azarkan, A. Allaoui, and A. Botteaux, “Interplay between predicted inner-rod and gatekeeper in controlling substrate specificity of the type III secretion system,” *Mol. Microbiol.*, vol. 87, no. 6, pp. 1183–1199, Mar. 2013.

[75] D.-K. Shen, N. Moriya, I. Martinez-Argudo, and A. J. Blocker, “Needle length control and the secretion substrate specificity switch are only loosely coupled in the type III secretion apparatus of Shigella,” *Microbiol. Read. Engl.*, vol. 158, no. Pt 7, pp. 1884–1896, Jul. 2012.

[76] G. Bange, N. Kümmerer, C. Engel, G. Bozkurt, K. Wild, and I. Sinning, “FlhA provides the adaptor for coordinated delivery of late flagella building blocks to the type III secretion system,” *Proc. Natl. Acad. Sci. U. S. A.*, vol. 107, no. 25, pp. 11295–11300, Jun. 2010.

[77] C. B. O’Connell, E. A. Creasey, S. Knutton, S. Elliott, L. J. Crowther, W. Luo, M. J. Albert, J. B. Kaper, G. Frankel, and M. S. Donnenberg, “SepL, a protein required for enteropathogenic Escherichia coli type III translocation, interacts with secretion component SepD,” *Mol. Microbiol.*, vol. 52, no. 6, pp. 1613–1625, Jun. 2004.

[78] E. A. Creasey, D. Friedberg, R. K. Shaw, T. Umanski, S. Knutton, I. Rosenshine, and G. Frankel, “CesAB is an enteropathogenic Escherichia coli chaperone for the type-III translocator proteins EspA and EspB,” *Microbiol. Read. Engl.*, vol. 149, no. Pt 12, pp. 3639–3647, Dec. 2003.

[79] P. Wattiau, B. Bernier, P. Deslée, T. Michiels, and G. R. Cornelis, “Individual chaperones required for Yop secretion by Yersinia,” *Proc. Natl. Acad. Sci. U. S. A.*, vol. 91, no. 22, pp. 10493–10497, Oct. 1994.

[80] T. Ramu, M. E. Prasad, E. Connors, A. Mishra, J.-L. Thomassin, J. Leblanc, J. K. Rainey, and N. A. Thomas, "A novel C-terminal region within the multicargo type III secretion chaperone CesT contributes to effector secretion," *J. Bacteriol.*, vol. 195, no. 4, pp. 740–756, Feb. 2013.

[81] C. Parsot, C. Hamiaux, and A.-L. Page, "The various and varying roles of specific chaperones in type III secretion systems," *Curr. Opin. Microbiol.*, vol. 6, no. 1, pp. 7–14, Feb. 2003.

[82] T. Izoré, V. Job, and A. Dessen, "Biogenesis, regulation, and targeting of the type III secretion system," *Struct. Lond. Engl. 1993*, vol. 19, no. 5, pp. 603–612, May 2011.

[83] T. Z. Grove, A. L. Cortajarena, and L. Regan, "Ligand binding by repeat proteins: natural and designed," *Curr. Opin. Struct. Biol.*, vol. 18, no. 4, pp. 507–515, Aug. 2008.

[84] K.-I. Kazetani, T. Minamino, T. Miyata, T. Kato, and K. Namba, "ATP-induced FliI hexamerization facilitates bacterial flagellar protein export," *Biochem. Biophys. Res. Commun.*, vol. 388, no. 2, pp. 323–327, Oct. 2009.

[85] C. Pozidis, A. Chalkiadaki, A. Gomez-Serrano, H. Stahlberg, I. Brown, A. P. Tampakaki, A. Lustig, G. Sianidis, A. S. Politou, A. Engel, N. J. Panopoulos, J. Mansfield, A. P. Pugsley, S. Karamanou, and A. Economou, "Type III protein translocase: HrcN is a peripheral ATPase that is activated by oligomerization," *J. Biol. Chem.*, vol. 278, no. 28, pp. 25816–25824, Jul. 2003.

[86] A. Andrade, J. P. Pardo, N. Espinosa, G. Pérez-Hernández, and B. González-Pedrajo, "Enzymatic characterization of the enteropathogenic Escherichia coli type III secretion ATPase EscN," *Arch. Biochem. Biophys.*, vol. 468, no. 1, pp. 121–127, Dec. 2007.

[87] C. A. Cooper, K. Zhang, S. N. Andres, Y. Fang, N. A. Kaniuk, M. Hannemann, J. H. Brumell, L. J. Foster, M. S. Junop, and B. K. Coombes, "Structural and biochemical characterization of SrcA, a multi-cargo type III secretion chaperone in Salmonella required for pathogenic association with a host," *PLoS Pathog.*, vol. 6, no. 2, p. e1000751, Feb. 2010.

[88] A. Gauthier and B. B. Finlay, "Translocated intimin receptor and its chaperone interact with ATPase of the type III secretion apparatus of enteropathogenic Escherichia coli," *J. Bacteriol.*, vol. 185, no. 23, pp. 6747–6755, Dec. 2003.

[89] K. Nam, J. Pu, and M. Karplus, “Trapping the ATP binding state leads to a detailed understanding of the F1-ATPase mechanism,” *Proc. Natl. Acad. Sci. U. S. A.*, vol. 111, no. 50, pp. 17851–17856, Dec. 2014.

[90] T. B. Walpole, D. N. Palmer, H. Jiang, S. Ding, I. M. Fearnley, and J. E. Walker, “Conservation of complete trimethylation of lysine 43 in the rotor ring of c-subunits of metazoan ATP synthase,” *Mol. Cell. Proteomics MCP*, Jan. 2015.

[91] M. Sekiya, R. Hisasaka, A. Iwamoto-Kihara, M. Futai, and M. Nakanishi-Matsui, “A unique mechanism of curcumin inhibition on F1 ATPase,” *Biochem. Biophys. Res. Commun.*, vol. 452, no. 4, pp. 940–944, Oct. 2014.

[92] M. J. Pallen, C. M. Bailey, and S. A. Beatson, “Evolutionary links between FliH/YscL-like proteins from bacterial type III secretion systems and second-stalk components of the FoF1 and vacuolar ATPases,” *Protein Sci. Publ. Protein Soc.*, vol. 15, no. 4, pp. 935–941, Apr. 2006.

[93] K. Paul, M. Erhardt, T. Hirano, D. F. Blair, and K. T. Hughes, “Energy source of flagellar type III secretion,” *Nature*, vol. 451, no. 7177, pp. 489–492, Jan. 2008.

[94] T. Minamino, Y. V. Morimoto, N. Hara, and K. Namba, “An energy transduction mechanism used in bacterial flagellar type III protein export,” *Nat. Commun.*, vol. 2, p. 475, 2011.

[95] T. Minamino, Y. V. Morimoto, M. Kinoshita, P. D. Aldridge, and K. Namba, “The bacterial flagellar protein export apparatus processively transports flagellar proteins even with extremely infrequent ATP hydrolysis,” *Sci. Rep.*, vol. 4, p. 7579, 2014.

[96] Y. Lai, I. Rosenshine, J. M. Leong, and G. Frankel, “Intimate host attachment: enteropathogenic and enterohaemorrhagic Escherichia coli,” *Cell. Microbiol.*, vol. 15, no. 11, pp. 1796–1808, Nov. 2013.

[97] A. S. Santos and B. B. Finlay, “Bringing down the host: enteropathogenic and enterohemorrhagic Escherichia coli effector-mediated subversion of host innate immune pathways,” *Cell. Microbiol.*, Jan. 2015.

[98] J. E. Deane, P. Abrusci, S. Johnson, and S. M. Lea, “Timing is everything: the regulation of type III secretion,” *Cell. Mol. Life Sci. CMLS*, vol. 67, no. 7, pp. 1065–1075, Apr. 2010.

[99] T. Tobe, H. Yen, H. Takahashi, Y. Kagayama, N. Ogasawara, and T. Oshima, “Antisense transcription regulates the expression of the enterohemorrhagic Escherichia coli virulence regulatory gene ler in response to the intracellular iron concentration,” *PloS One*, vol. 9, no. 7, p. e101582, 2014.

[100] R. Zarivach, M. Vuckovic, W. Deng, B. B. Finlay, and N. C. J. Strynadka, “Structural analysis of a prototypical ATPase from the type III secretion system,” *Nat. Struct. Mol. Biol.*, vol. 14, no. 2, pp. 131–137, Feb. 2007.

[101] G. Waksman and S. J. Hultgren, “Structural biology of the chaperone-usher pathway of pilus biogenesis,” *Nat. Rev. Microbiol.*, vol. 7, no. 11, pp. 765–774, Nov. 2009.

[102] J. E. Galán and H. Wolf-Watz, “Protein delivery into eukaryotic cells by type III secretion machines,” *Nature*, vol. 444, no. 7119, pp. 567–573, Nov. 2006.

[103] K. A. Datsenko and B. L. Wanner, “One-step inactivation of chromosomal genes in Escherichia coli K-12 using PCR products,” *Proc. Natl. Acad. Sci. U. S. A.*, vol. 97, no. 12, pp. 6640–6645, Jun. 2000.

[104] P.-J. Matteï, E. Faudry, V. Job, T. Izoré, I. Attree, and A. Dessen, “Membrane targeting and pore formation by the type III secretion system translocon,” *FEBS J.*, vol. 278, no. 3, pp. 414–426, Feb. 2011.

[105] K. Takeuchi and G. Wagner, “NMR studies of protein interactions,” *Curr. Opin. Struct. Biol.*, vol. 16, no. 1, pp. 109–117, Feb. 2006.

[106] M. Lilic, M. Vujanac, and C. E. Stebbins, “A common structural motif in the binding of virulence factors to bacterial secretion chaperones,” *Mol. Cell*, vol. 21, no. 5, pp. 653–664, Mar. 2006.

[107] D. Munera, V. F. Crepin, O. Marches, and G. Frankel, “N-terminal type III secretion signal of enteropathogenic Escherichia coli translocator proteins,” *J. Bacteriol.*, vol. 192, no. 13, pp. 3534–3539, Jul. 2010.

[108] H. Nikaido, “Isolation of outer membranes,” *Methods Enzymol.*, vol. 235, pp. 225–234, 1994.

[109] R. Lill, W. Dowhan, and W. Wickner, “The ATPase activity of SecA is regulated by acidic phospholipids, SecY, and the leader and mature domains of precursor proteins,” *Cell*, vol. 60, no. 2, pp. 271–280, Jan. 1990.

[110] G. Gouridis, S. Karamanou, M. Koukaki, and A. Economou, "*In vitro* assays to analyze translocation of the model secretory preprotein alkaline phosphatase," *Methods Mol. Biol. Clifton NJ*, vol. 619, pp. 157–172, 2010.

[111] G. Gouridis, S. Karamanou, M. F. Sardis, M. A. Schärer, G. Capitani, and A. Economou, "Quaternary dynamics of the SecA motor drive translocase catalysis," *Mol. Cell*, vol. 52, no. 5, pp. 655–666, Dec. 2013.

[112] K. F. Discola, A. Förster, F. Boulay, J.-P. Simorre, I. Attree, A. Dessen, and V. Job, "Membrane and Chaperone Recognition by the Major Translocator Protein PopB of the Type III Secretion System of Pseudomonas aeruginosa," *J. Biol. Chem.*, vol. 289, no. 6, pp. 3591–3601, Feb. 2014.

[113] P.-C. Lee, S. E. Zmina, C. M. Stopford, J. Toska, and A. Rietsch, "Control of type III secretion activity and substrate specificity by the cytoplasmic regulator PcrG," *Proc. Natl. Acad. Sci. U. S. A.*, vol. 111, no. 19, pp. E2027–2036, May 2014.

[114] G. W. Buchko, G. Niemann, E. S. Baker, M. E. Belov, R. D. Smith, F. Heffron, J. N. Adkins, and J. E. McDermott, "A multi-pronged search for a common structural motif in the secretion signal of Salmonella enterica serovar Typhimurium type III effector proteins," *Mol. Biosyst.*, vol. 6, no. 12, pp. 2448–2458, Dec. 2010.

[115] A. A. A. Amer, M. K. Åhlund, J. E. Bröms, Å. Forsberg, and M. S. Francis, "Impact of the N-terminal secretor domain on YopD translocator function in Yersinia pseudotuberculosis type III secretion," *J. Bacteriol.*, vol. 193, no. 23, pp. 6683–6700, Dec. 2011.

[116] K. S. Ramamurthi and O. Schneewind, "A synonymous mutation in Yersinia enterocolitica yopE affects the function of the YopE type III secretion signal," *J. Bacteriol.*, vol. 187, no. 2, pp. 707–715, Jan. 2005.

[117] R. Younis, L. E. H. Bingle, S. Rollauer, D. Munera, S. J. Busby, S. Johnson, J. E. Deane, S. M. Lea, G. Frankel, and M. J. Pallen, "SepL resembles an aberrant effector in binding to a class 1 type III secretion chaperone and carrying an N-terminal secretion signal," *J. Bacteriol.*, vol. 192, no. 22, pp. 6093–6098, Nov. 2010.

[118] G. Gouridis, S. Karamanou, I. Gelis, C. G. Kalodimos, and A. Economou, “Signal peptides are allosteric activators of the protein translocase,” *Nature*, vol. 462, no. 7271, pp. 363–367, Nov. 2009.